ERDC TR-21-8

US Army Corps
of Engineers®
Engineer Research and
Development Center

Long-Term Performance of Sustainable Pavements Using Ternary Blended Concrete with Recycled Aggregates

Gilson R. Lomboy, Douglas B. Cleary, Seth M. Wagner, Yusuf Mehta, Danielle E. Kennedy, Benjamin E. Watts, Peter G. Bly, and Jared I. Oren

May 2021

Engineer Research and Development Center

The U.S. Army Engineer Research and Development Center (ERDC) solves the nation's toughest engineering and environmental challenges. ERDC develops innovative solutions in civil and military engineering, geospatial sciences, water resources, and environmental sciences for the Army, the Department of Defense, civilian agencies, and our nation's public good. Find out more at www.erdc.usace.army.mil.

To search for other technical reports published by ERDC, visit the ERDC online library at https://erdclibrary.on.worldcat.org/discovery.

ERDC TR-21-8
May 2021

Long-Term Performance of Sustainable Pavements Using Ternary Blended Concrete with Recycled Aggregates

Gilson R. Lomboy, Douglas B. Cleary, Seth M. Wagner, and Yusuf Mehta

Rowan University
Center for Research and Education in Advanced Transportation Engineering Systems (CREATEs)
107 Gilbreth Parkway
Mullica Hill, NJ 08062-4446

Danielle E. Kennedy, Benjamin E. Watts, and Jared I. Oren

U.S. Army Engineer Research and Development Center (ERDC)
Cold Regions Research and Engineering Laboratory (CRREL)
72 Lyme Road
Hanover, NH 03755-1290

Peter G. Bly

U.S. Army Engineer Research and Development Center (ERDC)
Geotechnical and Structures Laboratory (GSL)
3909 Halls Ferry Road
Vicksburg, MS 39180-6199

Final Report

Prepared for Headquarters, U.S. Army Corps of Engineers
Washington, DC 20314-1000

Under PE 0602784A / Project T26, “Innovative Construction Materials for Cold Regions”

Abstract

Dwindling supplies of natural concrete aggregates, the cost of landfilling construction waste, and interest in sustainable design have increased the demand for recycled concrete aggregates (RCA) in new portland cement concrete mixtures. RCA repurposes waste material to provide useful ingredients for new construction applications. However, RCA can reduce the performance of the concrete.

This study investigated the effectiveness of ternary blended binders, mixtures containing portland cement and two different supplementary cementitious materials, at mitigating performance losses of concrete mixtures with RCA materials. Concrete mixtures with different ternary binder combinations were batched with four recycled concrete aggregate materials. For the materials used, the study found that a blend of portland cement, Class C fly ash, and blast furnace slag produced the highest strength of ternary binder. At 50% replacement of virgin aggregates and ternary blended binder, some specimens showed comparable mechanical performance to a control mix of only portland cement as a binder and no RCA substitution. This study demonstrates that even at 50% RCA replacement, using the appropriate ternary binder can create a concrete mixture that performs similarly to a plain portland cement concrete without RCA, with the added benefit of being environmentally beneficial.

Contents

Figures and Tables

Figures

Tables

Preface

This study was conducted for the U.S. Army Corps of Engineers under PE 0602784A / Project T26, "Innovative Construction Materials for Cold Regions."

The work was performed by Rowan University in conjunction with the Engineering Resources Branch (Dr. Caitlin A. Callaghan, Chief) of the Research and Engineering Division (Dr. George Calfas, Acting Chief), U.S. Army Engineer Research and Development Center, Cold Regions Research and Engineering Laboratory (ERDC-CRREL). Additional technical support was provided by the Airfields and Pavements Branch (Ms. Anna Miller Jordan, Chief) of the Engineering Systems and Materials Division (Mr. Justin Strickler, Chief), ERDC Geotechnical and Structures Laboratory (GSL). At the time of publication, Ms. Pam Kinnebrew was the Technical Director for Military Engineering. The Deputy Director of ERDC-CRREL was Mr. David B. Ringelberg, and the Director was Dr. Joseph L. Corriveau. The Deputy Director of ERDC-GSL was Mr. Charles W. Ertle II, and the Director was Mr. Bartley P. Durst.

COL Teresa A. Schlosser was Commander of ERDC, and Dr. David W. Pittman was the Director.

Acronyms and Abbreviations

AASHTO	American Association of State Highway and Transportation Officials
ACI	American Concrete Institute
ACPA	American Concrete Pavement Association
AVA	Air-Void Analyzer
B-RCA	Blended, Recycled Concrete Aggregate
C_2S	Dicalcium Silicate
C_3A	Tricalcium Aluminate
C_3S	Tricalcium Silicate
CCCA	Crushed Concrete Coarse Aggregate
CRREL	U.S. Army Cold Regions Research and Engineering Laboratory
DGABC	Dense-Graded Aggregate Base Course
ERDC	Engineer Research and Development Center
FAC	Fly Ash, Class C
FAF	Fly Ash, Class F
GGBFS	Ground, Granulated Blast Furnace Slag
GSL	Geotechnical and Structures Laboratory
HRWR	High-Range Water Reducer
LA	Los Angeles
NC	Normal Concrete
NJDOT	New Jersey Department of Transportation
PC	Portland Cement
RCA	Recycled Concrete Aggregate

SCM	Supplementary Cementitious Material
SF	Silica Fume
UFC	Unified Facilities Criteria
UFGS	Unified Facilities Guide Specifications
USACE	U.S Army Corps of Engineers

1 Introduction

1.1 Background

Because of the high production rate of portland cement concrete, demand for suitable aggregates and portland cement raises concerns for both the environmental and economic viability of these materials. The production of portland cement and aggregates plays a significant role in the creation of pollution in the concrete industry and depletes natural concrete aggregate sources. For many years, alternative materials have been used to either supplement or replace these in concrete materials to varying degrees of success.

Recycled concrete aggregate (RCA) or crushed concrete coarse aggregate (CCCA) is demolished concrete that has been crushed and graded to be used as aggregate (ACI Committee 555 2001; USACE 2004a). RCA consists of virgin aggregate coated fully or partially by hardened mortar from the previous mix. RCA tends to have higher porosity and poorer mechanical properties than virgin aggregates due to the presence of adhered mortar, which may be softer or less durable than the original aggregate. However, given appropriate constraints on usability, it may be possible to replace part or all of the required aggregates in a concrete mixture with RCA to yield mixture properties equivalent to more traditional concrete materials. In these cases, the demand for virgin aggregates may be reduced, preserving existing quarries. RCA may also be more readily available in some instances from on-site or local crushing facilities, reducing materials and transportation costs.

Like RCA, supplementary cementitious materials (SCMs) are a class of industrial byproducts that are used to replace a portion of the ingredients in a concrete mixture. SCMs are mineral admixtures that can be used in combination with portland cement to improve the fresh and hardened properties of concrete. These admixtures can be hydraulic such that they exhibit cementitious properties when reacted with water. They may also be pozzolanic, reacting with calcium hydroxide and water to provide additional strength. When two SCMs are combined with portland cement as the binder for concrete, the binder becomes a *ternary blended binder*.

Common SCMs include ground granulated blast furnace slag, fly ash, and silica fume. Blast furnace slag is a byproduct of iron production, fly ash is produced from coal-burning operations, and silica fume is a byproduct of silicon and ferrosilicon alloy production. In locations where these industrial processes create an excess of these byproducts, it is possible to reduce both the environmental impact and cost of concrete construction with their use. This is further enhanced by reducing the use of Portland cement, which has a large energy and carbon footprint.

There is little in the way of literature addressing the use of ternary blended cements in conjunction with RCA replacement in concrete mixes. However, ternary blended binders are actively researched for their benefits to concrete mixtures. In these cases, cementitious or pozzolanic mineral admixtures that have compounding beneficial properties can replace a significant portion of portland cement in a proposed binder. An example of this theory is the inclusion of fly ash to accelerate early strength gain in slag-portland cement binders, which typically produce high strength but slowly maturing concrete. The inclusion of fly ash creates a ternary-blended binder that benefits from both the fly ash and blast furnace slag. The individual properties of SCMs make some more desirable than others. Increasing the use of ternary blended binders also helps to reduce the rate at which these SCMs are consumed by replacing some part of commonly used binary binders with a third component. The overall benefits that can result from the use of a ternary binder may be uniquely useful in mitigating the performance detriments associated with use of RCA.

1.2 Objective

The U.S. Army Cold Regions Research and Engineering Laboratory (CRREL), in conjunction with Rowan University, studied the use of ternary binders and recycled aggregates in concrete. The overall goal of the project was to increase the use of RCA in concrete through portland cement concrete mixture development and long-term performance verification. The beneficial effects of optimized ternary binders on improving concrete strength and durability may offset the drawbacks of incorporating large quantities of RCA in concrete, with replacement percentages of coarse aggregate as high as 100%. The objective of this study was to develop guidance concerning the use of RCA for the design of portland cement concrete mixtures where virgin aggregates or approved building materials are not available.

1.3 Scope

The purpose of this research was to explore the interaction of ternary blended binders and crushed concrete coarse aggregates in developed concrete mixtures with a low water-to-binder ratio. This work included two tasks:

1. Determine an optimal ternary blended binder consisting of portland cement and two SCMs (blast furnace slag, Class C fly ash, Class F fly ash, or silica fume).
2. Assess the performance of concrete mixtures with varying amounts of recycled coarse aggregate from multiple sources and the effect of using a ternary blended binder in concrete mixtures with RCA replacement rates up to 100%.

1.4 Approach

This study was segmented into two tasks. Task 1 was cementitious material blend optimization, which included all procedures for optimizing the ternary binder composition that was used for RCA concrete mixtures. Mortar cubes for various binder combinations of portland cement and mineral admixtures were tested to determine the differences in the strengths. Isothermal calorimetry was conducted for each mixture to observe curing characteristics and to identify interactions between additives. Statistical analysis was performed on mortar cube strength data to determine an optimized binder proportioning that produced the highest predicted strength for each blend of mineral admixtures.

Larger batches of fresh mixture tests, surface resistivity, alkali-silica reaction, and concrete compression tests for each optimized ternary blend were made to compare strength gain and resistivity characteristics for each blend. From this data, a single blend for further testing in RCA concrete was chosen.

Task 2 was the testing of ternary blended concrete with RCA replacement. Additional concrete batches were mixed to compare fresh and hardened properties between a control and ternary blended concrete with varying levels of RCA replacement.

2 Literature Review

2.1 Ternary blended cement-based binder

Making portland cement requires an immense amount of energy and is known to release carbon dioxide into the environment. Including alternative admixtures as replacements for cement can reduce the environmental impact of concrete production. SCMs in portland cement concrete mixtures reduce the amount of portland cement needed in the concrete binder while incorporating other benefits, such as increased strength. Consequently, there is much interest in researching and standardizing the addition of SCMs in cement concrete (Ghosh et al. 2011).

SCMs have cementitious properties on their own or when combined with portland cement. Therefore, including them into concrete mixtures properly improves both fresh-mixture and hardened-concrete properties (Naval Facilities Engineering Command 2019). In many cases, the use of two supplementary materials compounds the benefits or overcomes the shortfalls of a binary binder, which includes only one of the two supplementary materials. For example, the long-term strength of portland-limestone cement can be improved by including high-grade slag. Thus, using multiple SCMs is very important in applications where a mix must meet many requirements for workability, early and late strength, durability, and so on.

Isothermal calorimetry can be used to measure and identify patterns in the heat of hydration of cement mixtures containing different supplements. This method measures the change in the heat of a substance undergoing a chemical reaction at a constant ambient temperature. This measurement correlates directly with the ultimate strength and durability of the concrete (Kim 2010). In general, the hydration of cement occurs in five distinct stages. On the first contact with water, a rapid heating process begins that lasts 15 to 30 minutes as a result of ions dissolving in the water and reacting with components of the cement (Stage 1 in Figure 1) (Wang et al. 2006). This period provides no strengthening characteristics to the concrete; however, it can reduce the reaction rate in the later stages (Kim 2010). The second part of hydration is a period of dormancy during which hydration stops temporarily (Stage 2). During this time, the concrete does not generate heat and is in a workable condition. This stage may last upward of 5 hours and can be retarded by including supplementary materials

and additives. Following the dormant phase, hydration of tricalcium silicate (C3S) and dicalcium silicate (C2S) accelerates in a concrete-strengthening reaction that produces a significant amount of heat (Stage 3). Following this accelerated hydration stage, hydrate layers thicken; and there is less available surface area of unhydrated particles, slowing the hydration reaction (Stage 4). During this portion of the reaction, tricalcium aluminate (C3A) hydration may occur and will cause a secondary peak in the heat of hydration. The magnitude of this secondary reaction is dependent on the inclusion of pozzolanic materials in the mixture and will increase significantly with their addition. Finally, the reaction reaches a steady state where little or no hydration occurs (Stage 5). The figure below shows the general heat of hydration curve for portland cement concrete.

Figure 1. Hydration curve for portland cement concrete.

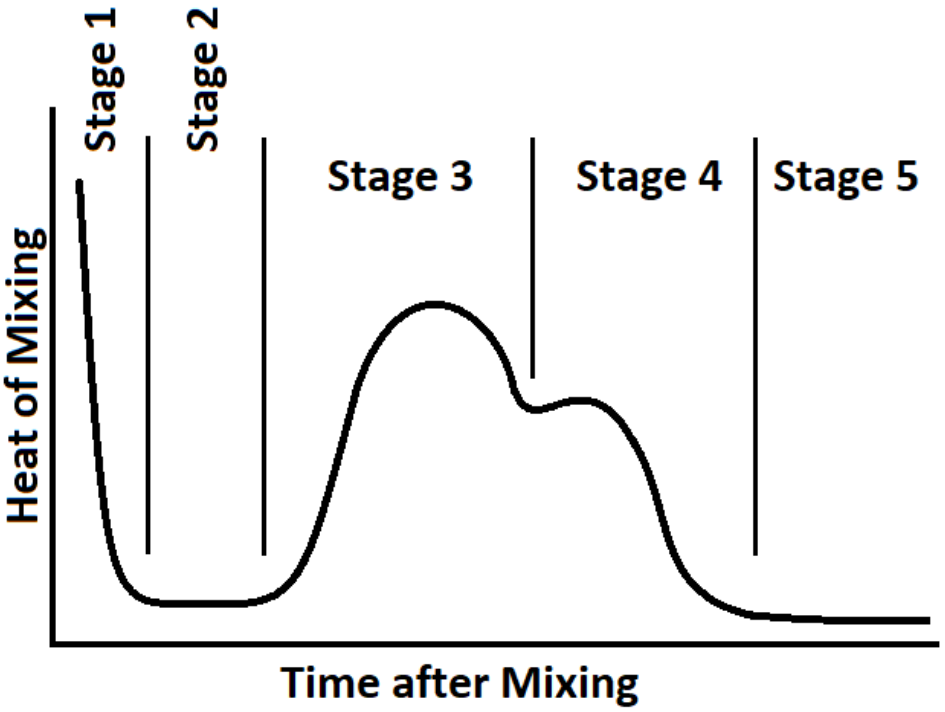

Total heat of hydration is an indicator of the completeness of the reaction in a mixture, and thus the analysis of these reactions through calorimetry is effective in explaining the strength and durability of individual ternary mixtures.

In addition to strength and durability, which may be predicted in part by calorimetry, there are additional properties of concrete to consider. Dewar

(2003) suggested considering the following parameters: consistency, stiffening rate, cohesion, density, strength, durability, and air content. Requirements in these categories impact the chosen mixture and the method of proportioning. Concerning individual tests, there are additional factors to consider in a real-world scenario. Materials should accurately represent those to be used in construction and should be in a similar condition to avoid discrepancies between laboratory and field evaluations. Smaller test batches will lose water content more easily to evaporation and absorption. Lastly, multiple initial tests are preferred when used as a representation of larger-scale mixtures.

Dewar (2003) has cataloged several mixture design methods. The British Ready Mixed Concrete Association proposes a mixture design based on the plastic properties of the concrete and measurement of hardened performance. Dewar (2003) proposed an addition to this process based on a computer model of gradation, bulk density, and the relative density of aggregates. The goal is to model the interaction between particles accurately to avoid needing preliminary trial mixing. The American Concrete Institute (ACI) suggests ACI 211.1-91 as a guideline for selecting proportions for cement concrete made with other cementitious materials (ACI Committee 211 2002). This document outlines the procedure for determining mixture proportions by weight equivalency and conversion of absolute volumes to weights, dependent on specifications regarding water-to-cement ratio, cement content, air content, required slump, aggregate size, and strength. The Kansas Department of Transportation (2012) provides a solution for absolute volume design dependent on the known required volumes of each component of the mixture.

The types of cementitious materials used may have a bearing on the mix design method used. SCMs may affect the desired water content, aggregate proportion, and so on. Hydraulic cements, such as portland cement, are materials that demonstrate cementitious properties when mixed with water. Excluding portland cement, these are considered secondary cementitious materials. Blended hydraulic cements are those that include portland cement along with other hydraulic SCMs. These types of SCMs include materials such as slag cement and Class C fly ash. Slag cement is a byproduct of the operation of iron blast furnaces, and it has been found to increase set time and concrete strength (Ayers et al. 2007). Fly ash is a byproduct of coal burning and is usually separated into two classes for use in

cement, Class C and Class F. Class C fly ash is described as sometimes exhibiting cementitious properties and contains more calcium oxide than Class F fly ash (Abdel-Hay 2015). Class F is a pozzolanic material. Both fly ashes can reduce the water required to achieve a set workability, increased strength, and reduced heat of hydration.

Pozzolans are another type of SCM that are not cementitious on their own but are cementitious when combined with calcium hydroxide, a chemical found in hydrating cementitious materials. Various types of pozzolans are added to portland cement concrete. These can include Class F fly ash, silica fume, and other natural pozzolans. Class F fly ash consumes calcium hydroxide and thus strengthens concrete beyond the initial hydraulic reaction by turning weak byproducts into more calcium silica hydrate. However, the pozzolanic reaction slows the initial hydration reaction and creates longer setting times. Silica fume is a byproduct of making silicon and ferrosilicon alloys. It is also pozzolanic but extremely reactive due to its high surface area from its small particle size (Kosmatka and Wilson 2016). The addition of silica fume increases the strength of the concrete, though the mixture requires a higher water-to-cement ratio or the inclusion of superplasticizer (Tutanji and El-Korchi 1995).

Using pozzolanic SCMs is advantageous in that cement production is a primary producer of carbon dioxide, and using replacement pozzolans helps lower greenhouse gas emissions. Natural pozzolans were originally used as SCMs and included materials such as volcanic ash, calcined clay, calcined shale, and metakaolin (Abdel-Hay 2015). One of the greater points of interest concerning SCMs is decreasing the amount of variability between producers as most SCMs are byproducts, and their actual compositions can differ depending on when they were produced. Decreased variability in the materials can lead to more accurate, consistent testing results.

Limestone is another material that may be used to lessen the environmental impact of concrete. Blending limestone and portland cement is a fairly new practice. In 2012, ASTM defined portland-limestone cement as containing 5% to 15% limestone (ASTM 2017a [C595]). Portland-limestone cement is made by intergrinding limestone and cement clinker. The limestone is softer than the clinker, so it may be crushed into finer particles than cement, creating a greater particle-size distribution in the binder. Limestone may affect the set time, compressive strength, and permeability of concrete (Goguen 2014). Finer limestone may decrease the setting time,

and these fine particles increase density and lower permeability. Low concentrations of limestone increase early strength. However, when the cement is more than 15% limestone, it may negatively impact compressive strength. When portland-limestone cement is incorporated in mixes with Class C Fly Ash and slag, the compressive strength of concrete increases (Goguen 2014).

2.1.1 Fresh ternary blended concrete properties

The inclusion of SCMs may affect the required setting time of a concrete mixture. Setting time affects construction logistics as the concrete needs to be transported and placed before setting occurs. After it is placed, it then needs to be consolidated or formed. Ghosh et al. (2011) found that when Class C fly ash is used to replace 20% of Type I portland cement, initial and final setting time can be increased by 96 and 189 minutes, respectively. (Type I portland cement is a general-purpose cement used in applications where specific properties such as early strength or sulfate resistance are not required.) Class C fly ash may be more effective than Class F at increasing setting time when Class F fly ash has a higher content of oxides or sulfur. Larger increases in setting time occurred when Class C fly ash was mixed into a ternary mixture with Class F. Time to set was increased by 402 minutes compared to a control mixture of portland cement only, which took 221 minutes to reach final cure (Ghosh et al. 2011).

2.1.2 Hardened ternary blended concrete properties

Bektas et al. (2014) investigated the trends that binary and ternary blended concretes exhibited in their hardened properties. The study found that in binary mixtures of additives and portland cement, adding Class C fly ash provided similar compressive strengths at 15% and 30% replacement of the cementitious component to that of control samples of only portland cement. Ternary blends of Class C fly ash and slag showed improved strengths. The inclusion of Class F fly ash lowered compressive strength at 28 days at all levels of inclusion; however, the use of slag and Class F fly ash together improved strength. Hariharan et al. (2011) analyzed the effects of ternary blended binders of fly ash and silica fume on compressive strength and chloride ion permeability. They observed that the use of silica fume increased the early and final strength of concrete compared to a control. When Class C fly ash was mixed with the silica fume, the silica fume also had a positive effect on the compressive strength of the concrete and accelerated the early strength. Using 30% Class C fly

ash and 6% silica fume resulted in an optimal compressive strength. The study also found that, except for the mixture designed for maximum strength, the difference in compressive strength between the control mixture and the binary and ternary blended concrete mixtures was negligible (Harihan et al. 2011).

There are several other properties to consider in the use of ternary blended binders. Air content and void structure may change depending on the particle size and composition of SCMs used. Air-void systems are described by the air content, spacing factor, and specific surface of voids (the ratio of void surface area to volume) in fresh and hardened concrete. Having a well-formed air-void system may increase the durability of concrete under freeze–thaw conditions. A good air-void system for resisting the effects of cyclic freezing and thawing has a spacing factor of less than 0.2 mm in hardened concrete. The addition of most SCMs does not have obvious effects on air-void systems. High dosages of silica fume may have a negative effect on air voids due to its small particle size relative to portland cement (Bektas et al. 2014; Bleszynski et al. 2002).

Freeze–thaw durability is a measure of the capacity of a hardened concrete mixture to resist cyclic degradation processes. In areas of harsh or varied weather conditions, freeze–thaw testing may gauge the effect that the environment will have on the finished concrete. Stundebeck (2007) offered that the air-void structure and air entrapment of a sample has a great effect on its freeze–thaw resistance. The use of silica fume creates a refined pore structure that may aid durability, though more than 5% silica fume was not found to increase resistance any further, as shown by Bleszynski et al. (2002) and Stundebeck (2007). Stundebeck also found that replacing portland cement with slag gives a greater risk of surface damage and freeze–thaw damage than replacement by fly ash.

When cement is mixed, a byproduct of the chemical reaction is the release of heat. In general, ternary blended concrete has a lower heat of hydration than portland cement alone (Hu et al. 2017). Portland cement with slag takes longer to set and, as such, releases heat over a longer period than portland cement alone. This leads to a lower or more delayed peak hydration temperature of mixtures with slag (Bleszynski et al. 2002). When the percentage of fly ash is increased and the percentage of slag is decreased, the overall heat signature decreases. This has significant implications for

larger concrete placements, where excessive heat production can lead to deleterious reactions and thermal cracking.

Due to sourcing and mixing procedures, drying shrinkage in ternary blended cement concretes is difficult to examine as the additives have inconsistent effects on the hardened properties (Bleszynski et al. 2002). The addition of high doses of silica fume or slag increases drying shrinkage. Reducing SCMs generally reduces shrinkage. At higher percent replacements such as 30% slag and 20% fly ash with portland cement, the mixture may be unable to resist drying shrinkage and may be more susceptible to cracking (Hu et al. 2017).

2.2 Blended cement mixtures with RCA (B-RCA)

When properly used, blended binders combined with recycled concrete aggregate (B-RCA) achieve the environmental, economic, and material property benefits of both binder admixtures and aggregate substitution. Mixtures including RCA and SCMs should account for both the variations in properties of recycled aggregates and for the changes in fresh and hardened properties caused by incorporating mineral admixtures. This can include the chemical and physical aggregate properties as well as binder properties and interactions.

2.2.1 Fresh B-RCA properties

Mixtures incorporating RCA require more water to maintain comparable workability to virgin aggregate concrete mixtures. Gurdián et al. (2014) found that concrete slump decreases when RCA levels increase; however, when 35% fly ash is added, the slump begins to stabilize and equal the control blend. Kim et al. (2013) found that adding 30% fly ash increases the slump of RCA mixtures by 45% to 100%. The density of concrete mixes only slightly changes when low levels of fly ash or RCA are introduced. Table 1 shows how density changes based on the concrete blend, as presented by Bleszynski et al. (2002) and gathered by Sadati et al. (2016), Cong (2006), Pepe (2015), Kou and Poon (2009), and Lima et al. (2013).

Table 1. Density of concrete with recycled concrete aggregates (Sadati et al. 2016; Cong 2006; Pepe 2015; Kou and Poon 2009; Lima et al. 2013).

Concrete Mixtures	Density (kg/m^3)
Conventional Materials	2211–2365
Fly Ash and Coarse RCA	1958–2324
Fly Ash and Fine RCA	1958–2299

The fresh density of concrete mixes decreased when RCA and fly ash increased. Mixes with a higher water-to-cement ratio were less affected than those with lower ratios when RCA and fly ash were introduced.

2.2.2 Hardened B-RCA properties

The presence of adhered mortar on recycled aggregates affects the ability of fresh mortar to adhere to RCA and may impact mixture strength. Akbari and Rushabh (2015) found that the compressive strength of recycled aggregate concrete with a ternary blended binder is typically at least 76% of that of a virgin mix. The strength of the recycled concrete portion and the strength of the new mix matrix contribute to the overall strength of a concrete mixture containing RCA. The percentage of RCA used and the aggregate size proportion also contribute to the strength of the mixture. The study found that compressive strength increased with increasing RCA replacement, with a maximum strength identified between 30% and 40% recycled aggregate replacement. When introducing SCMs, such as fly ash and silica fume, the adherence was improved between the recycled aggregate and the paste. The optimum percentage of SCM was found to be 5% silica fume and 20% fly ash without recycled aggregate and 20% fly ash and 10% silica fume with recycled aggregate at a replacement rate of 50% (Akbari and Rushabh 2015).

2.3 Recycled concrete aggregate (RCA)

Concrete is commonly recycled into RCA through the demolition of buildings and pavements (ACI Committee 555 2001). In addition to impurities that may be present in aggregate of this type due to the wide variety of sources, the presence of mortar alters the physical properties of the aggregate. The presence of these components tends to decrease concrete density and increase porosity and adsorption with respect to concrete with virgin aggregates (Pedro et al. 2014). RCA is primarily used in consideration of the economic and environmental impacts of concrete construction as a

cheaper or less-harmful alternative to virgin aggregates. The use of RCA prevents material from occupying landfills and limits the harvesting of virgin aggregates (Meddah et al. 2016). Depending on the cost and availability of virgin aggregates, using RCA may also prove to be an economical choice where there is less cost in recycling than in removing and disposing of rubble, particularly in cases where a mobile recycling operation can be brought onto the site (ACPA [American Concrete Pavement Association] 2010a).

RCA can differ greatly from virgin aggregates with respect to production and stockpiling. The production of RCA begins with the demolition of the site. ACI Committee 555 (2001) lists common types of structures that may be a part of this process. These include mass concrete structures, underground concrete structures, reinforced concrete structures, and prestressed/posttensioned concrete structures. Different types of structures require additional considerations in demolition to avoid accidental collapse. Demolition methods are selected based on safety, environmental impact, budgetary constraints, and the size and location of the site. Available methods of demolition include hand tools, vehicle-mounted equipment, explosive blasting, chemical demolition agents, mechanical splitters, heat demolition, and hydrodemolition.

Following successful demolition, reinforcement is removed from the debris, and the concrete is transported to a processing plant. Once at the plant, large rubble is crushed to a suitable size via several differently sized crushers. The aggregate size is reduced to a final maximum diameter of 20 to 25 mm* (ACI Committee 555 2001). Further processing is required to remove other contaminants in the concrete, which can vary by source. A magnet removes any additional rebar in the concrete. Other contaminants present in concrete removed from building demolitions include wood, plaster, plastic, oil, etc. ACI Committee 555 (2001) closely relates the operations at RCA processing plants to those of plants that process unused virgin aggregate.

There is some concern over stockpiling recycled aggregates. The ACPA has found RCA stockpiles are notably more alkaline as a result of calcium

* For a full list of the spelled-out forms of the units of measure used in this document, please refer to *U.S. Government Publishing Office Style Manual*, 31st ed. (Washington, DC: U.S Government Publishing Office, 2016), 248–252, https://www.govinfo.gov/content/pkg/GPO-STYLEMANUAL-2016/pdf/GPO-STYLEMANUAL-2016.pdf.

hydroxide being leached from the pile (ACPA 2010b). The calcium hydroxide reacts with carbon dioxide to form carbonates. Abbaspour et al. (2016) confirm these findings, noting increases in pH with stockpile aging as well as an increase in carbonate content. ACPA suggests stockpiling washed RCA to help avoid carbonate runoff from clogging drains. Additionally, the acidity of rain reacting to form the carbonates may reduce or potentially neutralize the alkalinity of the stockpile (Poon et al. 2006). There are no further known disadvantages to stockpiled RCA as opposed to virgin aggregate.

Production of crushed concrete coarse aggregate as an alternative source of coarse aggregate has a few notable environmental effects. Sources of virgin aggregate are finite and ever reducing, and recycling already-used materials helps to preserve these supplies (ACPA 2010a). In addition, reusing demolished concrete as RCA reduces the output of material from the construction industry into landfills. By processing RCA for a given project, the carbon dioxide emissions and energy consumption associated with quarrying can be reduced or eliminated (Meddah 2016). RCA production can be accomplished via mobile recycling operations placed on the construction site or fixed recycling plants that require materials transportation off-site (McIntyre et al. 2009). McIntyre et al. (2009) conducted a study that found that the optimal amount of RCA production depended on both cement consumption and transportation. If increasing the RCA replacement rate of a mix requires more cement to be added to maintain a target strength, RCA replacement begins to lose value. On-site recycling reduces the costs associated with materials transportation. McGinnis et al. (2017) quantified the land use, water use, energy demand, and carbon emissions associated with the production of natural and recycled aggregates via field study. Their study found that, in all four categories, recycled aggregate production required a fraction of the resources of virgin aggregate production. The study concluded that RCA production had a 55% reduced environmental impact over virgin aggregate. Additionally, the study investigated the economic possibilities of RCA and found that recycled aggregates cost as low as 74% of the price of virgin aggregates available for studied projects.

2.3.1 Aggregate properties

The increase in aggregate void space in RCA greatly affects their bulk density (ASTM 2017 [C29]). This is found via ASTM C29/C29M standard testing. Bulk density is essential for proportioning, voids calculation, and vol-

ume control. A low percentage of voids in aggregates is preferable for concrete production because less paste is required for mixing. Adding binder increases the cost of portland cement concrete. The presence of old, porous mortar adhered to recycled aggregates reduces the density of concrete with RCA. Specific gravity for recycled aggregates ranges from 2.2 to 2.6, lower than virgin aggregate, which has a range of 2.4 to 2.9 (Kosmatka et al. 2002; Limbachiya et al. 2000; Bairagi et al. 1993; Butler et al. 2011).

Absorption, porosity, and permeability are affected by the pore volume in the aggregate and between aggregates. These voids affect the strength, abrasion resistance, and freeze–thaw durability of a concrete mixture. Porosity is the ratio of the voids in the aggregate to the total volume of the aggregate and is found via ASTM (2017b) C29/29M. Porosity is higher in RCA than in virgin aggregates due to the adhered mortar content of recycled aggregates. Concrete mixtures using RCA thus require more water to maintain workability and may suffer a decrease in hardened strength and density.

The Los Angeles Abrasion Test measures the effect of degradation on aggregate while enduring impact, abrasion, and grinding. ASTM (2006) C131/131M outlines this process. The aggregate sample is placed in a steel drum containing steel spheres, which undergoes a specified number of revolutions. A higher percent loss of aggregate mass following the test procedure indicates less resistance to crushing while a load is applied. Virgin aggregates tend to have a loss value between 10% and 20% while RCA typically suffers a 20%–45% mass loss due to the removal of the adhered paste (Kosmatka et al. 2002; Berube et al. 2002).

ASTM (2014a) C136/136M details the process to determine the particle-size distribution of fine and coarse aggregates in a sample. Coarse aggregates are those retained on a 4.75 mm opening sieve whereas fine aggregates pass through. The particle-size distribution of aggregates is important. Fine aggregates are stronger when placed under load and have less pore space. Using more coarse aggregate reduces construction cost as less binder is required to cover the surface area of the aggregates. Therefore, a gradation with an appropriate blend of fine and coarse aggregates (well graded) is required to balance concrete strength with cost. A well-graded aggregate will result in small, tightly packed voids and a stable matrix structure. Fineness modulus, which is used in portland cement con-

crete mixture design and quality control checks during concrete production, is also determined from the gradation of fine aggregates. Typical values of fineness modulus for fine aggregates are between 2.3 and 3.1.

The flat and elongated test determines the shape of aggregates to be used in a mixture. ASTM (2010b) D4791 gives the process by which the percentage of elongated particles, flat particles, or flat and elongated particles is found for an aggregate sample. Flat or elongated particles have a greater chance to fracture and are harder to compact. The shape for typical virgin aggregates is blended between well-rounded smooth gravel and angular, rough crushed rock. RCA tends to be rougher due to the presence of adhered mortar (Anderson et al. 2009). The shape, texture, and angularity of aggregates determine the uncompacted void content percentage. If the void content increases, it may be attributed to a greater angularity, less sphericity, or a rougher surface of the aggregate. Angular aggregates create greater void space as angularity prohibits tight compaction (Anderson et al. 2009). They also require more binder material due to larger surface areas and subsequently increase mixture cost. However, increased angularity improves interlocking within the concrete matrix, increasing compressive strength. Rounded, smooth aggregates flow more easily in fresh concrete and may increase workability (Cleary 2013). Brown et al. (2001) concluded that the roundness of RCA produced commercially increased workability when compared with natural basalt aggregate.

Contaminants negatively affect the hardened properties of concrete. In a virgin aggregate blend, such contaminants are extraneous clays and organic material; however, RCA sources typically include contaminants from other demolished construction materials collected on-site. Most contaminants are found via a visible check at stockpiles and during mixing. Limiting the number of contaminants increases the strength of the concrete. Currently, the New Jersey Department of Transportation (NJDOT) limits the contaminant presence to 10% in RCA (NJDOT 2007). Standard processing procedures developed by ACI Committee 221 (2001) for removal and reuse of hardened concrete provide recommendations for the control of aggregate parameters, which include cleanliness and fine particle removal. RCA production processes follow this standard procedure closely and thus undergo the same treatment (ACI Committee 555 2001). The contaminants in virgin or recycled aggregates are primarily controlled through the quality control and quality assurance procedures at the quarries during crushing procedures.

Sulfate testing measures the capacity of aggregate to withstand intense weathering that occurs during freeze–thaw action. This test is conducted by placing the aggregate in magnesium sulfate or sodium sulfate for an extended time in accordance with ASTM (2018c) C88. These mixtures simulate the formation of ice crystals that can form on aggregates during winter. The Washington Department of Transportation found that both virgin and recycled aggregates pass the magnesium sulfate component of the test; however, only virgin aggregates are able to endure sodium sulfate testing based on acceptable mass losses. Because of the contradiction of the results between magnesium sulfate testing and sodium sulfate testing, agencies commonly waive RCA soundness testing (Anderson et al. 2009).

2.3.2 Fresh RCA concrete properties

The workability of concrete typically refers to how easily it can be set into place and finished. Workability depends on the consistency of concrete mixtures and is commonly indicated through a procedure known as slump testing as specified by ASTM (2015b) C143. In laboratory conditions for normal concrete, slump increases proportionally to water content and is inversely related to strength. The acceptable slump value for a concrete mixture depends on the structure in which the concrete will be used. These ranges typically fall between 50 and 100 mm for most applications (NJDOT 2007).

Workability is affected by the free water content of a fresh concrete mix. Recycled aggregates absorb more water due to high porosity. Barra et al. (2007) observed that concrete made with RCA requires approximately 5% more water than concrete made with virgin aggregates to achieve the same workability. Presaturating RCA prior to mixing can counteract this effect.

The permeability of concrete is its ability to remain well mixed and easily moveable under pressure (Jolin et al. 2009). This is an important characteristic of concrete because many structures require concrete pumps to place material. Concrete that is not readily pumpable will segregate or create pipe blockages. Many of the same measures used to enhance the workability of concrete made with RCA can be used to ensure pumpability. This includes the presoaking of recycled aggregates and strict slump control.

Water expands by approximately 9% when frozen (Hallet 2006). Concrete that is expected to experience freeze–thaw conditions is required to have air entrainment. Air entrainment produces more distributed air voids in a

concrete mixture, allowing water room to expand during freezing (Mamlouk and Zaniewski 2011). Wen et al. (2014) determined that the air content of RCA mixes was only marginally greater than concrete made with virgin aggregates, but the values had greater variability. However, the concrete with RCA and an air-entraining agent showed better resistance to cracking during freeze–thaw cycles.

To cure concrete, a procedure that takes place after mixing and placing concrete, the moisture and temperature are kept within a specific range for a certain amount of time (Mamlouk and Zaniewski 2011). Typical curing methods include membrane curing, steam curing, and the ponding method (Kosmatka et al. 2002). Membrane curing requires covering the wetted material with a waterproof surface for seven days to prevent the evaporation of water. Concrete cured using the steam method requires control of temperature and humidity to prevent the sample from drying out. Concrete cured via this method may achieve 70% of its ultimate strength after 18 hours. The ponding method entails submerging the concrete surface in water during the curing process. Amorim et al. (2012) found that curing conditions did not tend to affect concrete mixtures with RCA any differently than those with virgin aggregates.

2.3.3 Hardened RCA concrete properties

In general, the addition of RCA decreased the strength of concrete, though little difference in strength can be found for replacement rates below 30%. As the percentage of RCA goes up, the compressive strength of the specimen goes down (Limbachiya et al. 2000; Bairagi et al. 1993; Desai 2004; Desai and Limbachiya 2006). At 50% and 100% replacement, the compressive strength decreases by 16.6% and 26.4%, respectively (Davis et al. 2017).

Abdel-Hay (2015) observed the impact of curing conditions in RCA concrete strength gain. Through experimentation, that study found that water curing leads to increased 28-day compressive strength at 25% and 100% RCA replacement; however, air curing leads to higher strengths at all ages at 50% RCA replacement. This indicates no obvious link between curing condition and concrete strength at given RCA replacement rates. Abdel-Hay (2015) suggests a replacement rate of 50% to achieve maximum compressive strength for a concrete mixture with RCA. However, the compressive strength of RCA mixtures may vary with the RCA used. Corinaldesi

(2010) found that compressive strength was 8% lower using the same water-to-cement ratio when fine RCA was used rather than a strictly coarse blend of RCA. Corinaldesi (2010) attributed this strength difference to the variation of absorption, porosity, and the average dimension of the RCA particles. Davis et al. (2017) found that size #57 coarse aggregates made RCA 10%–15% percent weaker compared to RCA with smaller ASTM size #8 coarse aggregates.

Concrete does not have a linear stress-strain relationship. A chord modulus has traditionally been used when determining the elastic modulus of concrete as per ASTM C469 (Cleary 2013; ASTM 2014b). When recycled concrete aggregate is added to supplement virgin aggregate, the chord modulus of the concrete sample decreases. This decrease can vary widely due to the type and amount of RCA used. On average, the decrease in elastic modulus is 15%. A more dramatic reduction in elastic modulus can be seen with replacement by more than 50% RCA (Ann et al. 2007). However, the inclusion of mineral admixtures has been found to improve the elastic modulus when using RCA (Meinhold et al. 2001; Tam et al. 2007; Kou et al. 2007).

Porosity is a measurement of the amount of interconnected pores and air voids in a sample of concrete at the interfacial transition zone. This measurement is used to suggest the relative durability of a mixture against freeze–thaw and abrasion (Quattrone et al. 2016). Residual mortar present in recycled aggregates increases the porosity of RCA above virgin aggregate or gypsum. This high porosity allows for sorption into the concrete and the penetration of chemicals. Water absorption in the aggregate is increased, which may be detrimental to the concrete's durability (Cleary 2013). Large or connected voids in concrete may decrease strength and increase permeability (Mamlouk and Zaniewski 2011). ASTM (2013a) C642 presents the standard practice for determining voids in hardened concrete Additionally, ASTM (2010a) D4404 gives a method of porosity determination in aggregates by using mercury intrusion porosimetry. As this test is conducted by mercury intrusion under high pressure, it provides accurate analysis considering even very small pore spaces.

Larger pores in RCA create passageways for chemical seepage into the material. When chemicals such as chloride infiltrate a section of reinforced concrete, the steel corrodes and the structure weakens (Cleary 2013). A high permeability suggests a low strength value and high porosity of the

concrete (Mamlouk and Zaniewski 2011). Concrete with RCA can be up to six times more permeable than concrete with only virgin aggregate (ACI Committee 555 2001; Hansen 1986). Additionally, reducing the water-to-cement ratio by 5% to 10% may counteract the permeability issues of RCA. Abdel-Hay (2015) found that sample permeability is reduced by curing the RCA concrete in water. The 100 mm cube samples that were cured in water had sorptivity values that were 50% less compared to those obtained by curing in air at 28 days (Abdel-Hay 2015). Thomas et al. (2013) showed that the high porosity of RCA may lead to higher water and oxygen permeability in concretes that use recycled aggregates when compared to those without. This leads to concerns regarding the durability of RCA, especially in instances where aggressive deleterious processes, such as freeze–thaw action, occur. However, Andal et al. (2016) concluded that recycling concrete for aggregate while selecting material for original-mixture-quality preservation characteristics drastically reduced these concerns. This process excludes recycled materials that do not reflect the characteristics of the original mixture and thus reduces the amount of material that may be recycled on a job site.

Newly made concrete goes through a phase of drying shrinkage. Because of evaporation and chemical shrinkage, freshly cast concrete decreases in volume over time. After this initial shrinkage, the sample may continue to shrink as it settles, which causes cracking in the sample. Meinhold et al. (2001) concluded that drying shrinkage causes an increase in tensile stress and increases linearly as RCA replacement rates increase. Over the course of the first year, concrete made with RCA is expected to shrink 65% to 85% more than mixes with virgin aggregate. Xiao et al. (2013) showed that replacement rates of 50% and 100% RCA resulted in 17% and 59% higher shrinkage, respectively, over natural aggregate mixtures. Typical shrinkage values fall near 0.05% but may reach up to 0.1% for concrete containing RCA. Drying shrinkage was reduced when fly ash was included in the cementitious component of recycled aggregate mixes. Yamato et al. (1998) found that using shrinkage-reducing admixtures can counteract the effects of RCA. Drying shrinkage can be determined via ASTM (2017c) C596.

When water freezes within the pore spaces of concrete, it creates expansive pressure, which leads to cracking and deterioration of concrete. Over many cycles of freezing and thawing action, this deterioration accumulates and weakens concrete. Freeze–thaw durability performance may be assessed using ASTM (2012a) C666. While most studies agree that RCA replacement

may not notably impact concrete strength, the increased permeability of these mixtures allows freeze–thaw processes to deteriorate the concrete more quickly. Thus, the main concern with recycled aggregates is their impact on concrete durability. A study by Yamasaki and Tatematsu (1998) confirmed this, showing a marked decrease in freeze–thaw performance for samples with RCA replacement. The negative effects of recycled aggregates in recycled aggregate concrete mixtures can be limited effectively by mixture design and the use of additional additives. Yamato et al. (1998) suggested that this reduction in durability can be counteracted in part by limiting RCA replacement, reducing water-to-cement ratio, and increasing entrained air in the mixture. Salem et al. (2003) confirmed these findings and claimed that entrained air may neutralize the durability differences between virgin aggregate mixtures and RCA mixtures. Additionally, Wei et al. (2011) suggested that the addition of calcined diatomite in small amounts (2%) can reduce the permeability of recycled aggregate concrete mixtures and improve durability characteristics.

Huda and Alam (2015) found that increasing RCA replacement rates from 30% to 50% correlated with decreasing relative dynamic modulus throughout the testing. However, they found that all samples greatly exceeded the passing criteria set forth by ASTM (2012a) C666 of 60% of the initial elastic modulus at 300 cycles. This study concluded that the use of RCA does not have a significant detrimental impact on the durability of concrete in freeze–thaw conditions. Amorim et al. (2017) found similar results in the testing of concrete with 15% to 50% replacement rates, with instances of concrete with RCA replacement even surpassing the durability factor of samples containing only virgin aggregates.

In concrete subjected to sufficient moisture, it is possible for potassium and sodium compounds in cement paste to react with silica found in aggregates, causing swelling in the concrete (Obla 2005). This causes cracking in the material over time. Concrete swelling due to an alkali-silica reaction can be measured following ASTM (2015a) C1293. Li and Gress (2006) found that this reaction requires a pH threshold to be met within the mixture. The substitution of fly ash into the mixture at a rate of 25% effectively controlled this reaction. Li and Gress (2006) found that RCA mixtures at this replacement rate met all ASTM limitations for alkali-silica reaction swelling. This is due to the pozzolanic reaction depleting calcium in the mixture, which halts the alkali-silica reaction. A study by Thomas et al.

(2008) agrees that SCM such as fly ash, slag, or silica fume at threshold replacement levels effectively limited the alkali-silica reaction in concrete. The study also suggested the use of portland cement with low alkali content as a method of controlling this reaction in low- to moderate-risk scenarios but suggested a combination of this and SCM incorporation for high-risk cases.

2.3.4 Regulations

The U.S. Army Corps of Engineers (USACE) provides guidance in the Unified Facilities Criteria (UFC) documents concerning the use of recycled concrete aggregates in individual circumstances. These may include pavement surfaces, structures, airfields, heavy-duty pavements, and aggregate base courses. Detailed requirements for usage are as follows.

Concerning concrete pavements, UFC 3-250-04 states that recycled concrete may be crushed and used as both coarse and fine aggregate (USACE 2004a). This assumes the concrete is crushed to a proper gradation following standard ASTM (2018a) C33 guidelines. The UFC requires recycled aggregates to be washed only if they are contaminated with base or subgrade material. If the aggregate comes from D-cracked pavement, it must be crushed to a maximum size of 20 mm. (D-cracked pavement shows damage starting along edges or joints and is caused by coarse aggregates susceptible to freeze–thaw.) Implementing a maximum size prevents D-cracking from occurring when concrete is recycled in the new mixture. Load transfer capacity between interlocked aggregates in a concrete matrix is reduced, but using short concrete panel lengths in construction addresses this issue (USACE 2004b).

UFC 3-250-07 details the procedure for the production and use of crushed concrete aggregate (USACE 2004b). CCCA may be collected from both pavements and structures as long as asphalt, subbase, and subgrade materials are removed as thoroughly as possible and all steel reinforcement is removed. Once recycled aggregates are crushed, stockpiled, and have met all requirements for normal aggregates for the intended purpose, they may be treated as such and are usable as unbound or bound cement-treated bases as per UFC 3-250-04, *Standard Practice for Concrete Pavements* (USACE 2004a).

United Facilities Guide Specifications (UFGS) 32 13 13.06 provides additional information on the use of recycled aggregates in pavements and site

facilities (Naval Facilities Engineering Command 2011). RCA is allowed as a recycled aggregate material if it complies with ASTM (2019a) D6155 and the material's gradation follows ASTM (2018a) C33/C33M. ASTM D6155 addresses these standards for coarse aggregates only. Aggregates for use in airfield and other heavy-duty pavement concrete surfaces covered by UFGS-32 13 14.13 require a thorough source, service record, and petrographic survey of all materials (USACE 2019). Current specifications preclude the use of recycled aggregate for these applications.

UFGS-32 11 23 allows the use of crushed concrete aggregates in the base course for road use (USACE 2017). Recycled materials must meet ASTM gradation requirements for coarse aggregate. Before use in airfield pavement coarse bases, additional alkali-silica reaction testing must be completed in accordance with the Innovative Pavement Research Foundation (2006) IPRF-01-G-002-03-5, which outlines evaluation techniques for recycled materials to be used in airfield pavement base. For both road and airfield uses, subgrade soil must contain 0.3% or lower sulfates to avoid ettringite reactions with recycled aggregates. This is an expansive reaction that causes cracking and swelling. Additionally, airfield projects require a risk assessment to determine the feasibility of using RCA for construction (Air Force Civil Engineer Support Agency 2019). This avoids concrete failures, such as cracking, and damage to adjacent facilities.

Lastly, UFGS-32 11 36.13 also allows the use of recycled aggregates in lean concrete (low cement content) base courses provided it meets the ASTM standards and strength required for the intended use (Naval Facilities Engineering Command 2019). While the range of applications for RCA is extensive within UFC and UFGS guidance, there is not currently guidance for use of RCA at very high replacement percentages. This study makes an initial attempt to rectify this.

3 Materials and Methods

Section 3.1 describes and characterizes the materials used for the research. The materials include different types of binders and aggregates. Section 3.2 presents the test methods employed in optimizing the ternary combinations of binders, and section 3.3 presents the test methods for the concrete mixes.

3.1 Materials

Table 2 provides the raw materials used in this research and their suppliers. The virgin coarse aggregate was diabase trap rock, with 25 mm nominal maximum aggregate size and meeting ASTM (2018a) C33 grading #56. The fine aggregate was river sand, with a fineness modulus of 2.65. The four RCAs were sourced from different areas of New Jersey's northern and southern regions. RCA1 was grading #56, specifically graded by the producer for concrete coarse aggregates. To evaluate different sources of RCA, RCA2 to RCA4 aggregates were collected as a dense-graded aggregate base course (DGABC) with a nominal maximum aggregate size of 25 mm. Being DGABC, RCA2 to RCA4 were passed through a 4.75 mm sieve to remove sand-sized material. This study observed by visual inspection that RCA3 contained aggregates with asphalt. This is likely due to the source of the aggregate, which was not sold as an ingredient for concrete. By manual separation following the residual mortar content procedure, it was determined that RCA3 consisted of 26.8% asphalt by weight.

This study addressed portland cement and four supplementary mineral admixtures: ground, granulated blast furnace slag; Class C fly ash; Class F fly ash; and silica fume. X-ray fluorescence was used to determine the oxide composition of each mineral, as given in Table 3. The test used a Rigaku ZSX Primus II Sequential Wavelength-Dispersive XRF Spectrometer. Based on the oxide composition, the cementitious materials meet their respective ASTM requirements for the type/class of cementitious materials.

Figure 2 provides the gradations for the aggregates used in these experiments. Table 4 provides additional characteristics for each aggregate. The study found residual mortar content for all RCAs following the Abbas et al. (2009) procedure, which was developed to improve the mixture proportioning of concrete containing RCA. By this method, 3 kg of each sample

were fully submerged in a 26% by weight sodium sulfate solution and subjected to six freeze–thaw cycles of 16 hours at −5°C and 8 hours at 80°C. The aggregate samples were washed over a 2.5 mm sieve, and the remaining portion was oven-dried at 105°C and weighed.

Table 2. Materials.

Material	Designation	Source
Portland Cement, Type I	PC	Keystone Cement Co.
Silica Fume	SF	BASF Co.
Ground, Granulated Blast Furnace Slag, Grade 100	GGBFS	Lehigh Hanson, Inc.
Fly Ash, Class C	FAC	Headwaters, Inc.
Fly Ash, Class F	FAF	Salomone Bros., Inc.
Recycled Concrete Aggregate (#56)	RCA1	Salomone Bros., Inc.
Recycled Concrete Aggregate (DGABC)	RCA2	Tilcon NY Inc., Kearny NJ
Recycled Concrete Aggregate (DGABC)	RCA3	A.E. Stone, Inc.
Recycled Concrete Aggregate (DGABC)	RCA4	Tilcon NY Inc., Oxford NJ
Virgin Coarse Aggregate (#56), Trap Rock		F. J. Fazzio, Inc.
Fine Aggregate (Fineness Modulus: 2.65)		F. J. Fazzio, Inc.
Air-Entraining Admixture		Sika Corp.
Water-Reducing Admixture		Sika Corp.

Table 3. Cementitious material oxide composition by percent.

Component	Portland Cement	Class C Fly Ash	Class F Fly Ash	GGBFS	Silica Fume
SiO_2*	19.32	28.13	39.01	25.69	94.23
Al_2O_3	5.77	13.49	22.75	10.35	0.37
Fe_2O_3	2.38	8.97	24.79	0.51	0.32
CaO	61.55	37.30	5.97	56.33	2.23
MgO	2.63	2.87	0.63	3.54	0.27
SO_3	4.56	3.02	1.47	1.76	0.30
Na_2O	0.33	1.00	0.37	0.13	—
K_2O	0.97	0.85	2.98	0.45	1.55
TiO_2	—	2.08	1.43	0.77	—
P_2O_5	—	1.28	0.35	0.02	0.16
ZnO	—	—	0.03	—	0.26
MnO	—	—	—	0.22	0.09
Others	2.49	1.01	0.22	0.24	0.13

* For a full list of the spelled-out forms of the chemical elements used in this document, please refer to *U.S. Government Publishing Office Style Manual*, 31st ed. (Washington, DC: U.S Government Publishing Office, 2016), 265, https://www.govinfo.gov/content/pkg/GPO-STYLEMANUAL-2016/pdf/GPO-STYLEMANUAL-2016.pdf.

Figure 2. Aggregate gradations.

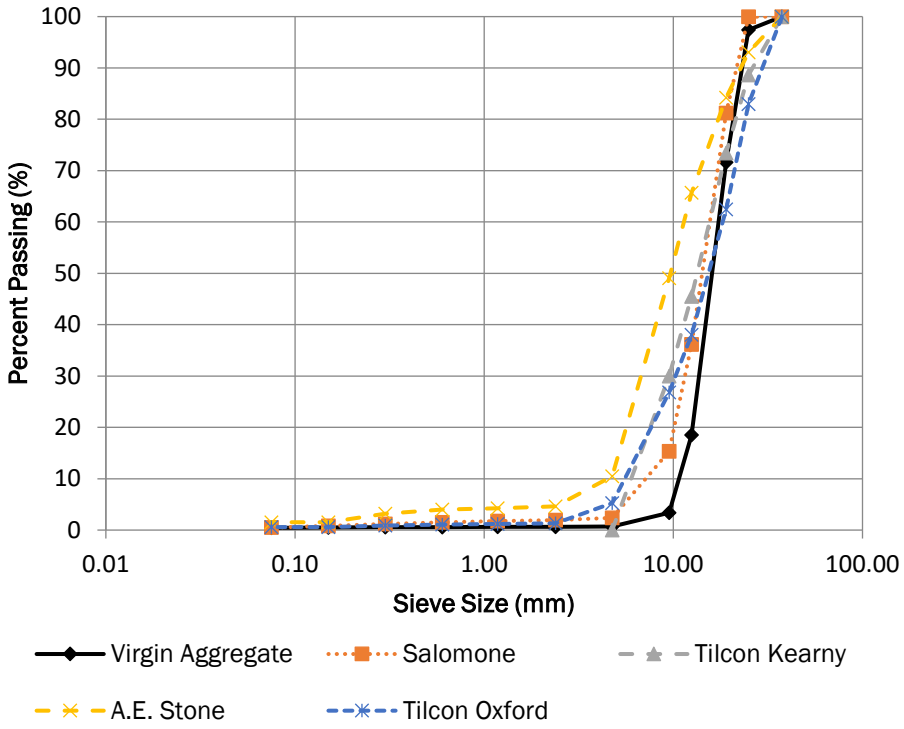

Table 4. Aggregate properties.

Sample Type	Bulk Specific Gravity, Saturated Surface Dry	Absorption (%)	Residual Mortar Content (%)
RCA, Salomone	2.49	4.71	42.00
RCA, Tilcon Kearny	2.32	4.20	34.83
RCA, A.E. Stone	2.35	3.50	34.83
RCA, Tilcon Oxford	2.31	5.71	27.50
Virgin Coarse Aggregate	2.77	0.20	-
Fine Aggregate	2.62	1.04	-

3.2 Blend Optimization

3.2.1 Mortar compressive strength

This study evaluated the performance of 25 unique blends of cementitious materials to determine the optimal blend of cementitious materials to use. Mixture proportions, listed in Table 5, were determined by percentage mass of total cementitious material to create a design matrix. The notation includes each mineral component followed by that component's percentage by mass. For example, PC75FAC25 denotes a binder blend of 75% portland cement and 25% Class C fly ash.

The study used maximum replacement rates of 30% slag, 25% Class C fly ash, 25% Class F fly ash, and 5% silica fume. These limits were based on recommended practice from NJDOT and from a previous study conducted by Taylor (2014), who suggests a maximum portland cement replacement rate of 60%. Rupnow (2012) also observed improved physical properties for some combinations of ternary blended cements at 50% portland cement replacement and recommended a maximum portland cement replacement rate of 70%. The intermediate replacement rates chosen were equal intervals between the minimum (0%) and the maximum replacement rates used for this study. Thus, one mix was portland cement, four were binary blended cements, and the remainder were ternary mixes.

Table 5. Tested mixture matrix by percent.

Mixture	Portland Cement (PC)	Class C Fly Ash (FAC)	Class F Fly Ash (FAF)	Silica Fume (SF)	Blast Furnace Slag (GGBFS)
PC100	100	0	0	0	0
PC75FAC25	75	25	0	0	0
PC75FAF25	75	0	25	0	0
PC95SF5	95	0	0	5	0
PC70GGBFS30	70	0	0	0	30
PC45FAC25GGBFS30	45	25	0	0	30
PC55FAC25GGBFS20	55	25	0	0	20
PC65FAC25GGBFS10	65	25	0	0	10
PC57.5FAC12.5GGBFS30	57.7	12.5	0	0	30
PC67.5FAC12.5GGBFS20	67.5	12.5	0	0	20
PC77.5FAC12.5GGBFS10	77.5	12.5	0	0	10
PC70FAC25SF5	70	25	0	5	0
PC72.5FAC25SF2.5	72.5	25	0	2.5	0
PC82.5FAC12.5SF5	82.5	12.5	0	5	0
PC85FAC12.5SF2.5	85	12.5	0	2.5	0
PC45FAF25GGBFS30	45	0	25	0	30
PC55FAF25GGBFS20	55	0	25	0	20
PC65FAF25GGBFS10	65	0	25	0	10
PC57.5FAF12.5GGBFS30	57.7	0	12.5	0	30
PC67.5FAF12.5GGBFS20	67.5	0	12.5	0	20
PC77.5FAF12.5GGBFS10	77.5	0	12.5	0	10
PC70FAF25SF5	70	0	25	5	0
PC72.5FAF25SF2.5	72.5	0	25	2.5	0
PC82.5FAF12.5SF5	82.5	0	12.5	5	0
PC85FAF12.5SF2.5	85	0	12.5	2.5	0

This study used 50 mm mortar cubes following ASTM (2016a) C109. The mortar water-to-binder ratio was 0.45, and the ratio of the binder to fine aggregate by mass was 0.50. Triplicates were produced for each mix to be tested for compressive strength at 28 and 56 days. Mixtures with SCMs typically continue to gain strength after 56 days. In the study conducted by Rupnow (2012), tests were conducted up to 90 days. However, the strengths that were compared did not change relative to one another from 56 days. Hence, for this study, 56 days was sufficient to identify which combinations would produce the highest strengths.

Batches were mixed and molded following ASTM C109. Cube specimens in molds were stored in a moist closet for 24 hours, at which point cubes were demolded and placed in a lime-saturated water curing bath. Prior to testing, cubes were removed from the bath, surface dried, and cleared of any debris. The compression testing configuration conformed to ASTM C109 at a loading rate of 1350 N ± 450 N per second. Peak load at sample failure was recorded for each test.

3.2.2 Isothermal calorimetry

This study used isothermal calorimetry to measure the energy release of paste samples during the hydration process and identified patterns in the heat of hydration of cement mixtures containing different supplementary materials. Kim (2010) also presented that the test results correlate with the gain and ultimate strength of concrete. Total heat of hydration is an indicator of the extent of the reaction in a mix, and thus the analysis of these reactions through calorimetry is effective in explaining the strength and durability of individual ternary mixes.

A high-precision isothermal calorimeter meeting ASTM (2017d) C1679 was used to measure the energy released during hydration. The machine was calibrated using a manufacturer-supplied calcium sulfate hemihydrate. The testing of the cementitious pastes followed ASTM C1679. All test samples consisted of 50 g of cementitious material proportioned by mass according to Table 5 with a water-to-binder ratio of 0.50. Prior to testing, materials were stored at 20°C for 24 hours to minimize the temperature differential at the beginning of testing. Samples were hand mixed for 45 seconds with a plastic stirrer in manufacturer-provided sample containers. The date and time were recorded at the beginning of mixing, approximated to the nearest minute. Two tests were conducted simultaneously, and heat flow measurements were collected once per minute for 72

hours. The cumulative heat of hydration (joules) and power (watts/gram cement) were recorded for each test.

3.3 Ternary blended concrete with RCA replacement

Mixtures were prepared to assess the performance of RCA in a ternary blended concrete. A mixture with only portland cement as the binder and no RCA substitution was prepared as a control. Then, a mixture with 30% coarse aggregate replacement by RCA from Salomone was prepared to identify the effects of RCA replacement. Third, a 30% replacement mixture using the ternary blended binder was produced to assess the performance alterations due to the proposed binder blend. Lastly, a mixture was prepared using the ternary-blended binder at 50% Salomone RCA replacement to assess high replacement strength and durability. For the additional recycled aggregate sources, mixes were produced with 50% replacement, 50% replacement and ternary blended binder, and 100% replacement and ternary blended binder. These sources were tested at higher replacement rates to determine the feasibility of much higher amounts of RCA in concrete.

For each mix that included a recycled aggregate, the RCA portion of the coarse aggregate was presoaked 24 hours before mixing to saturate the aggregate and to minimize the effects of high porosity on fresh mix properties. Chapter 4 shows all mixture proportions. Table 6 provides a schedule of conducted tests and applicable testing standards. In all cases, fresh and hardened concrete test procedures follow the addressed ASTM standard. Compressive strength, elastic modulus, and resistivity were tested at 3, 7, 14, 28, 56, and 90 days. Modulus of rupture was tested at 28 and 90 days. Concrete cylinders were cured in a lime-water bath in a climate controlled indoor space.

Fresh properties were tested to ensure mixtures were comparable. In all cases, the slump was controlled via the addition of a water reducer to maintain a target of 50 ± 25 mm. Control for workability ensured that the hardened properties of each batch could be compared to the assumption that fresh mixture behavior is similar. Target air-void content was 6.5% ± 1.5% to promote proper durability to freeze–thaw cycling. Unit weight and setting time were recorded for logistical purposes.

Table 6. Ternary blend recycled concrete aggregates (RCA) test schedule.

Property	Test Method
Fresh Concrete Properties	
Slump	ASTM (2015b) C143
Air Content	ASTM (2017e) C231
Air-Voids System	AASHTO (2013) T 348
Unit Weight	ASTM (2017f) C138
Setting Time	ASTM (2016b) C403
Hardened Concrete Properties	
Compressive Strength	ASTM (2018b) C39
Electrical Resistivity	ASTM (2012b) C1760
Alkali-Silica Reaction	ASTM (2013b) C1567
Modulus of Rupture	ASTM (2018e) C78
Elastic Modulus	ASTM (2014b) C469
Drying Shrinkage	ASTM (2017g) C157
Resistance to Cyclic Freeze–Thaw	ASTM (2012a) C666

4 Results and Analysis

4.1 Binder optimization

4.1.1 Mortar cube strength

Figure 3 shows the results for average 28-day and 56-day mortar cube compressive strength. In the figure, the bars represent (*from left*) compressive strength of mortar with only a portland cement binder (colored red), then binary binders (in blue), while the remaining results are from ternary binders. The ternary binders are grouped by Class C fly ash with slag (FAC-GGBFS, purple), Class C fly ash with silica fume (FAC-SF, green), Class F fly ash with slag (FAF-GGBFS, orange), and Class F fly ash with silica fume (FAF-SF, yellow), all with portland cement. Full tabulated strength data is available in Appendix A.

Comparing the binary combination results to the control mixture with only portland cement (PC), replacement of PC with Class C fly ash or silica fume is shown to effectively increase compressive strength at 28 and 56 days. On the other hand, replacement of PC with Class F fly ash or GGBFS has a slight lowering effect on compressive strength at 25% and 30% replacement, respectively.

Comparing the ternary combination results to the PC results, the ternary combinations with Class C fly ash produce higher strengths than PC alone, except for PC45FAC25GGBSF30, which has the least amount of portland cement in the group. This may indicate reduced performance at lower fractions. With the Class F fly ash and GGBFS combination, the compressive strength is less than the strength of plain portland cement with Class F fly ash at 25% replacement, except for PC65FAF25GGBFS10, which has a similar 56-day strength to PC 56-day strength. This indicates a resource depletion in the hydration reaction when combining high fractions of Class F fly ash and slag. Based on the chemical composition of the materials used, 45% to 65% PC would not be able to produce enough calcium hydroxide after hydration to fully react with 25% FAF. This is based on a calculation with a 1.63 calcium-to-silica ratio and calculation that 100 grams of the PC used will produce 27.7 grams of calcium hydroxide.

Figure 3. Mortar compressive strength results for 28-day (*solid bars*) and 56-day (*hatched bars*) strength for mixtures tested, with control mixtures in *red*, binary mixtures in *blue*, PC-FAC-GGBFS blends in *purple*, PC-FAC-SF blends in *green*, PC-FAF-GGBFS mixtures in *orange*, and PC-FAF-SF mixtures in *yellow*.

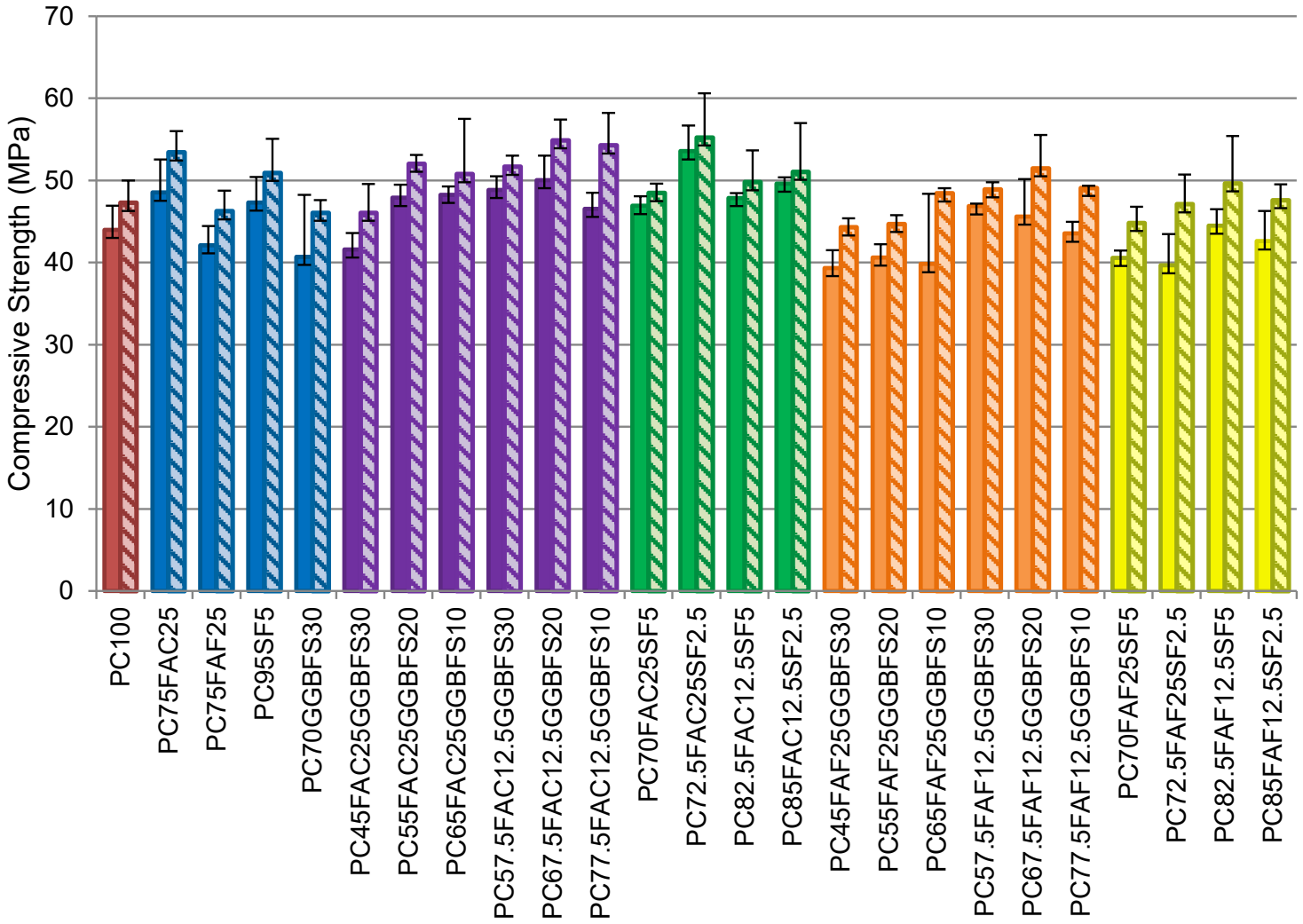

For the Class F fly ash and silica fume combination, the compressive strengths are lower or equal in strength to PC strength, except for PC82.5FAF12.5SF5, which has a higher 56-day compressive strength compared to PC compressive strength. As with Class F fly ash and slag, this may indicate that Class F fly ash and silica fume compete for similar insufficient resources in the hydration reaction. Based on the PC composition, it would need the 82.5% PC to produce sufficient calcium hydroxide for the pozzolanic reaction of 5% SF.

4.1.2 Isothermal calorimetry

Calorimetry tests were conducted on all binder combinations listed in Table 5. Figures 4 through 8 present the heat of hydration curves plotted as the thermal power emitted by the binder hydration and reactions over time. The figures are grouped by blend compositions.

The first group includes Type I cement paste and four binary blended binders (Figure 4). The cement paste heat of hydration curve shows the main peak in heat at 11.5 hours and a sulfate depletion point at 16 hours. The initial thermal peak is due to a C3S hydration reaction. The peak heat of hydration produced by cement is higher than that of the binary blends, the hydration of portland cement being the main source of heat. The pattern of the heat of hydration with 5% silica fume is similar to the cement curve, only that lower values were produced. The curve for a binary blend with 25% Class F fly ash has a lower peak heat than the cement paste, which peaks at a similar time. It has a secondary peak in thermal activity at 28 hours, which is due to the C3A reaction (Kosmatka and Wilson 2016).

However, the heat of hydration curve for the binder with 25% Class C fly ash had its main peak 4 hours after the portland cement paste. Its second peak is also higher than its main peak. With the paste containing 30% GGBFS, the main peak is lower than the main peak of the paste with only portland cement but occurs at a similar time. Its second peak is slightly lower than its main peak, much more pronounced than the Class F fly ash curve, and not as high as the Class C fly ash curve. Comparing the presence of GGBFS and Class C fly ash in the binder indicates that the GGBFS has more hydrating calcium silicates while Class F fly ash had more calcium aluminates reacting during the early age. This subset of calorimetry results shows how the heat of hydration is reduced by mineral admixtures and how pozzolanic admixtures alter the reaction by delaying or extending

peak thermal output. Note that the heat of hydration curves of the ternary blends are combinations of the heat of hydration of the binary blends. The patterns of the curves are additive, which indicates that the effects of combining SCMs are also additive, implying little or no interaction between the SCMs.

Figure 4. Plot of thermal power vs. time of Type I cement and binary binders.

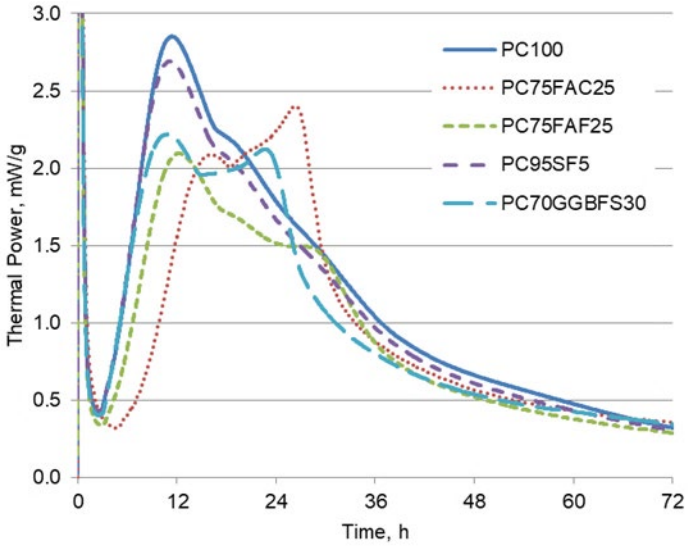

Figure 5 presents results for ternary blends of Class C fly ash and GGBFS. In cases of very high replacement rates, the secondary reactions shown by the second peak overtake the initial C2S and C3S reactions by a significant margin. This manifests as a delayed strength gain in the curing process. Low replacement mixes (see PC77.5FAC12.5GGBFS10) maintain a more significant C2S, C3S reaction. Figure 6 shows blends of Class F fly ash and GGBFS. These mixes are characterized by a markedly lower peak thermal output with respect to other mixes as a result of high replacement rates with Class F fly ash in addition to significant replacement by pozzolanic materials.

Figure 5. Plot of thermal power vs. time of ternary blends of PC-FAC-GGBFS.

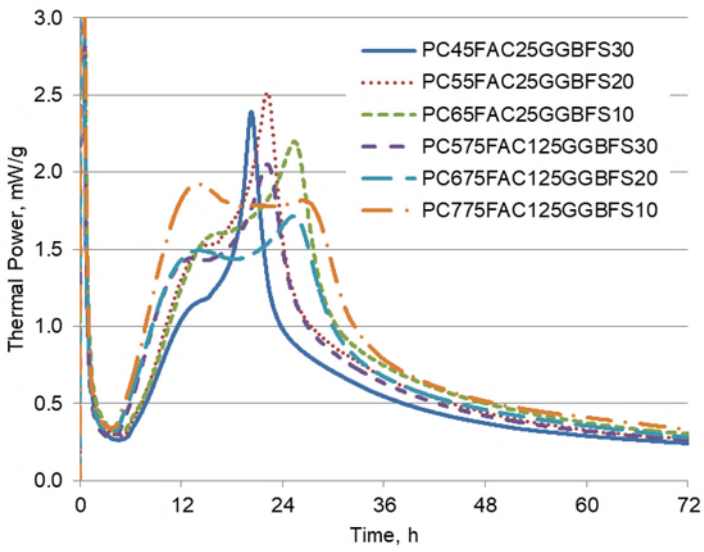

Figure 6. Plot of thermal power vs. time of ternary blends of PC-FAF-GGBFS.

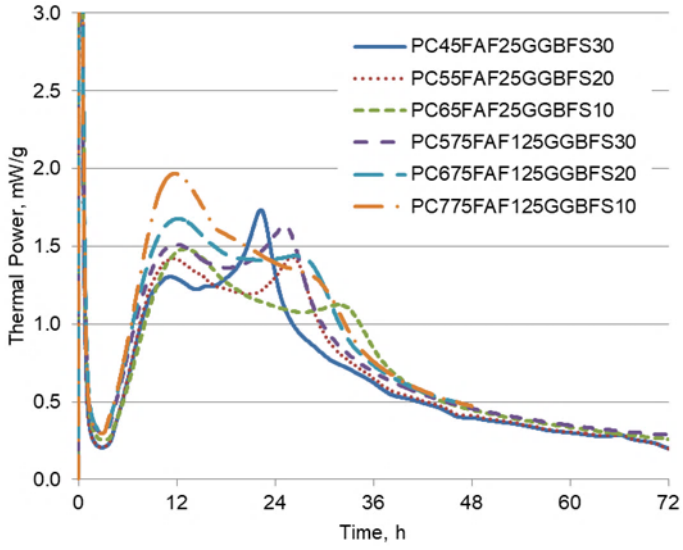

Figure 7 shows mixes containing Class C fly ash and silica fume. Shown previously, high replacement with Class C fly ash favors the C3A reaction. There is no apparent interaction with silica fume in this ternary mixture. Figure 8 gives Class F fly ash and silica fume combinations. These are marked by low thermal peaks and further-reduced heat with an increase in either supplementary material.

Figure 7. Plot of thermal power vs. time of ternary blends of PC-FAC-SF.

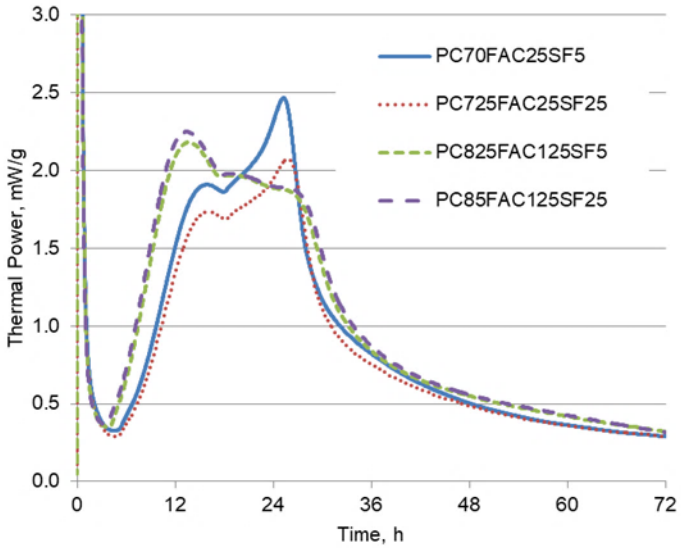

Figure 8. Plot of thermal power vs. time of ternary blends of PC-FAF-SF.

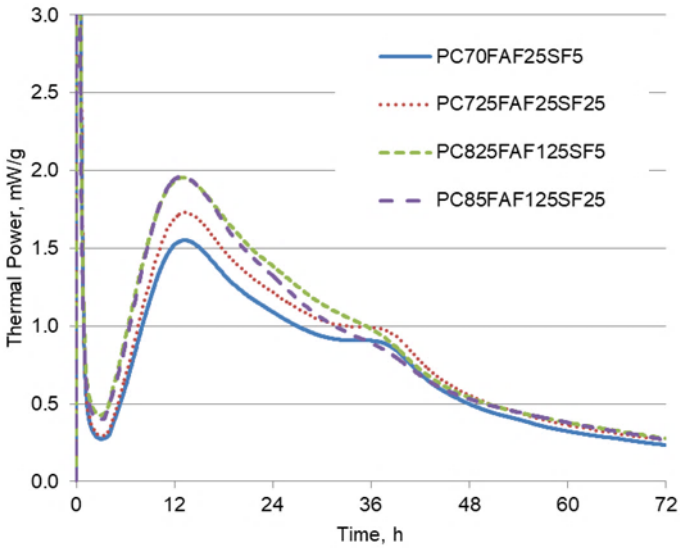

The total heat of hydration is determined from thermal power plots by integrating the area under the curve. Figure 9 compares all conducted tests. There is a consistent trend of reduced heat of hydration with an increase in SCM use for ternary blended cements. However, the total heat did not necessarily correlate with peak thermal activity. As such, it is not clear that there is a reduced completion of the reaction in low-heat blends. It is also possible that total heat evolution was simply retarded in cases of high SCM

replacement percent. From the binary blends, GGBFS has greater reactivity compared to the fly ashes. Even with greater portland cement replacement, the paste with GGBFS released more heat compared to the paste with fly ash. In the Class C fly ash and GGBFS combinations, the GGBFS complements the fly ash. In the Class F fly ash and GGBFS combination, the heat of hydration indicates little or no additional heat from the combination of SCM; with about the same level of total replacement, a higher proportion of GGBFS will produce a higher amount of heat of hydration relative to Class F fly ash. In silica fume and fly ash combinations, Class C fly ash with silica fume tends to have a higher heat of hydration. A lower proportion of silica fume to the amount of Class C fly ash seems to favor reducing the heat of hydration, while a high proportion of silica fume to Class F fly ash seems to increase the heat of hydration.

Figure 9. Total heat of hydration for all blends.

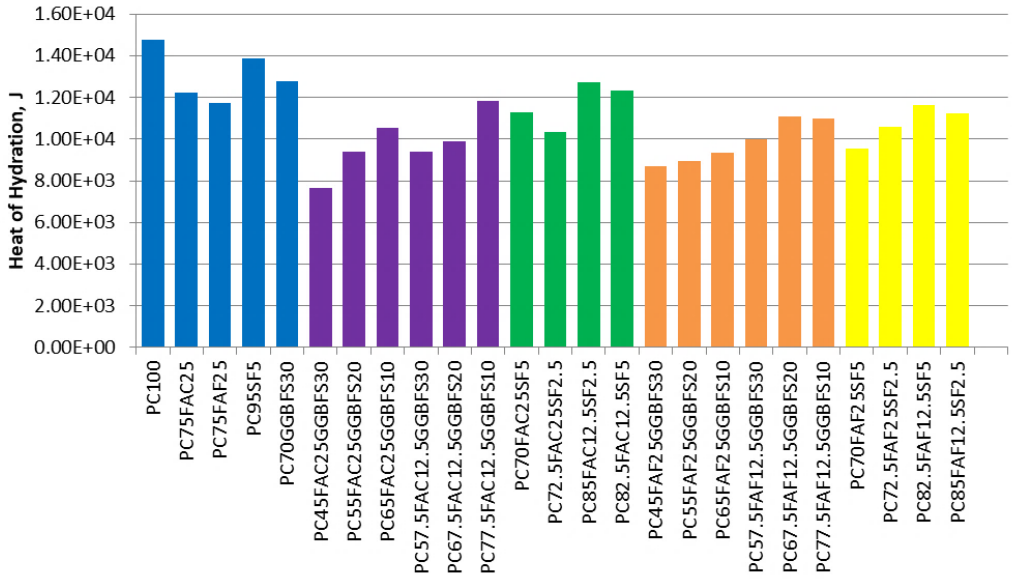

4.1.3 Statistical analysis

This study analyzed the compressive strength data by using statistical analysis software, JMP, to determine the statistical significance of cementitious elements in each blend. Surface plots were made to model the relationship between the replacement rates of supplementary cementitious materials and the predicted compressive strength from the data collected in the mortar cube tests. The x- and y-axes each represent the percent replacement of one SCM being analyzed and range from 0% to the highest tested replacement rate along each of these axes. Thus, the origin point represents no replacement (Type I portland cement), and data points that

lie on an axis represent binary blends with replacement by only a single SCM. Four plots were created, representing the studied combinations of SCMs (Figures 10–13). Optimal mix designs were selected based on the 56-day strength analysis as this closest represents the ultimate strength of the mix. The 56-day strength better captures the ultimate strength of the mixtures due to later reactions of binders with supplementary cementitious materials. The strengths of the mixtures increased beyond 28-day strength, but the relationship of the strength between mixtures of the same binder type does not change, as observed in Figure 3.

Table 7 is a result of this binder optimization analysis. These results include optimal SCM replacement rates for each ternary blend within the studied percent replacement. They also include total replacement rates and predicted mortar compressive strengths for each combination.

Appendix A lists the compressive strength data and predicted strength for the different ternary blend combinations. In the case of the PC-FAF-SF, an optimum combination excludes FAF, which makes it a binary binder. Among the three SCM combinations in Table 7 that are ternary combinations, FAC-GGBFS has the highest strength and highest total heat of hydration at 72 hours, curing within the studied range of percent replacement of Type I portland cement. FAC-SF has the lowest total heat of hydration but is second highest in strength. The predicted 56-day compressive strength of the optimal mixes was compared to the experimentally found compressive strength at 56 days. The models have a root-mean-square error range of 3.92 to 2.16 MPa to its predictions.

Table 7. Optimized ternary blends.

SCM	PC (%)	FAC (%)	FAF (%)	GGBFS (%)	SF (%)	% SCM by Weight	Predicted 56-Day Strength (MPa)	Tested 56-Day Strength (MPa)	RMSE of prediction model (MPa)	Total Heat of Hydration for 50 g (kJ)
FAF-SF	95	—	0	—	5	5	51.1	47.3	3.42	13.86
FAF-GGBFS	77.5	—	12.5	10	—	22.5	50.7	49.1	2.16	11.0
FAC-SF	72.5	25	—	—	2.5	27.5	52.5	55.3	3.92	10.36
FAC-GGBFS	77.5	12.5	—	10	—	22.5	55.24	54.3	3.23	11.81

Figure 10. Class F fly ash and silica fume data surface plot.

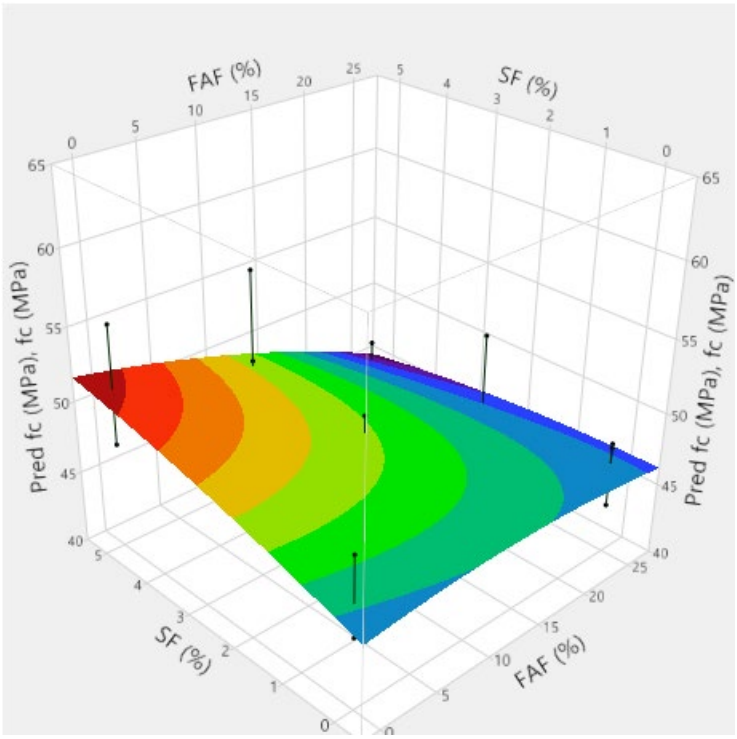

Figure 11. Class F fly ash and slag data surface plot.

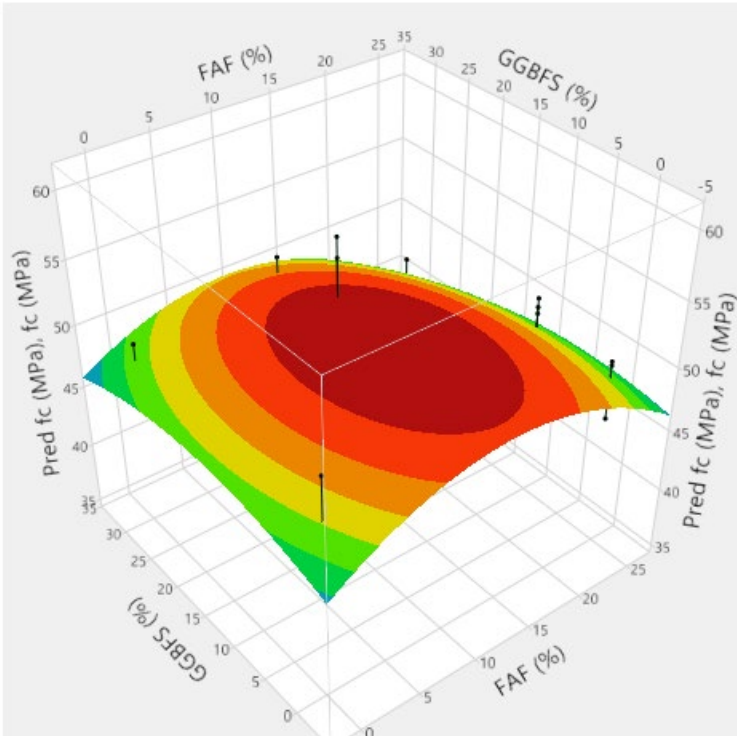

Figure 12. Class C fly ash and silica fume data surface plot.

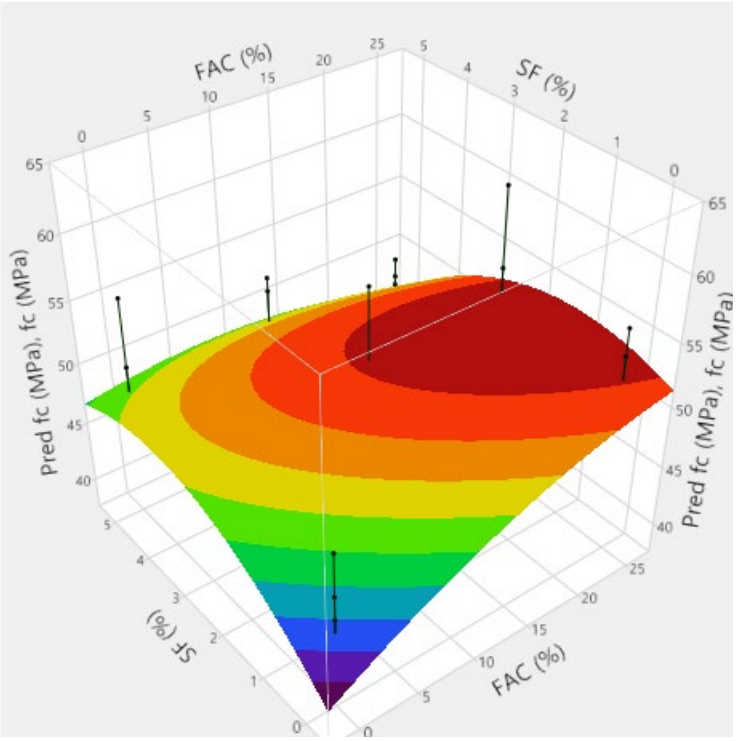

Figure 13. Class C fly ash and slag surface plot.

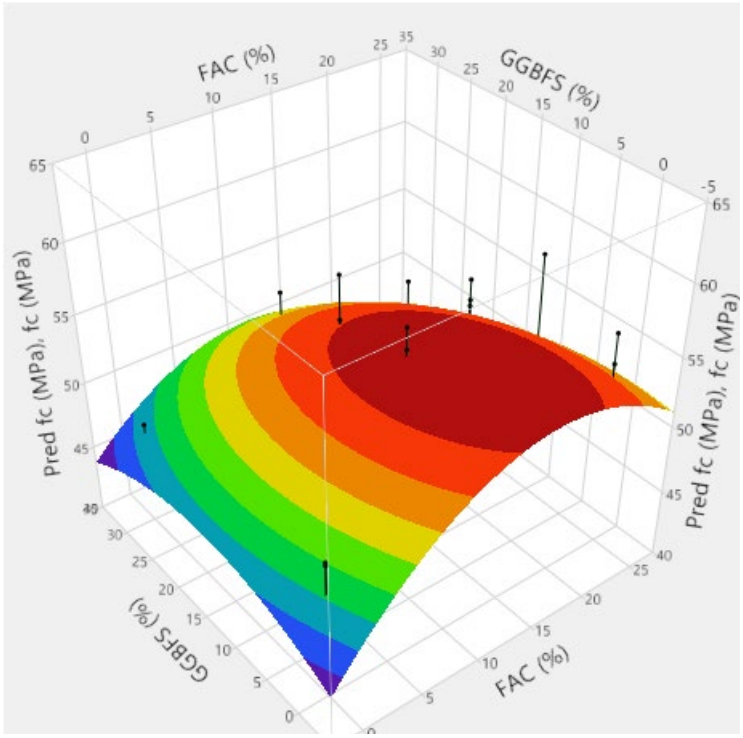

4.1.4 Ternary blended concrete

Additional testing of ternary blended concrete used the optimized proportioning in Table 7. Triplicate 100 mm diameter concrete cylinders for each of the three ternary binder proportions were tested (FAF-GGBFS, FAC-SF, FAC-GGBFS). Table 8 gives the mixture proportions used. Proportions for a comparable control mix are available in Table 10.

Table 8. Mixture proportions of ternary blended concrete per cubic meter.

Material	PC77.5FAF12.5GGBFS10 Mix 1	PC72.5FAC25SF2.5 Mix 2	PC77.5FAC12.5GGBFS10 Mix 3
Cement (kg)	204.8	247.0	240.8
Fly Ash (kg)	44.5	88.2	53.5
Slag (kg)	106.9	-	62.4
Silica Fume (kg)	-	17.6	-
Water (kg)	160.3	158.8	160.5
Sand (kg)	866.9	866.9	866.9
Virgin Aggregate (kg)	916.5	916.5	916.5
Air-Entraining Agent (ml/100 kg)	117	143	130

The fresh and hardened mixture properties for each of the three blends were recorded. All points in Figures 14 through 16 were from average measurements of three replicate specimens. Full tabulated data is available in Appendix A, tables A-3 through A-6. Table 9 shows the recorded fresh mixture properties for each of these concrete blends. Slump and air content were maintained for all blends. This indicated that none of the proposed ternary blends have a significant effect on workability or air content. Table 9 also provides data recorded with an air-void analyzer (AVA). This data includes calculations of air content, specific surface (a ratio of surface area to volume), and spacing factor (or the maximum distance to an air void in the matrix). Due to the stiffness of the mixtures, samples were not necessarily fully broken apart by the stirring mechanism, which may have introduced error into the AVA-measured percent air.

Table 9. Ternary blended concrete fresh properties.

Property	PC77.5FAF12.5GGBFS10	PC72.5FAC25SF2.5	PC77.5FAC12.5GGBFS10
Slump (mm)	25	38.1	31.75
Air Content (%)	5.50	5.50	5.00
Unit Wt. (kg/m^3)	2376.5	2381.3	2300.2
Mix Temp (°C)	18	18	18
Air-Void Analyzer			
% Air Voids in Concrete	2.3	3.1	2.9
Specific Surface (mm^{-1})	17.0	15.8	19.1
Spacing Factor (mm)	0.50	0.47	0.49

Figures 14 through 16 provide the evolution of strength, electrical resistivity, and alkali-silica reaction for each blend. All mixtures have similar late-age strength and resistivity values. PC77.5FAC12.5GGBFS10 had the slowest strength-gain trend; however, ultimately all mixtures performed nearly identically. The similarity in strength between these blends when tested as concrete comes from a few sources. First, concrete cylinders were mixed in a drum mixer, which has higher mixing energy than the process used to mix mortar cubes and may provide better mix consistency or uniformity. Additionally, the inclusion of coarse aggregates introduces interfacial transition zones (considered weak portions in a hardened concrete mixture) and anisotropy to the mix, which may be the controlling factor for failure behavior rather than binder strength. Likewise, alkali-silica reactivity is similar for all mixtures. The alkali-silica reaction testing was conducted for up to 30 days to assess late-age trends in reactivity, which is beyond the 16-day standard method indicated by ASTM (2014c) C1260. All samples maintained low-risk compliance at the 30-day testing mark, based on ASTM (2014c) C1260.

To select a blend for RCA testing, mortar cube analysis and concrete physical properties were considered. The study found that PC77.5FAC12.5GGBFS10 was the optimal ternary binder blend based on both higher predicted strength values from the mortar tests and the results from this concrete testing.

Figure 14. Ternary blended concrete compressive strength.

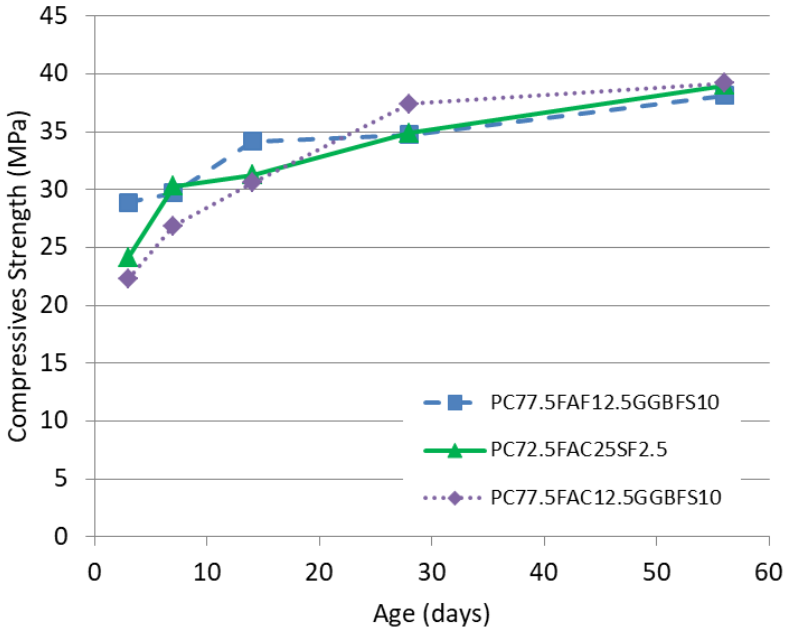

Figure 15. Ternary blended concrete electrical resistivity.

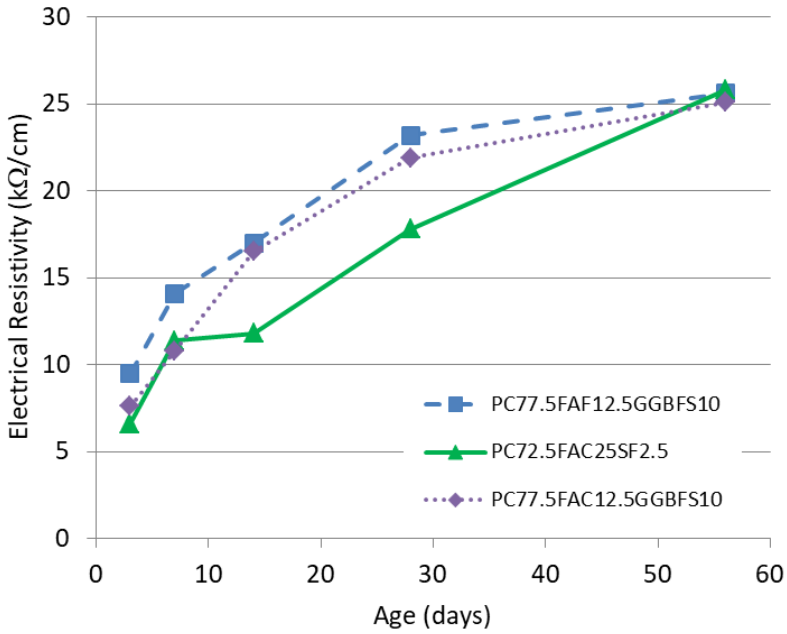

Figure 16. Ternary blended concrete alkali-silica reaction.

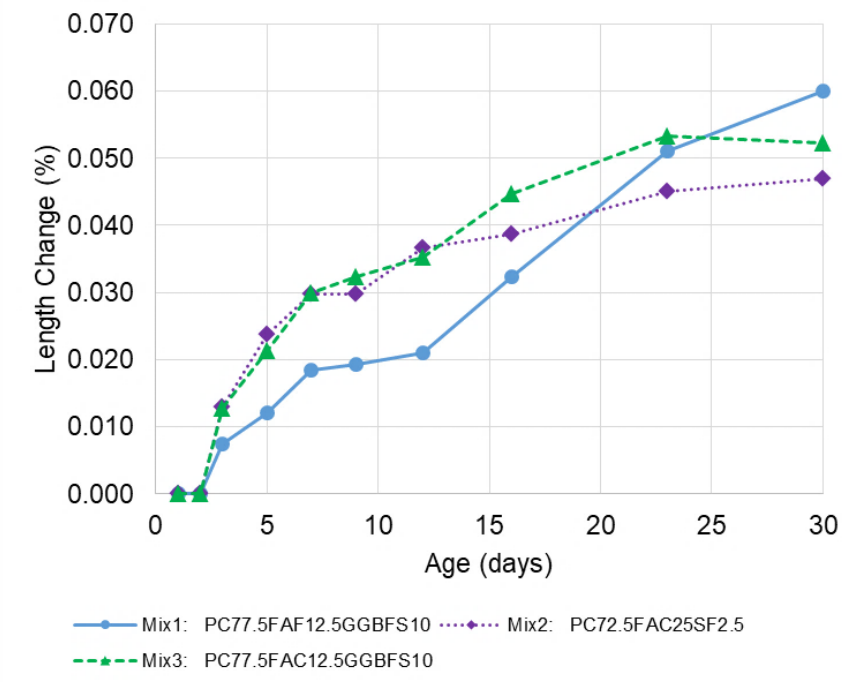

4.2 Ternary blended concrete with RCA replacement

Table 10 shows proportions per cubic yard for each mixture with and without RCA and SCM. In this table, NC (normal concrete) describes the control mix with only virgin aggregates and portland cement binder. RCA1-30 indicates that 30% of the coarse aggregate in the mix was replaced with RCA from Salomone. RCA1-30T indicates that the ternary blended binder was then implemented for the third iteration at 30% RCA. RCA1-50T indicates that recycled aggregate content was then increased to 50%. RCA2, RCA3, and RCA4 indicate mixes using Tilcon Kearny, A.E. Stone, and Tilcon Oxford recycled concrete coarse aggregates, respectively.

Table 11 gives the recorded fresh properties. For all mixes, the slump was maintained at 25 mm ± 6 mm. Mixtures with increasing content of RCA1 and RCA4 required an increasing dosage of high-range water reducer (HRWR) to maintain the same slump. The main contributing factor to this would be the mixture temperature. Mixtures with RCA2 and RCA3 did not have the same need of HRWR and had lower mix temperatures. Air content met or exceeded the target of 5%–8% in all mixtures. AVA analysis indicated much lower air content; however, for all AVA tests, the mortar samples were not properly broken apart during mechanical stirring. There was a slight pattern of loss of slump with an increasing RCA replacement

rate. This may be in part due to an increased mixing temperature and a higher amount of finer materials in RCA compared to the natural coarse aggregate. A higher dose of water reducer was required to counteract the loss of slump at constant water content across all mixtures. The increase in RCA content also increased air content and reduced mixture unit weight. Variations in mix temperature were due to the outdoor mixing environment and may have contributed to variations in setting time. This likely does not extend to hardened properties, however, as cylinders were cured in a room-temperature climate-controlled space after mixing.

Figures 17 through 20 show the progression of settings for each mixture. There is a clear increase in setting time of approximately 45 to 60 minutes when supplementary cementitious materials are included in the binder.

Table 10. Ternary blended RCA mixture proportions.

Material	Mix 4 NC	Mix 5 RCA1-30	Mix 6 RCA1-30T	Mix 7 RCA1-50T	Mix 8 RCA2-50	Mix 9 RCA2-50T	Mix 10 RCA2-100T	Mix 11 RCA3-50	Mix 12 RCA3-50T	Mix 13 RCA3-100T	Mix 14 RCA4-50	Mix 15 RCA4-50T	Mix 16 RCA4-100T
Cement (kg)	389.7	389.7	298.4	298.4	389.7	298.4	298.4	389.7	298.4	298.4	389.7	298.4	298.4
Fly Ash C (kg)	-	-	48.1	48.1	-	48.1	48.1	-	48.1	48.1	-	48.1	48.1
Slag (kg)	-	-	38.5	38.5	-	38.5	38.5	-	38.5	38.5	-	38.5	38.5
Water (kg)	155.9	155.9	154.0	154.0	155.9	154.0	154.0	155.9	154.0	154.0	155.9	154.0	154.0
Sand (kg)	864.6	864.6	864.6	864.6	864.6	864.6	864.6	864.6	864.6	864.6	864.6	864.6	864.6
Natural Aggregate (kg)	914.1	639.9	639.9	457.1	457.1	457.1	-	457.1	457.1	-	457.1	457.1	-
RCA (kg)	-	246.5	246.5	410.9	382.8	382.8	765.6	387.7	387.7	775.5	381.3	381.2	762.3
AEA (ml/100 kg)	260.5	260.5	260.5	260.5	260.5	260.5	260.5	260.5	260.5	260.5	260.5	260.5	260.5
HRWR (ml/100 kg)	-	188.8	198.6	439.6	384.2	195.4	0.0	0.0	81.4	0.0	97.7	267.0	325.6

Table 11. Ternary blended RCA fresh properties.

Property	Mix 4 NC	Mix 5 RCA1-30	Mix 6 RCA1-30T	Mix 7 RCA1-50T	Mix 8 RCA2-50	Mix 9 RCA2-50T	Mix 10 RCA2-100T	Mix 11 RCA3-50	Mix 12 RCA3-50T	Mix 13 RCA3-100T	Mix 14 RCA4-50	Mix 15 RCA4-50T	Mix 16 RCA4-100T
Slump (mm)	32	25	25	19	19	32	32	19	19	22	25	25	25
Air Content (%)	6.0	6.0	6.0	7.0	7.0	6.00	6.00	7.00	7.20	5.50	6.00	7.00	5.50
Unit Wt. (kg/m^3)	2322	2338	2338	2275	2291	2307	2211	2275	2275	2259	2275	2259	2227
Mix temp (°C)	24	25	24	31	16	13	12	15	13	13	18	22	28
Air-Void Analyzer													
Air (% Concrete volume)	1.1	1.5	1.9	3.1	3.5	8.0	7.1	1.8	3.6	5.3	1.0	0.6	0.4
Specific Surface (mm^{-1})	13.0	9.3	12.7	11.6	28.9	45.2	75.9	25.9	38.0	54.1	84.5	26.2	18.0
Spacing Factor (mm)	0.88	1.10	0.65	0.61	0.27	0.11	0.07	0.37	0.17	0.10	0.16	0.56	0.94
Setting Time													
Initial (h:min)	3:30	3:20	5:15	4:55	4:40	6:00	5:40	4:15	4:10	5:50	3:33	4:35	4:40
Final (h:min)	5:15	5:10	6:35	6:30	6:40	7:40	7:20	6:20	6:10	7:25	4:35	6:20	6:25

Figure 17. NC and RCA1 setting time.

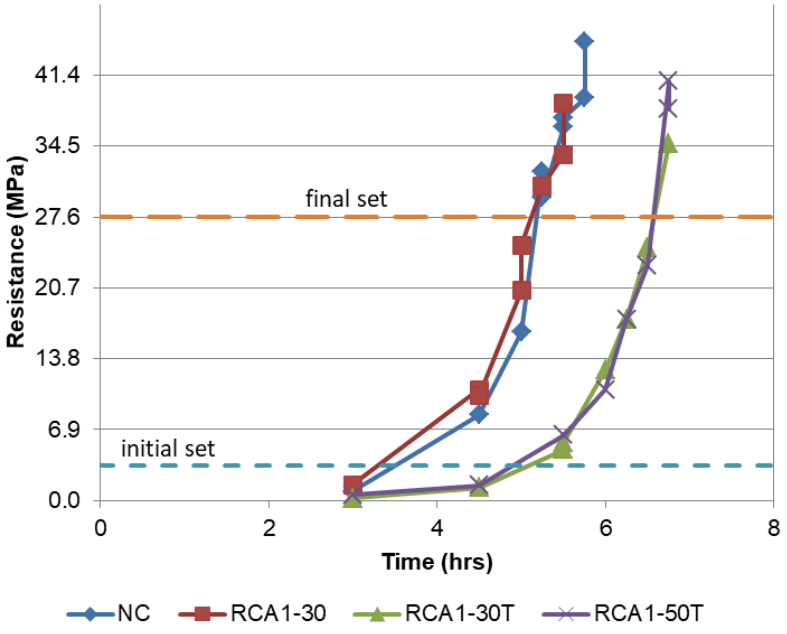

Figure 18. RCA2 setting time.

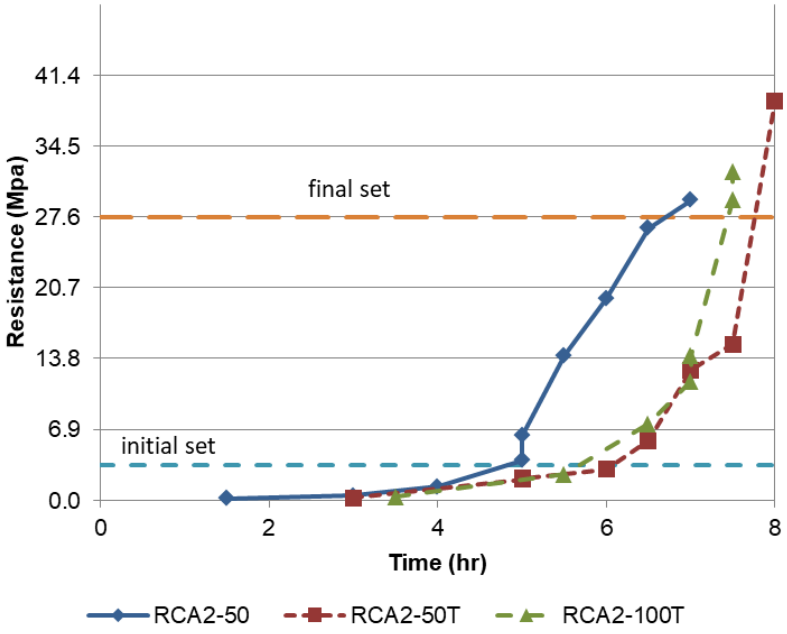

Figure 19. RCA3 setting time.

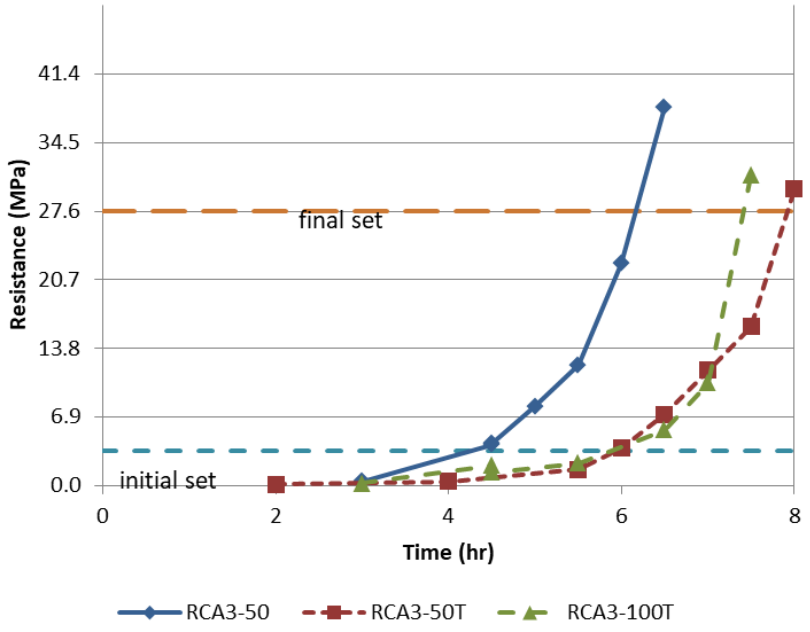

Figure 20. RCA4 setting time.

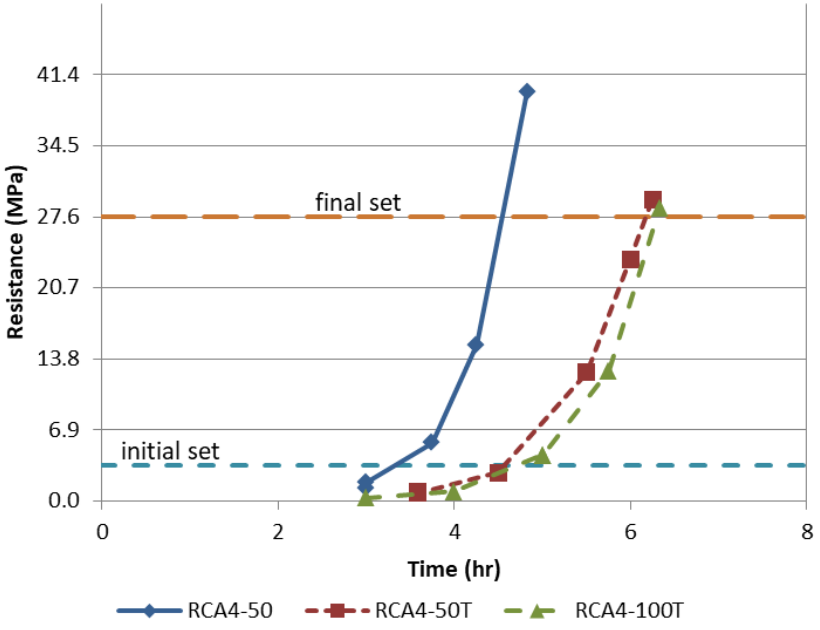

Trends in hardened properties for each mixture were analyzed. All tabulated data is available in Appendix A. Figures 21 through 24 show the compressive strength of the mixtures batched over time. For RCA1, there is an increase in compressive strength at up to 50% recycled aggregate replacement. At 30% replacement, the ternary blended mixture had reduced early

strength. However, late-age strength appeared to increase after 56 days in ternary blends. This increase in strength with RCA1 content may be attributed to the quality of the RCA. For the other RCAs tested, ternary-blended binder marginally improved compressive strength at 50% replacement. In all cases, strength reduced significantly at 100% RCA use. Additionally, in all cases except RCA3, 50% replacement mixtures reached 35 MPa at 28 days. Unlike the other mixtures, RCA3 was contaminated with asphalt. The asphalt residue tended to be much weaker than aggregate or binder present in the mixtures and thus influenced hardened mechanical properties for mixes using this recycled aggregate. It is likely that residual asphalt also resulted in poor bonding between the aggregate and cementitious paste.

Figure 21. NC and RCA1 compressive strength.

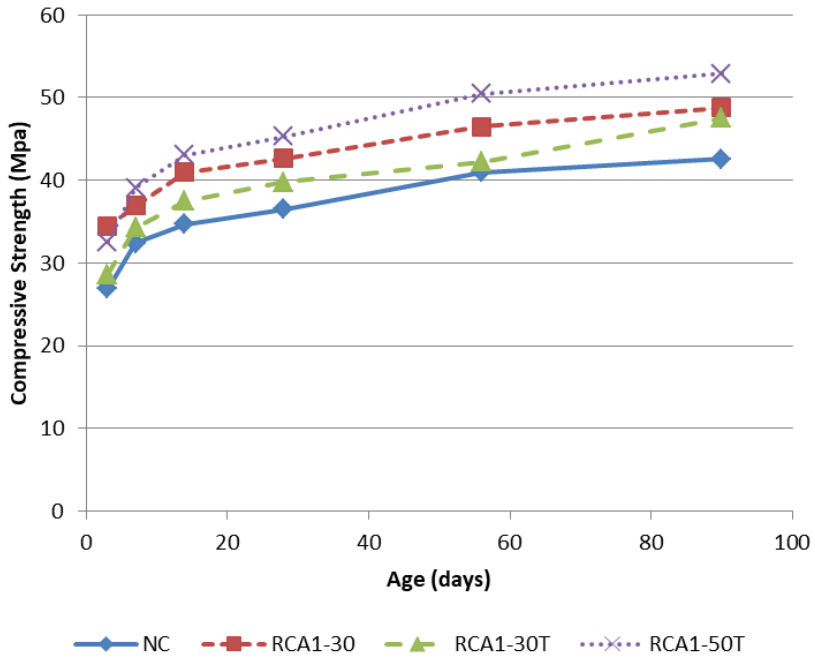

Figure 22. RCA2 compressive strength.

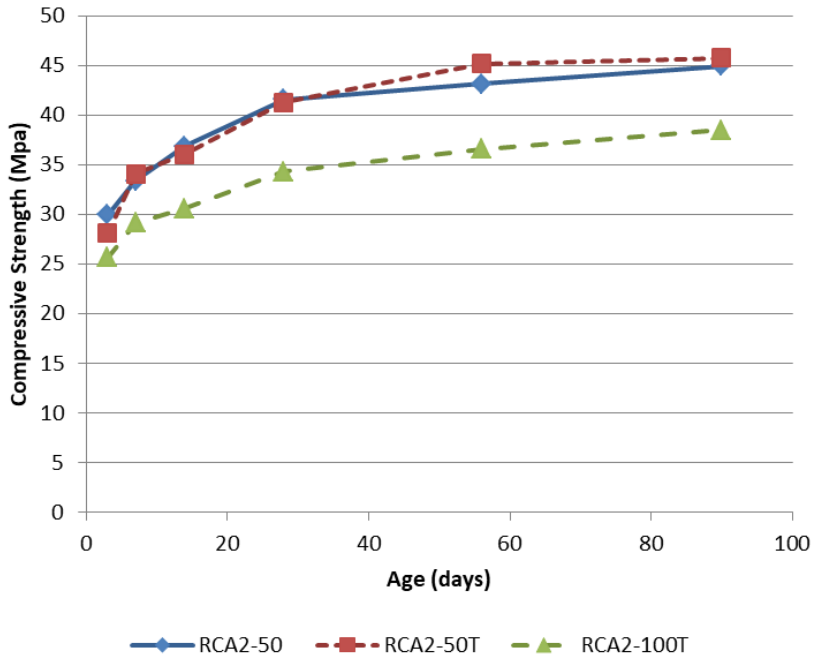

Figure 23. RCA3 compressive strength.

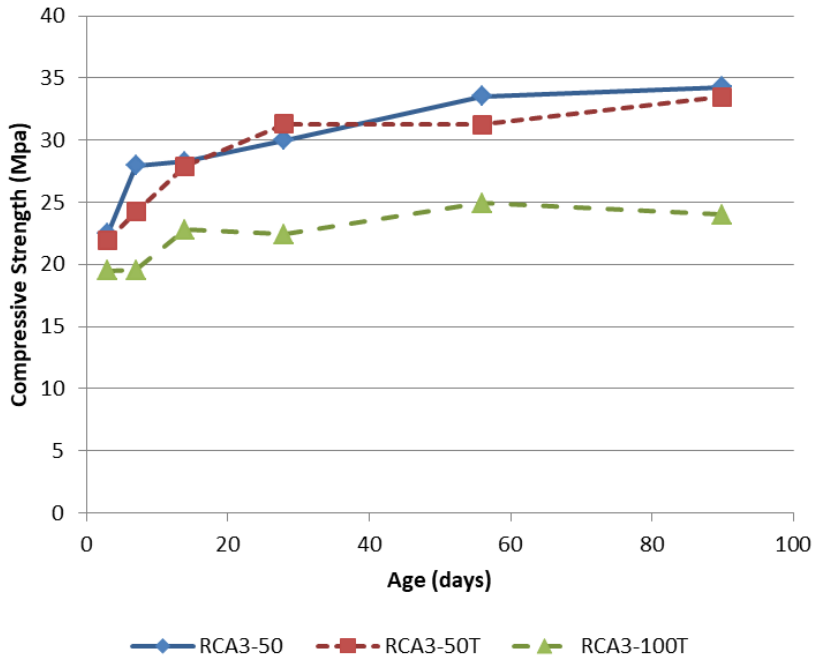

Figure 24. RCA4 compressive strength.

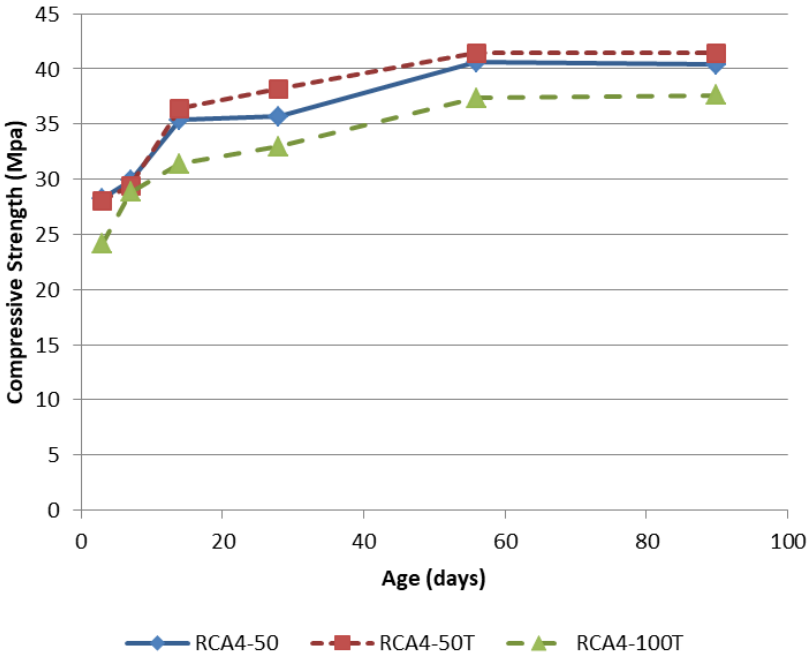

Figure 25. NC and RCA1 elastic modulus.

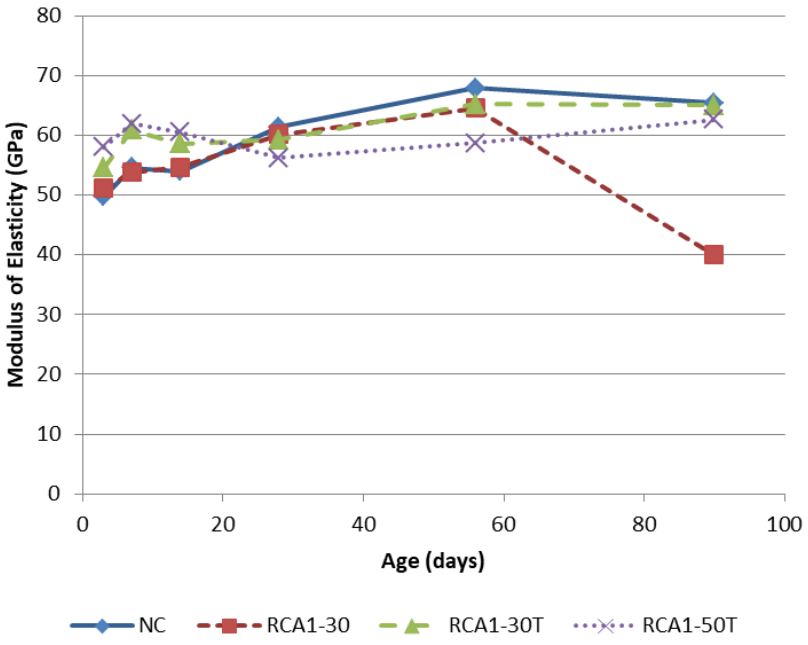

Figure 26. RCA2 elastic modulus.

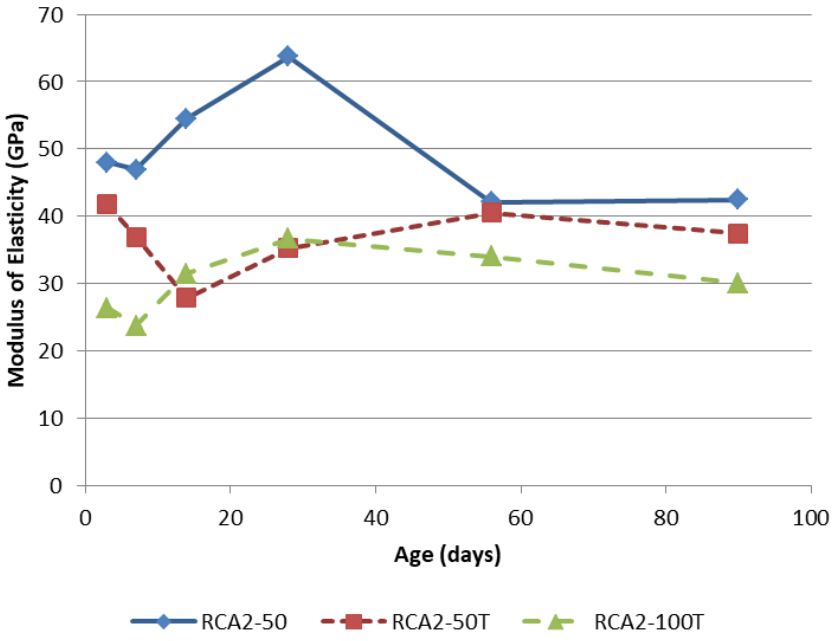

Figure 27. RCA3 elastic modulus.

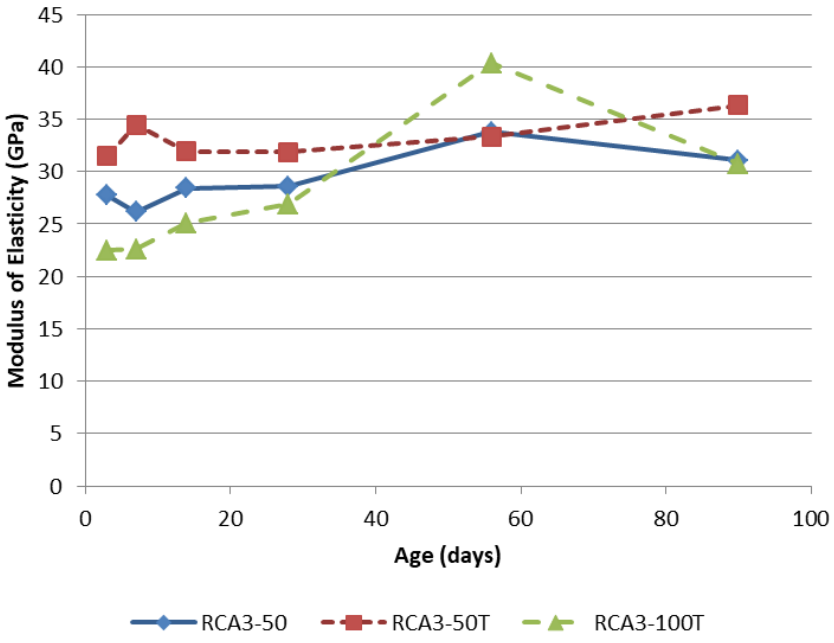

Figure 28. RCA4 elastic modulus.

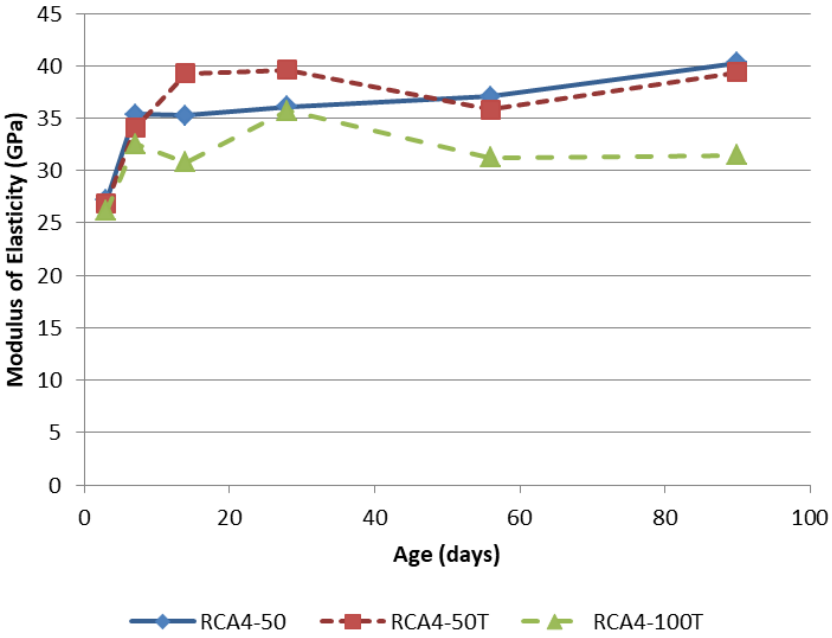

Figures 25 through 28 show results for the elastic modulus of the mixtures. NC and mixtures with RCA1 had a higher modulus compared to the other mixtures.

Figures 29 through 32 show modulus of rupture at 28 days and 90 days. In RCA1, mixtures with RCA replacement had greater flexural strength than the control. At 90 days, both mixtures with SCM had a higher modulus of rupture than either the control or the 30% RCA mixture without mineral admixtures. At 90 days, the modulus of rupture for the ternary blended mixtures RCA2, RCA3, and RCA4 met or exceeded their respective nonternary blend. In all cases, 100% replacement mixtures performed markedly worse.

Figure 29. NC and RCA1 modulus of rupture.

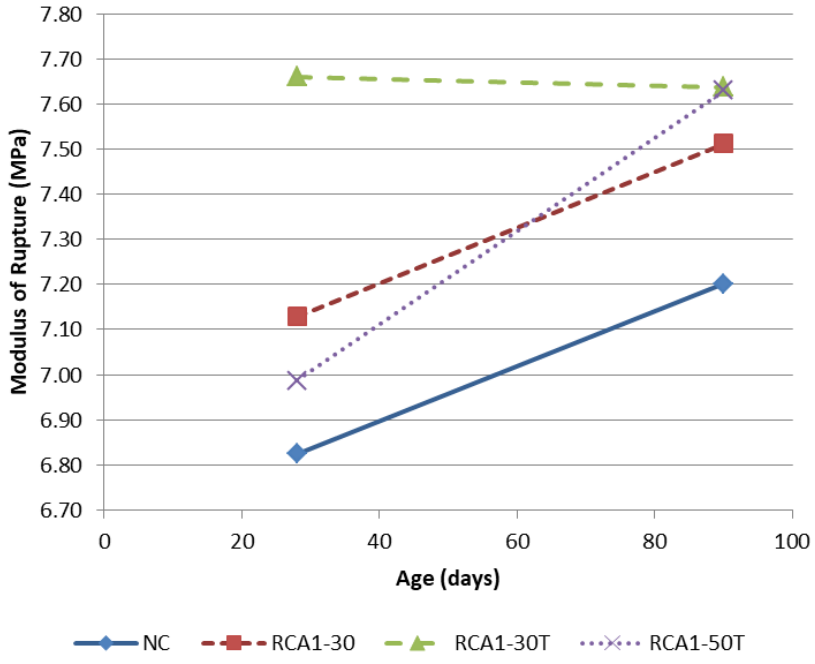

Figure 30. RCA2 modulus of rupture.

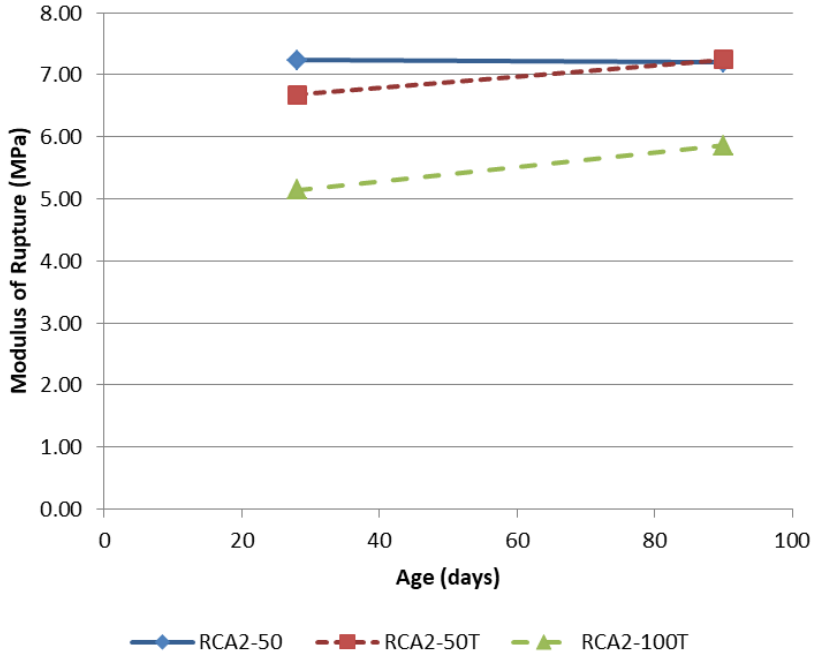

Figure 31. RCA3 modulus of rupture.

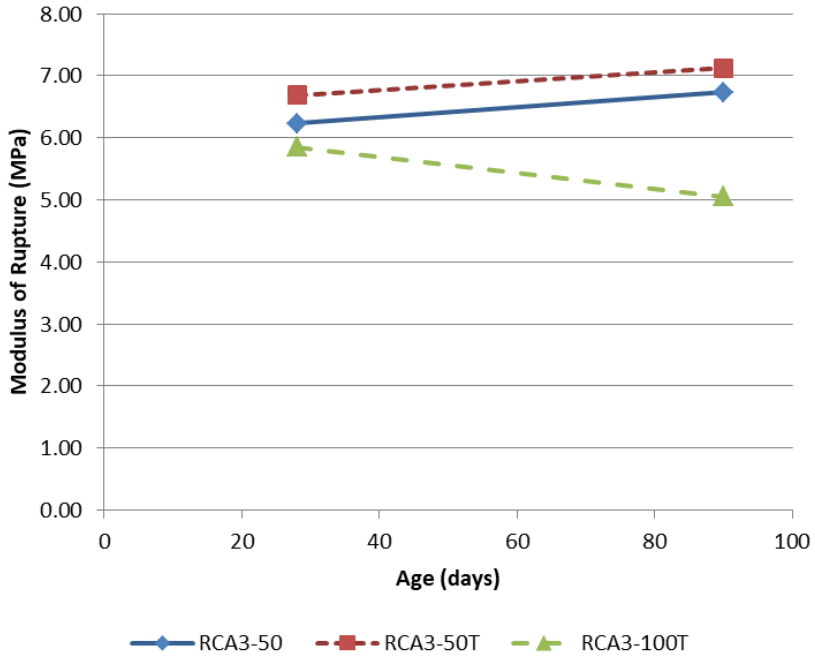

Figure 32. RCA4 modulus of rupture.

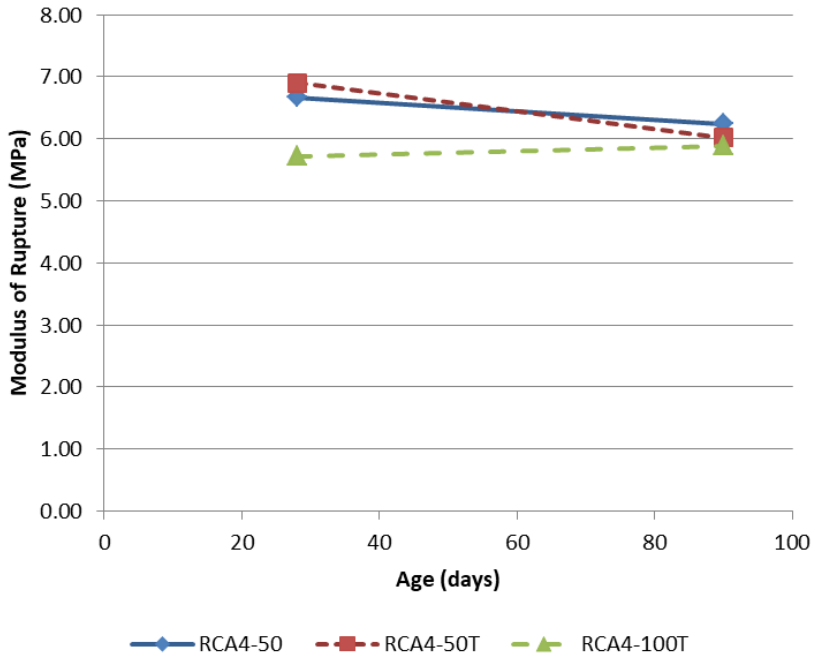

Figure 33 shows the electrical resistivity development for RCA1 mixtures. At 28 days, the control mixture maintained higher surface resistivity than the 30% RCA mixture. However, surface resistivity improved in both ternary blended mixtures. RCA1-30T (30% RCA, ternary blended) performed

best, indicating that RCA had a negative effect on the surface resistivity of the mixtures and that the addition of SCM counteracted this effect. A similar trend is apparent in the resistivity of RCA2 through RCA4 (Figures 34–36). At 50% replacement, the ternary blended mixture had a higher resistivity in all cases. However, at 100% replacement, resistivity fell to a similar level as the 50% replacement mix without SCM. The increase in resistivity with the use of the ternary blended binder is attributed to the decrease in permeability (Kosmatka and Wilson 2016), while the decrease in resistivity with the additional replacement with RCA is due to the increase in concrete porosity brought by the high porosity of the RCAs.

Figure 33. NC and RCA1 surface resistivity.

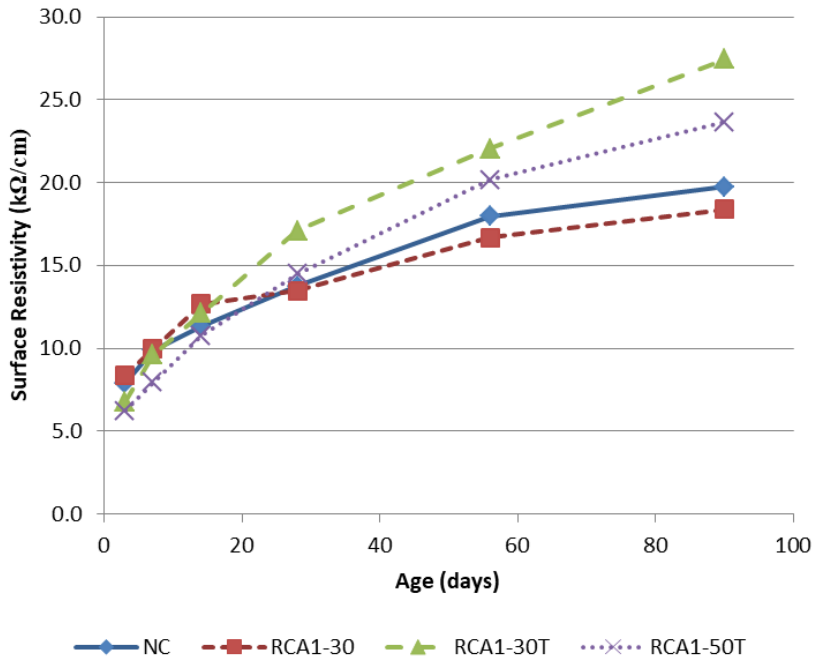

Figure 34. RCA2 surface resistivity.

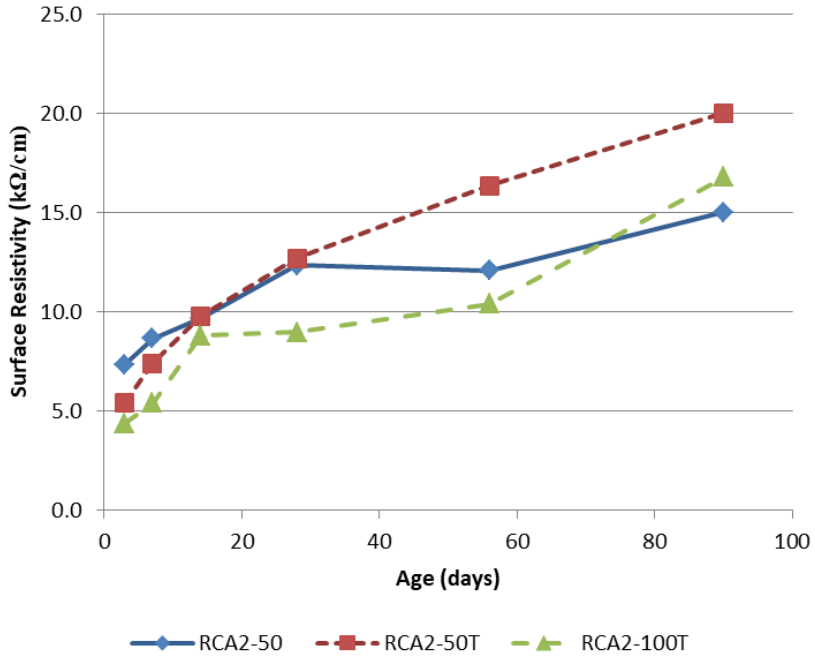

Figure 35. RCA3 surface resistivity.

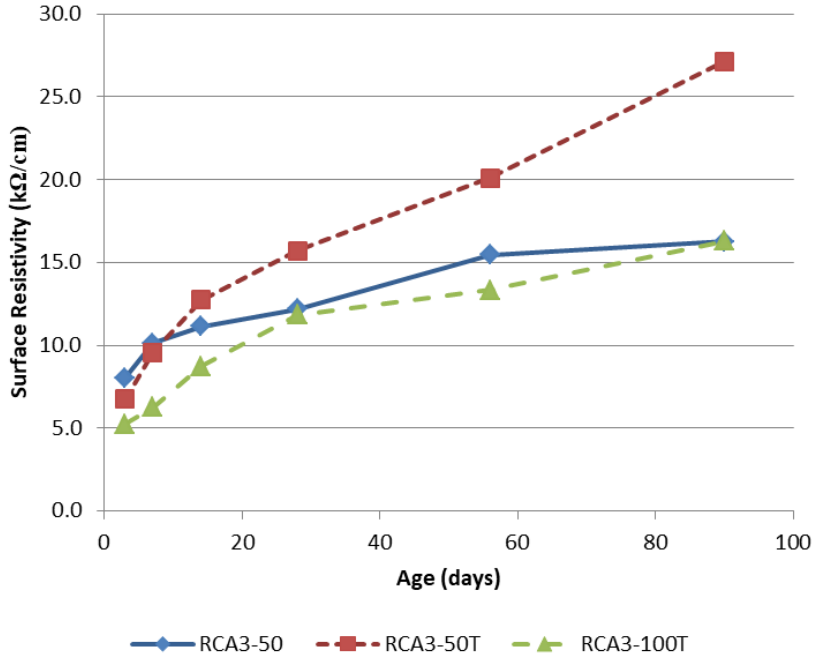

Figure 36. RCA4 surface resistivity.

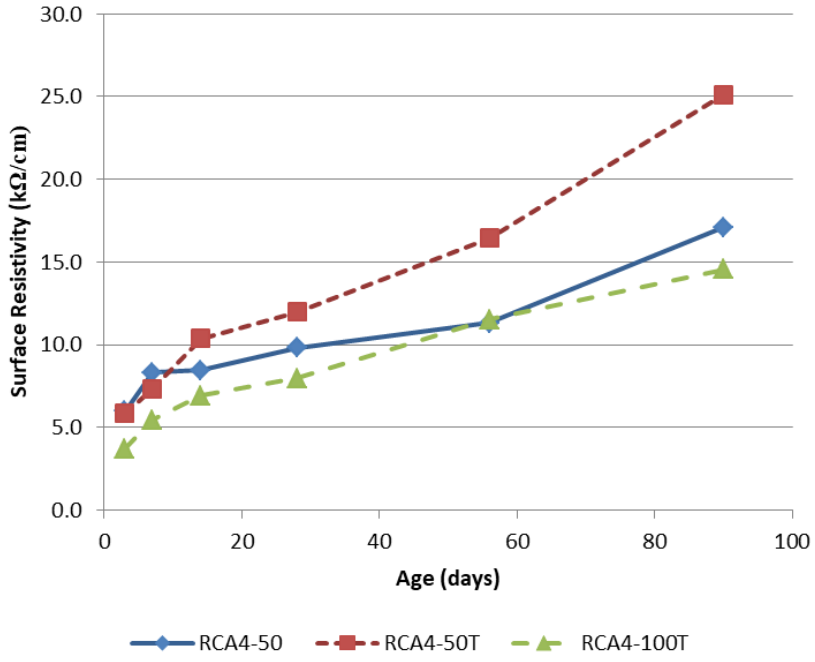

Figures 37 through 40 show data for drying shrinkage. The control blend showed the least change in length for the duration of testing. RCA1-30 (30% RCA) showed the highest change in length of the first four mixtures. A similar trend was observed in all mixtures for RCA2, RCA3, and RCA4 in which the addition of SCM reduced shrinkage below that of the mix without the blended binder. These results indicated that the use of the SCM reduces drying shrinkage caused by the addition of RCA. Higher permeability enables more surface drying due to climate exposure. The tested samples show this trend of higher shrinkage due to drying.

Figure 37. NC and RCA1 drying shrinkage.

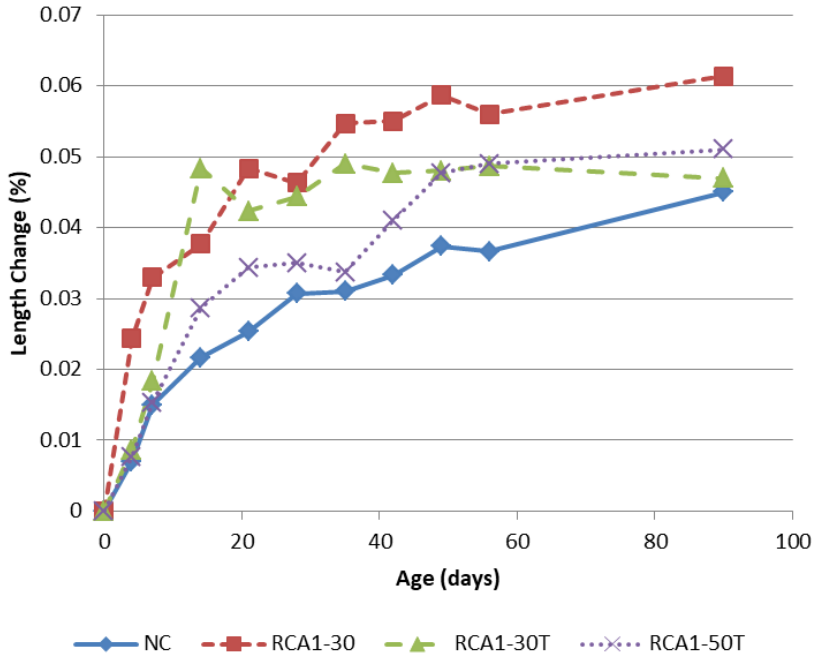

Figure 38. RCA2 drying shrinkage.

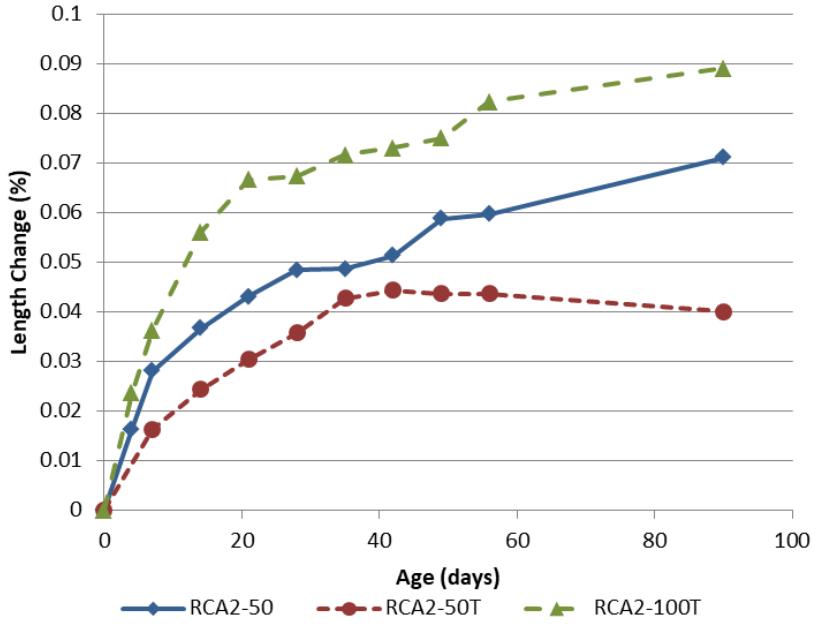

Figure 39. RCA3 drying shrinkage.

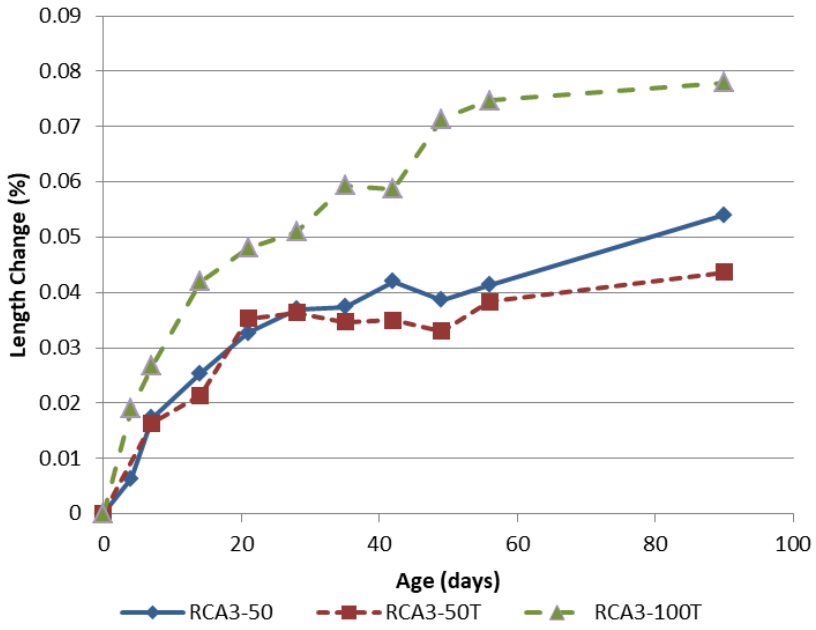

Figure 40. RCA4 drying shrinkage.

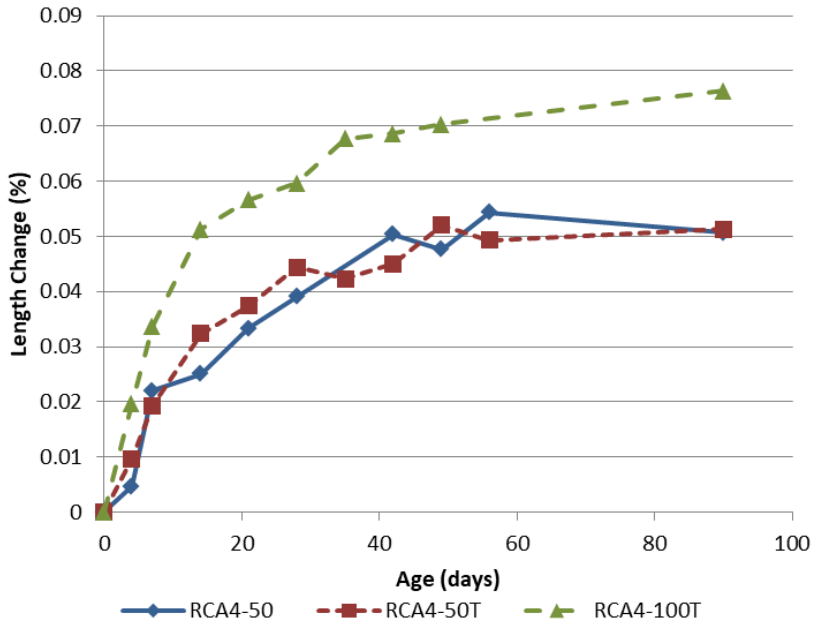

Figures 41 through 44 show freeze–thaw durability testing for all mixtures. NC and mixtures with RCA1 reached 300 freeze–thaw cycles while maintaining a relative dynamic modulus above 95%. RCA2 and RCA3 samples

began to decrease lower than 95% beyond 240 cycles and 120 cycles, respectively. Mixtures with RCA3 had a relative dynamic modulus less than 80% after 260 cycles.

Figure 41. NC and RCA1 freeze–thaw durability.

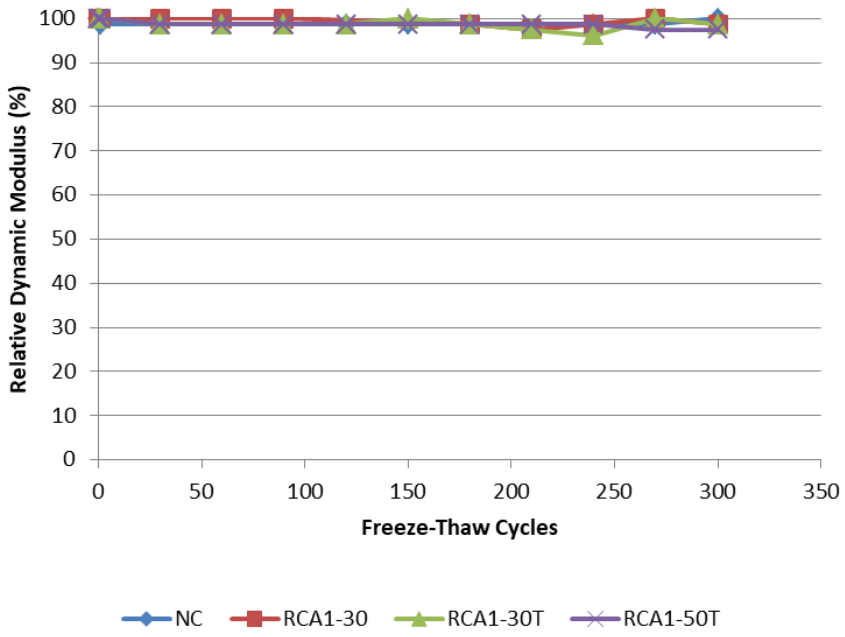

Figure 42. RCA2 freeze–thaw durability.

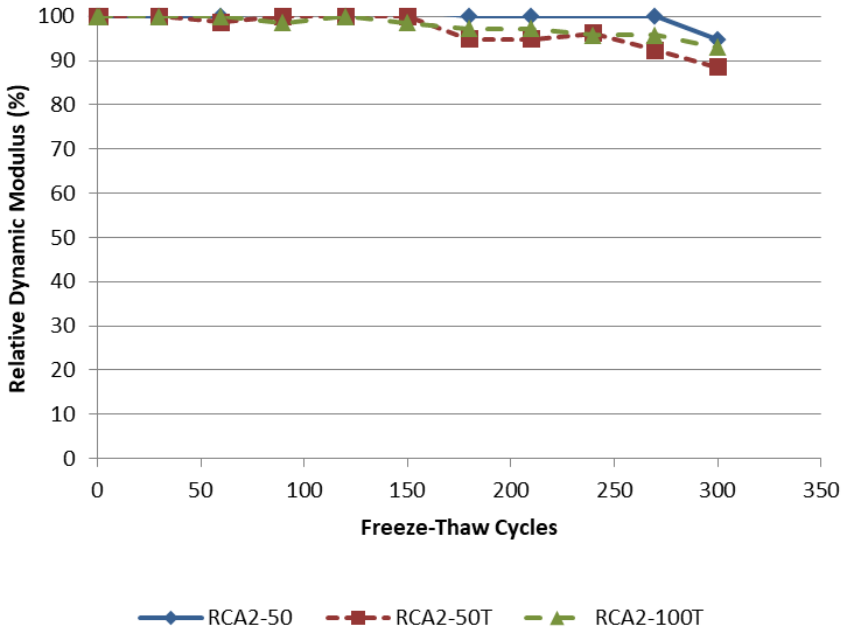

Figure 43. RCA3 freeze–thaw durability.

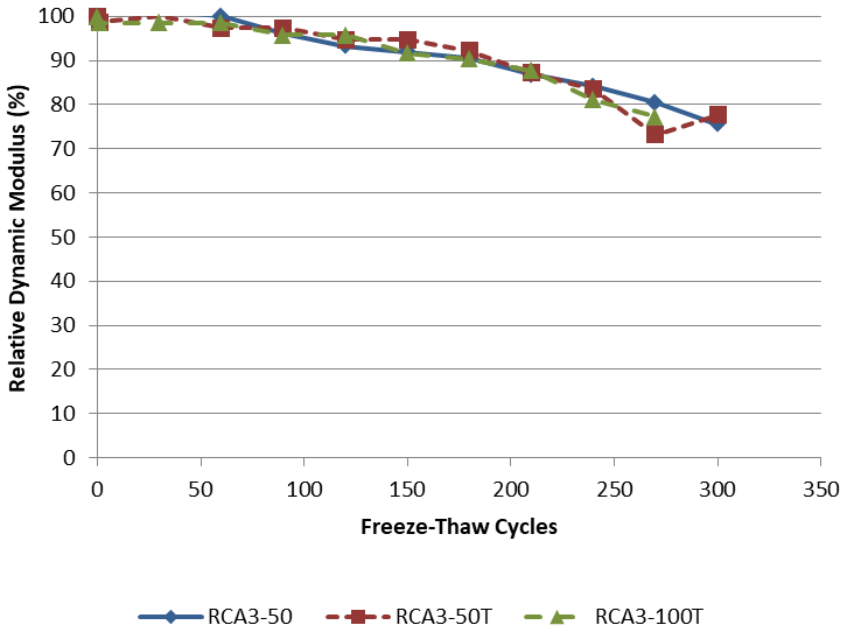

Figure 44. RCA4 freeze–thaw durability.

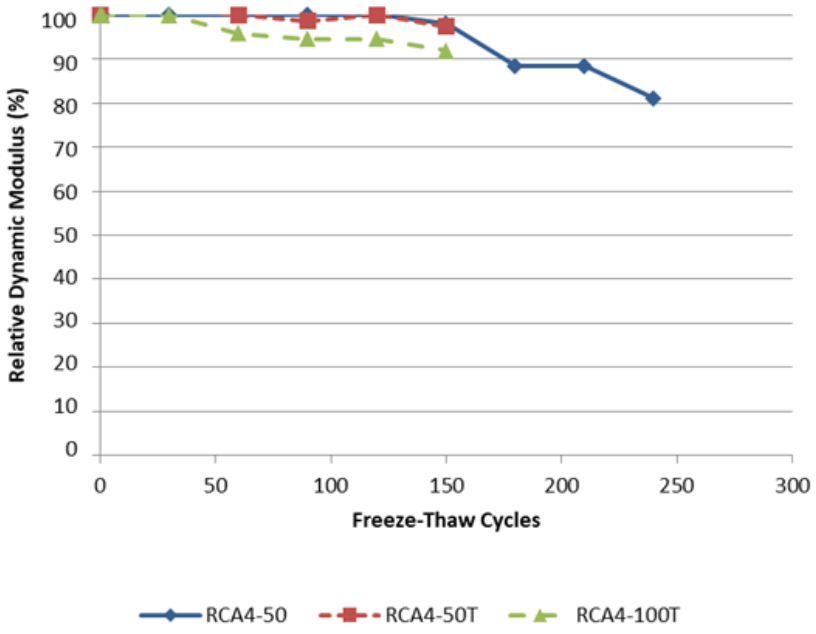

Figure 45 presents the alkali-silica reactivity for mixtures NC through RCA1-50T. Figures 46 through 48 show alkali-silica reactivity data for RCA2, RCA3, and RCA4, respectively. Length change over time increased with higher replacement rates of RCA. At 50% RCA replacement, the RCA1 samples failed to meet the 16-day low-risk limit for length change (0.10%).

The Class F fly ash and slag blend, PC72.7FAF12.5GGBFS10, was then tested at 50% replacement to analyze the effect of using a different binder (RCA1-50Tb). As previously shown, this blend performed very similarly to the chosen ternary binder blend in compressive strength, resistivity, and alkali-silica reactivity in mixtures without RCA. The alternate blend had a similar alkali-silica reaction potential to the control mixture. Class F fly ash is more efficient at reducing alkali-silica reaction due to its lower CaO content compared to the Class C fly ash.

A similar trend occurred for RCA2. At 100% replacement, the alternative binder reduced length change below the 16-day low-risk limit. RCA3 had the largest reduction in expansion with the addition of the blended binder. RCA4 had a significant amount of asphalt contamination, which lowered the available silica for the reaction to occur.

Figure 45. NC through RCA1-50T alkali-silica reaction.

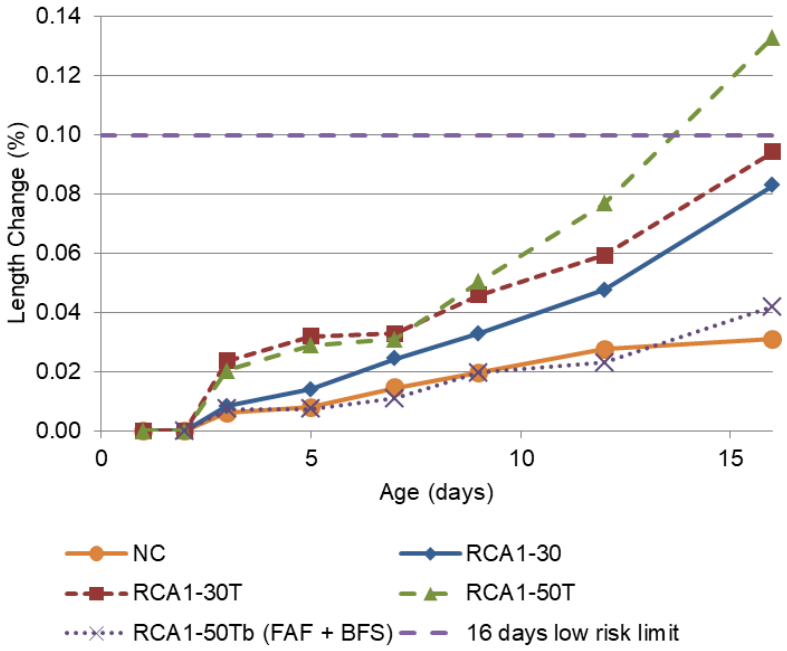

Figure 46. RCA2 alkali-silica reaction.

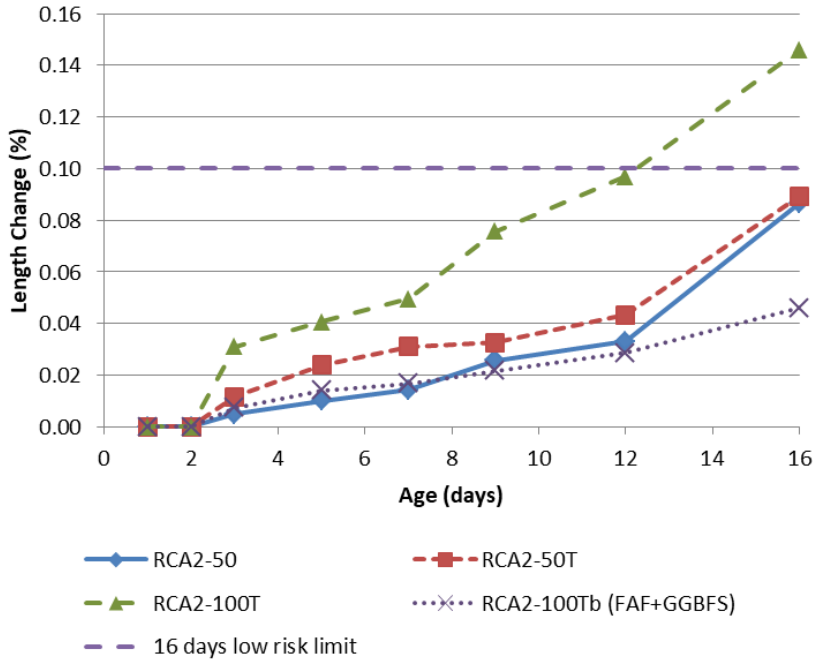

Figure 47. RCA3 alkali-silica reaction.

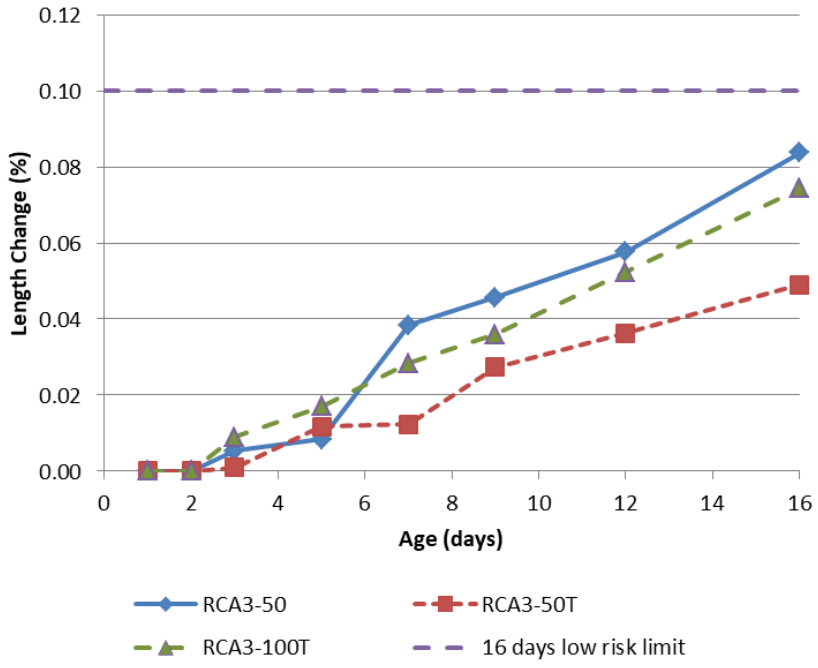

Figure 48. RCA4 alkali-silica reaction.

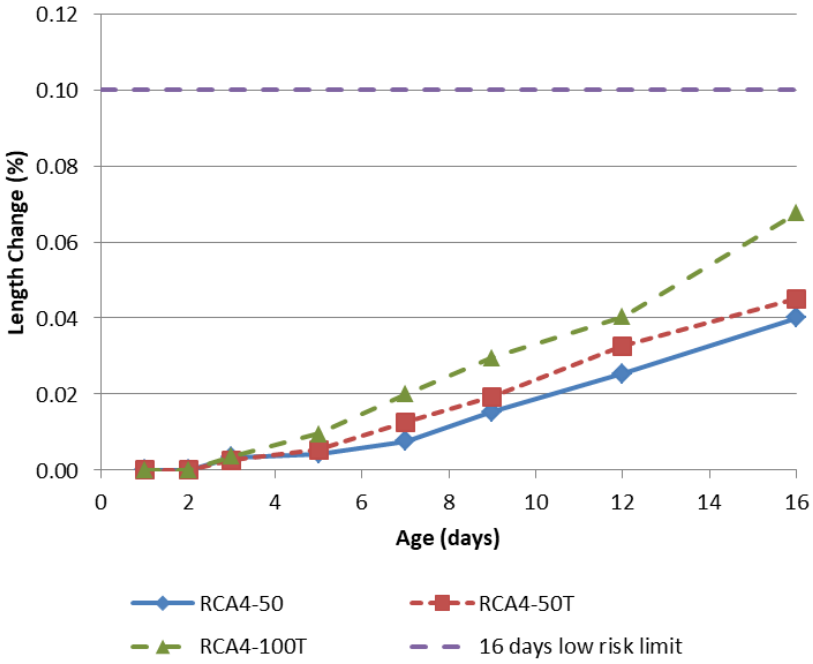

5 Summary and Conclusions

This study analyzed ternary blended cement binders at different proportions to optimize a concrete binder blend for the best concrete strength. Mortar cube compressive strength was recorded at 28 and 56 days for 25 unique cement blends, varying the mineral admixture replacement rate from 0% to 55% of the binder by weight. Isothermal calorimetry was used to identify curing properties by analyzing thermal activity and hydration heat for each blend. Concrete compressive testing and statistical analysis concluded that a blend of 77.5% portland cement, 12.5% Class C fly ash, and 10% slag will produce the best compressive strengths among ternary blends produced with the materials in this study. RCA from four sources were studied with different levels of replacement and with or without a ternary blended binder. Strength and durability tests were conducted on the concrete mixtures with the different combinations of binders and RCA.

5.1 Summary of findings

1. At 56 days, ternary combinations with SCM replacements up to 55% Class C fly ash produced higher strengths than portland cement.
2. At 56 days, ternary combinations with Class F fly and slag produced higher or similar strengths to portland cement when the replacement was up to 57.5%.
3. Ternary combinations of 12.5% Class F fly ash with 5% silica fume may produce strengths higher than PC at 56 days, but 5% silica fume alone with portland cement produced higher strength than the ternary blend.
4. The use of SCM tended to reduce the main peak in the heat of hydration and the total amount of heat measured in the first 72 hours of hydration. Class C fly ash and slag had a strong secondary C3A reaction, which may produce heat greater than the main C3S and C2S peak.
5. There was a consistent trend of reduced heat of hydration for ternary blended cements in the first 72 hours of hydration. The optimum strength with the low heat of hydration was the replacement of portland cement with 25% Class C fly ash and 2.5% silica fume, while the ternary blend with the highest compressive strength was replacement with 12.5% Class C fly ash and 10% slag.
6. Less than 55% portland cement in a ternary blend led to a decrease in mean strength compared to 100% portland cement strength at 56 days.
7. Compressive strength and elastic modulus tended to decrease significantly beyond 50% RCA replacement.

8. Flexural strength was maintained at up to 30% Salomone RCA use. The proposed ternary blended binder maintained or improved 90-day flexural strength above the portland cement mixtures.
9. Aggregate contamination (by asphalt in this experiment) significantly hindered mechanical properties as observed in RCA3 mixtures.
10. The 50 mm maximum slump and 5%–8% air content were consistently achieved with the proposed mix design for all iterations of binder implementation and RCA replacement studied.
11. Surface resistivity decreased, drying shrinkage increased, and alkali-silica reaction increased with RCA use. However, the proposed ternary blended binder improved concrete performance in these tests.

5.2 Conclusions

Concrete mixtures were tested with an increasing replacement rate of recycled concrete coarse aggregate and with the optimized ternary blended binder proportions. Fresh concrete properties were collected to check the consistency of workability and air content between mixtures. Hardened concrete properties were analyzed periodically up to 90 days to compare the strength and durability of each mixture. This study concluded the following based on the specific set of materials tested:

1. For use in concrete with a fraction of recycled coarse aggregates, a binder proportion of 77.5% Type I portland cement, 12.5% Class C fly ash, and 10% ground granulated blast furnace slag was optimal with respect to concrete strength, surface resistivity, and the limiting of drying shrinkage and alkali-silica reaction, for the materials considered in this study. The process conducted in the study can be followed to determine optimum combinations of SCM that are different in type and composition as the materials studied here.
2. Based on the RCA tested, screened and graded recycled concrete aggregate of appropriate physical characteristics may replace up to 50% of the coarse material in concrete mixtures without detrimentally affecting the strength, modulus, or durability of the concrete. Note that RCA can be a highly variable construction material. Laboratory testing of the processed stockpiled materials is necessary to determine the supplied material's properties to ensure quality and uniform concrete can be produced.
3. The porosity of RCA necessitated presoaking prior to batching and the potential use of workability-improving admixture to maintain consistent fresh mix workability at high coarse aggregate replacement by RCA.

4. The use of supplementary cementitious materials increased setting time consistently across trials. This has logistical application though may require additional planning to account for an additional 80 minutes to set time over portland cement mixtures.
5. Proper air entrainment (5%–8%) was sufficient to ensure the marginal loss of freeze–thaw durability characteristics at 50% RCA use.
6. Durability characteristics were properly controlled at 50% RCA by incorporating the optimized ternary blended binder.

5.3 Future work

This study proves the utility of ternary blended binders applied in concrete mixtures that use recycled concrete coarse aggregates. This topic would benefit from additional avenues of research:

1. This study addresses the use of Class C fly ash, Class F fly ash, silica fume, and ground granulated blast furnace slag. Several mineral admixtures commonly used could be examined through similar experimentation. These include limestone, metakaolin, etc. Other acceptable ternary binder combinations may exist that include these admixtures.
2. Different sources of RCA will have varying strength and durability characteristics. Designing unified guidelines for the use of RCA based on aggregate quality as it relates to the tests conducted in this study would allow a broader understanding of the mechanics that govern the usability of recycled aggregates.

The present work demonstrates a method for optimizing ternary binders based on mortar strength, then evaluates those binders in combination with RCA for concrete strength and durability performance. The process is important to consider due to the variability in the composition of SCM and when combining more than one type of SCM in a binder. RCA is also a product that varies significantly in properties and performance. However, this study showed that an optimized ternary blend would be able to offset the detrimental effect of RCA, if any, up to 50% replacement of RCA based on the tested mixtures. The combination of RCA and ternary blended binders could reduce costs compared to natural concrete aggregates while maintaining the same level of performance as plain portland cement concrete with natural concrete aggregates. These mixtures, RCA with ternary blended binders, will also contribute to a more sustainable construction practice.

References

AASHTO. 2013. Standard Method of Test for Air-Void Characteristics of Freshly Mixed Concrete by Buoyancy Change. AASHTO T 348-13. Washington, DC: American Association of State and Highway Transportation Officials.

Abbas, A., G. Fathifazl, B. Fournier, O. B. Isgor, R. Zavadil, A. G. Razaqpur, and S. Foo. 2009. "Quantification of the Residual Mortar Content in Recycled Concrete Aggregates by Image Analysis." *Materials Characterization* 60:716–728.

Abbaspour, A., B. F. Tanyu, and B. Cetin. 2016. "Impact of Aging on Leaching Characteristics of Recycled Concrete Aggregate." *Environmental Science and Pollution Research* 23:20835–20852.

Abdel-Hay, A. S. 2015. "Properties of Recycled Concrete Aggregate under Different Curing Conditions." *HBRC Journal* 13 (2): 271–276.

ACI Committee 211. 2002. *Standard Practice for Selecting Proportions for Normal, Heavyweight, and Mass Concrete*. ACI 211.1-91. Farmington Hills, MI: American Concrete Institute.

ACI Committee 221. 2001. *Guide for Use of Normal Weight and Heavyweight Aggregates in Concrete*. ACI 221R-96. Farmington Hills, MI: American Concrete Institute.

ACI Committee 555. 2001. *Removal and Reuse of Hardened Concrete*. ACI 555R-01. Farmington Hills, MI: American Concrete Institute.

ACPA. 2010a. "Why Recycle Concrete Pavements?" *Concrete Pavement Technology Series*, TS043.1P. Skokie, IL: ACPA. http://1204075.sites.myregisteredsite.com/downloads/TS/EB043P/TS043.1P.pdf.

———. 2010b. "Properties and Characteristics of RCA." Concrete Pavement Technology Series, TS043.3P. Skokie, IL: ACPA. http://1204075.sites.myregisteredsite.com/downloads/TS/EB043P/TS043.3P.pdf.

Air Force Civil Engineer Support Agency (Preparing Agency). 2019. Engineering Technical Letter (ETL) 07-6: *Risk Assessment Procedure for Recycling Portland Cement Concrete (PCC) Suffering from Alkali-Silica Reaction (ASR) in Airfield Pavement Structures*. HQ AFCESA/CEOA, ETL-07-6. Washington, DC: U.S. Army Corps of Engineers, Naval Facilities Engineering Command, and Air Force Civil Engineer Support Agency. https://www.wbdg.org/FFC/DOD/STC/tspwg_m_3-250-07_07-6.pdf.

Akbari, Y. V., and D. Rushabh. 2015. "Behavior of Recycled Coarse Aggregate in Ternary Blended Concrete with Microsilica and Flyash." *International Journal for Scientific Research & Development* 3 (3): 1617–1622.

Amorim, N. S., Jr., G. A. O. Silva, and D. V. Ribeiro. 2017. "Effects of the Incorporation of Recycled Aggregate in the Durability of the Concrete Submitted to Freeze-Thaw Cycles." *Construction and Building Materials* 161:723–730. https://doi.org/10.1016/j.conbuildmat.2017.12.076.

Amorim, P., J. de Brito, and L. Evangelista. 2012. "Concrete Made with Coarse Concrete Aggregate: Influence of Curing on Durability." *ACI Materials Journal* 109 (2): 195–204.

Andal, J., M. Shehata, and P. Zacarias. 2016. "Properties of Concrete Containing Recycled Concrete Aggregate of Preserved Quality." *Construction and Building Materials* 125:842–855.

Anderson, K. W., J. S. Uhlmeyer, and M. Russell. 2009. *Use of Recycled Concrete Aggregate in PCCP: Literature Search*. Special Report WA-RD 726.1. Olympia, WA: Washington State Department of Transportation.

Ann, K. Y., Y. B. Kim, H. Y. Moon, and J. Ryou. 2007. "Durability of Recycled Concrete Using Pozzolanic Materials." *Waste Management* 28:993–999.

ASTM. 2006. *Standard Test Method for Resistance to Degradation of Small-Size Coarse Aggregate by Abrasion and Impact in the Los Angeles Machine*. ASTM C131/C131M-14. West Conshohocken, PA: ASTM International.

———. 2010a. *Standard Test Method for Determination of Pore Volume and Pore Volume Distribution of Soil and Rock by Mercury Intrusion Porosimetry*. ASTM D4404-10. West Conshohocken, PA: ASTM International.

———. 2010b. *Standard Test Method for Flat Particles, Elongated Particles, or Flat and Elongated Particles in Coarse Aggregate*. ASTM D4791-10. West Conshohocken, PA: ASTM International.

———. 2012a. *Standard Test Method for Resistance of Concrete to Rapid Freezing and Thawing*. ASTM C666. West Conshohocken, PA: ASTM International.

———. 2012b. *Standard Test Method for Bulk Electrical Conductivity of Hardened Concrete*. ASTM C1760-12. West Conshohocken, PA: ASTM International.

———. 2013a. *Standard Test Method for Density, Absorption, and Voids in Hardened Concrete*. ASTM C642-13. West Conshohocken, PA: ASTM International.

———. 2013b. *Standard Test Method for Determining the Potential Alkali-Silica Reactivity of Combinations of Cementitious Materials and Aggregate (Accelerated Mortar-Bar Method)*. ASTM C1567-13. West Conshohocken, PA: ASTM International.

———. 2014a. *Standard Test Method for Sieve Analysis of Fine and Coarse Aggregates*. ASTM C136/C136M-14. West Conshohocken, PA: ASTM International.

———. 2014b. *Standard Test Method for Static Modulus of Elasticity and Poisson's Ratio of Concrete in Compression*. ASTM C469/C469M-10. West Conshohocken, PA: ASTM International.

———. 2014c. *Standard Test Method for Potential Alkali Reactivity of Aggregates (Mortar-Bar Method)*. ASTM C1260-14. West Conshohocken, PA: ASTM International.

——. 2015a. *Standard Test Method for Determination of Length Change of Concrete Due to Alkali-Silica Reaction*. ASTM C1293. West Conshohocken, PA: ASTM International.

——. 2015b. *Standard Test Method for Slump of Hydraulic-Cement Concrete*. ASTM C143/C143M-15a. West Conshohocken, PA: ASTM International.

——. 2016a. *Standard Test Method for Compressive Strength of Hydraulic Cement Mortars (Using 2-in. or [50-mm] Cube Specimens)*. ASTM C109/C109M-16. West Conshohocken, PA: ASTM International.

——. 2016b. *Standard Test Method for Time of Setting of Concrete Mixtures by Penetration Resistance*. ASTM C403/403M-16. West Conshohocken, PA: ASTM International.

——. 2017a. *Standard Specification for Blended Hydraulic Cements*. ASTM C595/C595M-17. West Conshohocken, PA: ASTM International.

——. 2017b. *Standard Test Method for Bulk Density ("Unit Weight") and Voids in Aggregate*. ASTM C29/C29M-17a. West Conshohocken, PA: ASTM International.

——. 2017c. *Standard Test Method for Drying Shrinkage of Mortar Containing Hydraulic Cement*. ASTM C596-09. West Conshohocken, PA: ASTM International.

——. 2017d. *Standard Practice for Measuring Hydration Kinetics of Hydraulic Cementitious Mixtures Using Isothermal Calorimetry*. ASTM C1679-17. West Conshohocken, PA: ASTM International.

——. 2017e. *Standard Test Method for Air Content of Freshly Mixed Concrete by the Pressure Method*. ASTM C231/C231M-17a. West Conshohocken, PA: ASTM International.

——. 2017f. *Standard Test Method for Density (Unit Weight), Yield, and Air Content (Gravimetric) of Concrete*. ASTM C138/138M-17a. West Conshohocken, PA: ASTM International.

——. 2017g. *Standard Test Method for Length Change of Hardened Hydraulic-Cement Mortar and Concrete*. ASTM C157/C157M-17. West Conshohocken, PA: ASTM International.

——. 2018a. *Standard Specification for Concrete Aggregates*. ASTM C33/C33M-18. West Conshohocken, PA: ASTM International.

——. 2018b. *Standard Test Method for Compressive Strength of Cylindrical Concrete Specimens*. ASTM C39/C39M-18. West Conshohocken, PA: ASTM International.

——. 2018c. *Standard Test Method for Soundness of Aggregates by Use of Sodium Sulfate or Magnesium Sulfate*. ASTM C88/C88M-18. West Conshohocken, PA: ASTM International.

——. 2018d. *Standard Specification for Slag Cement for Use in Concrete and Mortars*. ASTM C989/C989M-18a. West Conshohocken, PA: ASTM International.

——. 2018e. *Standard Test Method for Flexural Strength of Concrete (Using Simple Beam with Third-Point Loading)*. ASTM C78/78M-18. West Conshohocken, PA: ASTM International.

——. 2019a. *Standard Specification for Nontraditional Coarse Aggregates for Asphalt Paving Mixtures*. ASTM D6155-19. West Conshohocken, PA: ASTM International.

——. 2019b. *Standard Specification for Coal Fly Ash and Raw or Calcined Natural Pozzolan for Use in Concrete*. ASTM C618-19. West Conshohocken, PA: ASTM International.

Ayers, M. E., A. Davis, G. J. Fick, J. Gajda, J. Grove, D. Harrington, B. Kerkhoff, S. H. Kosmatka, H. C. Ozyildirim, J. M. Shilstone., K. Smith, S. M. Tarr, P. D. Tennis, P. C. Taylor, T. J. Van Dam, G. F. Voigt, and S. Waalkes. 2007. *Integrated Materials and Construction Practices for Concrete Pavement: A State-of-the-Practice Manual*. Report No. FHWA HIF-07-004. Washington, DC: Federal Highway Administration.

Bairagi, N. K., K. Ravande, and V. K. Pareek. 1993. "Behaviour of Concrete with Different Proportions of Natural and Recycled Aggregate." *Resources, Conservation and Recycling* 9 (1–2): 109–126.

Barra, M., M. Etxeberria, A. Marí, and E. Vázquez. 2007. "Influence of Amount of Recycled Coarse Aggregates and Production Process on Properties of Recycled Aggregate Concrete." *Cement and Concrete Research* 37 (5): 735–742.

Bektas, F., H. Ceylan, P, Taylor, and E. Yurdakul. 2014. "Effect of Water-to-Binder Ratio, Air Content, and Type of Cementitious Materials on Fresh and Hardened Properties of Binary and Ternary Blended Concrete." *Journal of Materials in Civil Engineering* 26 (60).

Berube, M. A., M. Angers, J. Frenette, and B. Marquis. 2002. "Frost-Resistance of Concrete Incorporating Coarse Aggregates Made of Recycled Concrete." In *Proceedings, 2nd Material Specialty Conference of the Canadian Society for Civil Engineering*, 5–8 June, Montreal, Quebec.

Bleszynski, R., R. D. Hooton, M. D. A. Thomas, and C. A. Rogers. 2002. "Durability of Ternary Blend Concrete with Silica Fume and Blast-Furnace Slag: Laboratory and Outdoor Exposure Site Studies" *ACI Materials Journal* 99 (5): 499–508.

Brown, T., K. K. Sagoe-Crentsil, and A. H. Taylor. 2001. "Performance of Concrete Made With Commercially Produced Coarse Recycled Concrete Aggregate." *Cement and Concrete Research* 31 (5): 707–712.

Butler, L., J. S. West, and S. L. Tighe. 2011. "The Effect of Recycled Concrete Aggregate Properties on the Bond Strength Between CCCA Concrete and Steel Reinforcement." *Cement and Concrete Research* 41 (10): 1037–1049.

Cleary, D. B. 2013. *Recycled Concrete Aggregate in Portland Cement Concrete*. FHWA-NJ-2013-001. New York: University Transportation Research Center. http://hdl.handle.net/10929/26462.

Cong, K. 2006. "Reusing Recycled Aggregates in Structural Concrete." PhD diss. Hong Kong Polytechnic University.

Corinaldesi, V. 2010. "Mechanical and Elastic Behavior of Concrete Made of Recycled-Concrete Coarse Aggregate." *Construction and Building Materials* 24:1616–1620.

Davis, M., A. de la Rosa, Y. Kurama, and M. McGinnis. 2017. "Strength and Stiffness of Concrete with Recycled Concrete Aggregates." *Construction and Building Materials* 154:258–269.

Desai, S. 2004. "Appreciation of Risks in Specifying and Designing Concrete Structures." *Building Engineer* 79 (6): 26–29.

Desai, S. B., and M. C. Limbachiya. 2006. "Coarse Recycled Aggregate—A Sustainable Concrete Solution." *Indian Concrete Journal* 80 (7): 17–23.

Dewar, J. 2003. "Concrete Mix Design." In *Advanced Concrete Technology: Processes*, ed. J. Newman and B. S. Choo, 3–40. Oxford, UK: Elsevier, Butterworth-Heinemann. https://doi.org/10.1016/B978-075065686-3/50287-1.

Ghosh, P., S. Hanson, P. Taylor, P. Tikalsky, and K. Wang. 2011. *Development of Performance Properties of Ternary Mixtures: Laboratory Study on Concrete*. Report No. DTFH61-06-H-00011. Ames, IA: National Concrete Pavement Technology Center.

Goguen, C. 2014. "Portland-Limestone Cement." *Precast Magazine*, 2 June 2014. http://precast.org/2014/06/portland-limestone-cement/.

Gurdián, H., E. García-Alcocel, F. Baeza-Brotons, P. Garcés, and E. Zornoza. 2014. "Corrosion Behavior of Steel Reinforcement in Concrete with Recycled Aggregates, Fly Ash and Spent Cracking Catalyst." *Materials* 7 (4): 3176–3197.

Hallet, B. 2006. "Why Do Freezing Rocks Break?" *Science* 314 (5802): 1092–1093.

Hansen, T. C. 1986. "Recycled Aggregates and Recycled Aggregate Concrete Second State-of-the-Art Report Developments 1945–1985." *Materials and Structures* 1 (111): 201–246.

Hariharan, A. R., A. S. Santhi, and G. Mohan Ganesh. 2011. "Effect of Ternary Cementitious System on Compressive Strength and Resistance to Chloride Ion Penetration." *International Journal of Civil and Structural Engineering* 1 (4): 700–701.

Hu, X., C. Shi, X. Shi, B. Tong, and D. Wang. 2017. "Early Age Shrinkage and Heat of Hydration of Cement-Fly Ash-Slag Ternary Blends." *Construction and Building Materials* 153:858–865.

Huda, S. B., and M. S. Alam. 2015. "Mechanical and Freeze-Thaw Durability Properties of Recycled Aggregate Concrete Made with Recycled Coarse Aggregate." *Journal of Materials in Civil Engineering* 27 (10): 04015003.

Innovative Pavement Research Foundation. 2006. *Evaluation, Design and Construction Techniques for Airfield Concrete Pavement Used as Recycled Material for Base*. IPRF-01-G-002-03-5. Skokie, IL: Innovative Pavement Research Foundation.

Jolin, M., D. Burns, B. Bissonnette, F. Gagnon, and L.-S. Bolduc. 2009. "Understanding the Pumpability of Concrete." In *Proceedings, Shotcrete for Underground Support XI*, 7–10 June. https://dc.engconfintl.org/shotcrete/17.

Kansas Department of Transportation. 2012. *5.3 Mix Design Methods*. Construction Manual. Topeka, Kansas: Kansas DOT.

Kim, K., M. Shin, and S. Cha. 2013. "Combined Effects of Recycled Aggregate and Fly Ash Towards Concrete Sustainability." *Construction and Building Materials* 48:499–507.

Kim, S. G. 2010. "Effect of Heat Generation from Cement Hydration on Mass Concrete Placement." MS thesis. Iowa State University.

Kosmatka, S. H., and M. L. Wilson. 2016. *Design and Control of Concrete Mixtures*. 16th ed. Skokie, IL: Portland Cement Association.

Kosmatka, S. H., B. Kerkhoff, and W. C. Panarese. 2002. *Design and Control of Concrete Mixtures*. Skokie, IL: Portland Cement Association.

Kou, S., and C. Poon. 2009. "Properties of Self-Compacting Concrete Prepared with Coarse and Fine Recycled Concrete Aggregates." *Cement and Concrete Composites* 31 (9): 622–627.

Kou, S. C., C. S. Poon, and C. Dixon. 2007. "Influence of Fly Ash as Cement Replacement on the Properties of Recycled Aggregate Concrete." *Journal of Materials in Civil Engineering* 19 (9): 709–717.

Li, X., and D. L. Gress. 2006. "Mitigating Alkali-Silica Reaction in Concrete Containing Recycled Concrete Aggregate." *Transportation Research Record* 1979 (1): 30–35.

Lima, C., A. Caggiano, C. Faella, E. Martinelli, M. Pepe, and R. Realfonzo. 2013. "Physical Properties and Mechanical Behaviour of Concrete Made with Recycled Aggregates and Fly Ash." *Construction Building Materials* 47:547–559.

Limbachiya, M. C., T. Leelawat, and R. K. Dhir. 2000. "Use of Recycled Concrete Aggregate in High-Strength Concrete." *Materials and Structures* 33 (233): 574–580.

Mamlouk, M. S., and J. P. Zaniewski. 2011. *Materials for Civil and Construction Engineers*. 3rd ed. Upper Saddle River, NJ: Pearson Education Limited.

McGinnis, M. J., M. Davis, A. de la Rosa, B. D. Weldon, and Y. C. Kurama. 2017. "Quantified Sustainability of Recycled Concrete Aggregates." *Magazine of Concrete Research* 69 (23): 1203–1211. https://doi.org/10.1680/jmacr.16.00338.

McIntyre, J., S. Spatari, and H. L. MacLean. 2009. "Energy and Greenhouse Gas Emissions Trade-Offs of Recycled Concrete Aggregate Use in Nonstructural Concrete: A North American Case Study." *ASCE Journal of Infrastructure Systems* 15 (4): 361–370.

Meddah, M. S. 2016. "Recycled Aggregates in Concrete Production: Engineering Properties and Environmental Impact." *MATEC Web of Conferences* 101:05021. https://doi.org/10.1051/matecconf/201710105021.

Meinhold, U., G. Mellmann, and M. Maultzsch. 2001. "Performance of High-Grade Concrete with Full Substitution of Aggregates by Recycled Concrete." In SP-202: Third Canmet/ACI International Symposium: Sustainable Development of Cement and Concrete. https://www.concrete.org/publications/internationalconcreteabstractsportal.aspx?m=details&ID=10775.

Naval Facilities Engineering Command (Preparing Agency). 2011. *Portland Cement Concrete Pavement for Roads and Site Facilities*. UFGS 32 13 13.06. Washington, DC: U.S. Army Corps of Engineers, Naval Facilities Engineering Command, Air Force Civil Engineer Support Agency, National Aeronautics and Space Administration. https://www.wbdg.org/ffc/dod/unified-facilities-guide-specifications-ufgs/ufgs-32-13-13-06.

———. 2019. *Lean Concrete Base Course*. UFGS 32 11 36.13. Washington, DC: U.S. Army Corps of Engineers, Naval Facilities Engineering Command, Air Force Civil Engineer Support Agency, National Aeronautics and Space Administration. https://www.wbdg.org/ffc/dod/unified-facilities-guide-specifications-ufgs/ufgs-32-11-36-13.

NJDOT (New Jersey Department of Transportation). 2007. Standard Specifications for Road and Bri*dge Construction*, 321, Table 901.10.02-1. Trenton, NJ: New Jersey Department of Transportation.

Obla, K. 2005. "Alkali Silica Reactions." *Concrete in Focus*, Spring 2005:45–47. https://www.nrmca.org/research/NRCQ_0105_45-47.pdf.

Pedro, D., L. de Brito, and L. Evangelista. 2014. "Influence of the Use of Recycled Concrete Aggregates from Different Sources on Structural Concrete." *Construction and Building Materials* 71:141–151.

Pepe, M. 2015. "A Conceptual Model for Designing Recycled Aggregate Concrete for Structural Applications." PhD diss., University of Salerno/Civil Engineering. http://elea.unisa.it/bitstream/handle/10556/1956/tesi_di_dottorato_M_Pepe.pdf?sequence=1&isAllowed=y.

Poon, C.-S., X. C. Qiao, and D. Chan. 2006. "The Cause and Influence of Self-Cementing Properties of Fine Recycled Concrete Aggregates on the Properties of Unbound Sub-Base." *Waste Management* 26 (10): 1166–1172.

Quattrone, M., B. Cazacliu, Angulo, S. C., E. Hamard , and A. Cothenet. 2016. "Measuring the Water Absorption of Recycled Aggregates, What is the Best Practice for Concrete Production?" *Construction and Building Materials* 123:690–703. https://doi.org/10.1016/j.conbuildmat.2016.07.019.

Rupnow, T. D. 2012. *Evaluation of Ternary Cementitious Combinations*. Tech Summary. Baton Rouge, LA: Louisiana Transportation Research Center.

Sadati, S., M. Arezoumandi, K. H. Khayat, and J. S. Volz. 2016. "Shear Performance of Reinforced Concrete Beams Incorporating Recycled Concrete Aggregate and High-Volume Fly Ash." *Journal of Cleaner Production* 115:284–293.

Salem, R. M., E. G. Burdette, and N. M. Jackson. 2003. "Resistance to Freezing and Thawing of Recycled Aggregate Concrete." *ACI Materials Journal* 100 (3): 216–221.

Stundebeck, C. J. 2007. "Durability of Ternary Blended Cements in Bridge Applications." Masters thesis, University of Missouri-Columbia. https://mospace.umsystem.edu/xmlui/bitstream/handle/10355/5082/research.pdf?sequence=3.

Tam, V. W. Y., C. M. Tam, and Y. Wang. 2007. "Optimization on Proportion for Recycled Aggregate in Concrete Using Two-Stage Mixing Approach." *Construction and Building Materials* 21 (10): 1928–1939.

Taylor, P. 2014. "The Use of Ternary Mixtures in Concrete." *InTrans Project Reports* 74. http://lib.dr.iastate.edu/intrans_reports/74.

Thomas, C., J. Setién, J. A. Polanco, P. Alaejos, and M. Sánchez De Juan. 2013. "Durability of Recycled Aggregate Concrete." *Construction and Building Materials* 40:1054–1065.

Thomas, M. D. A., B. Fournier, and K. J. Folliard. 2008. *Report on Determining the Reactivity of Concrete Aggregates and Selecting Appropriate Measures for Preventing Deleterious Expansion in New Concrete Construction*. Washington, DC: Federal Highway Administration.

Tutanji, H., and T. El-Korchi. 1995. "The Influence of Silica Fume on the Compressive Strength of Cement Paste and Mortar." *Cement and Concrete Research* 25 (7): 1591–1602.

USACE (U.S. Army Corps of Engineers) (Preparing Agency). 2004a. *Standard Practice for Concrete Pavements*. UFC 3-250-04. Washington, DC: U.S. Army Corps of Engineers and Air Force Civil Engineer Support Agency. https://www.wbdg.org/ffc/dod/unified-facilities-criteria-ufc/ufc-3-250-04.

———. 2004b. *Standard Practice for Pavement Recycling*. UFC 3-250-07. Washington, DC: U.S. Army Corps of Engineers, Naval Facilities Engineering Command, and Air Force Civil Engineer Support Agency. https://www.wbdg.org/ffc/dod/unified-facilities-criteria-ufc/ufc-3-250-07.

———. 2017. *Aggregate Base Courses*. UFGS-32 11 23. Washington, DC: U.S. Army Corps of Engineers, Naval Facilities Engineering Command, Air Force Civil Engineer Support Agency, National Aeronautics and Space Administration. https://www.wbdg.org/ffc/dod/unified-facilities-guide-specifications-ufgs/ufgs-32-11-23.

———. 2019. *Concrete Paving for Airfields and Other Heavy-Duty Pavements*. UFGS-32 13 14 13. Washington, DC: U.S. Army Corps of Engineers, Naval Facilities Engineering Command, Air Force Civil Engineer Support Agency, National Aeronautics and Space Administration. https://www.wbdg.org/ffc/dod/unified-facilities-guide-specifications-ufgs/ufgs-32-13-14-13.

Wang, K., Z. Ge, J. Grove, J. Mauricio Ruiz, and R. Rasmussen. 2006. *Developing a Simple and Rapid Test for Monitoring the Heat Evolution of Concrete Mixtures for Both Laboratory and Field Applications*. InTrans Project Reports 153. Ames, IA: Iowa State University, Center for Transportation Research and Education. https://lib.dr.iastate.edu/intrans_reports/153.

Wei, Y., Y. Meng, and Q. Sun. 2011. "Effects of Calcined Diatomite on Resistance to Permeability and Freeze-Thaw of Recycled Aggregate Concrete (RAC)." *Applied Mechanics and Materials* 121–126:2690–2694.

Wen, H., D. I. McLean, S. R. Boyle, T. C. Spry, and D. G. Mjelde. 2014. *Evaluation of Recycled Concrete as Aggregate in New Concrete Pavements*. WA-RD 826.1. Olympia, WA: Washington State Deptepartment of Transportation. https://www.wsdot.wa.gov/research/reports/fullreports/826.1.pdf.

Xiao, J.-Z., X.-D. Xu, and Y.-H. Fan. 2013. "Shrinkage and Creep of Recycled Aggregate Concrete and Their Prediction by ANN Method." *Journal of Building Materials* 16 (5): 752–757.

Yamasaki, J., and K. Tatematsu. 1998. "Strength and Freeze-Thaw Resistance Properties of Concrete Using High-Quality Recycled Aggregate." *Transactions of the Japan Concrete Institute* 20:45–52.

Yamato, T., Y. Emoto, and M. Soeda. 1998. "Mechanical Properties, Drying Shrinkage and Resistance to Freezing and Thawing of Concrete Using Recycled Aggregate." In Proceedings, Recent Advances in Concrete Technology, 7–11 June, Tokushima, Japan, 105–121.

Appendix A: Additional Tabulated Data

Table A-1. The 28-Day mortar cube compressive strength.

Mixture	Compressive Strength (psi)			Average	Standard Deviation
PC100	6839.30	6306.70	5996.10	6380.70	426.443
PC75FAC25	6482.70	7648.40	6980.30	7037.13	584.924
PC75FAF25	6384.50	5726.70	6208.80	6106.67	340.586
PC95SF5	6605.80	7379.10	6598.10	6861.00	448.704
PC70GGBFS30	5135.90	4564.60	6673.00	5457.83	1090.44
PC45FAC25GGBFS30	6052.10	6311.60	5733.80	6032.50	289.398
PC55FAC25GGBFS20	6779.10	7209.40	6852.10	6946.87	230.272
PC65FAC25GGBFS10	7025.70	7129.80	6842.10	6999.20	145.669
PC57.5FAC12.5GGBFS30	6837.30	7320.70	7095.60	7084.53	241.89
PC67.5FAC12.5GGBFS20	6830.50	7692.00	7247.10	7256.53	430.827
PC77.5FAC12.5GGBFS10	6436.10	6836.80	6984.70	6752.53	283.842
PC70FAC25SF5	6770.90	6987.10	6651.50	6803.17	170.111
PC72.5FAC25SF2.5	7676.30	8261.50	7367.00	7768.27	454.286
PC82.5FAC12.5SF5	6905.40	7040.10	6878.00	6941.17	86.7672
PC85FAC12.5SF2.5	7247.70	7074.70	7269.20	7197.20	106.631
PC45FAF25GGBFS30	5767.60	5366.10	5987.10	5706.93	314.914
PC55FAF25GGBFS20	5627.10	6059.10	5987.90	5891.37	231.614
PC65FAF25GGBFS10	5834.70	5716.30	3628.60	5059.87	1240.93
PC57.5FAF12.5GGBFS30	6840.30	6802.20	6752.90	6798.47	43.8194
PC67.5FAF12.5GGBFS20	6457.90	7339.30	6043.30	6613.50	661.863
PC77.5FAF12.5GGBFS10	6384.90	6475.40	6084.30	6314.87	204.74
PC70FAF25SF5	5822.10	6029.90	5803.50	5885.17	125.687
PC72.5FAF25SF2.5	5122.00	6099.70	6041.60	5754.43	548.473
PC82.5FAF12.5SF5	6298.00	6281.50	6787.20	6455.57	287.321
PC85FAF12.5SF2.5	5584.80	6627.50	6324.50	6178.93	536.375

1 psi = 0.006894757 MPa

Table A-2. The 56-Day mortar cube measured and predicted compressive strength.

Mixture	Compressive Strength (psi)			Average	Standard Deviation
PC100	4508.40	6502.80	5199.00	5403.40	1012.79
PC75FAC25	6164.00	6074.70	5750.00	5996.23	217.869
PC75FAF25	4936.20	5049.10	5378.90	5121.40	230.035
PC95SF5	6324.30	6703.30	5666.20	6231.27	524.772
PC70GGBFS30	6480.40	6917.50	6654.30	6684.07	220.065
PC45FAC25GGBFS30	7241.30	6245.60	6558.40	6681.77	509.185
PC55FAC25GGBFS20	7718.40	7428.60	7494.40	7547.13	151.926
PC65FAC25GGBFS10	6519.20	7154.90	8426.60	7366.90	971.211
PC57.5FAC12.5GGBFS30	7353.70	7418.20	7715.20	7495.70	192.809
PC67.5FAC12.5GGBFS20	8356.20	7895.40	7639.80	7963.80	363.065
PC77.5FAC12.5GGBFS10	8084.20	7230.20	8305.40	7873.27	567.788
PC70FAC25SF5	7207.00	6996.60	6890.70	7031.43	161.001
PC72.5FAC25SF2.5	7915.80	7291.00	8831.60	8012.80	774.867
PC82.5FAC12.5SF5	7462.90	7620.60	6590.40	7224.63	554.893
PC85FAC12.5SF2.5	7160.30	8361.50	6693.20	7405.00	860.648
PC45FAF25GGBFS30	6356.60	6604.00	6317.50	6426.03	155.359
PC55FAF25GGBFS20	6309.30	6535.70	6605.60	6483.53	154.885
PC65FAF25GGBFS10	7116.30	6946.20	7017.30	7026.60	85.4305
PC57.5FAF12.5GGBFS30	7031.60	7235.30	7026.70	7097.87	119.046
PC67.5FAF12.5GGBFS20	7691.00	7911.20	6801.30	7467.83	587.641
PC77.5FAF12.5GGBFS10	7146.20	7138.60	7082.00	7122.27	35.0784
PC70FAF25SF5	6509.00	6781.80	6221.60	6504.13	280.132
PC72.5FAF25SF2.5	6493.10	7433.00	6573.40	6833.17	521.02
PC82.5FAF12.5SF5	7135.50	8068.70	6405.30	7203.17	833.762
PC85FAF12.5SF2.5	6889.90	7192.00	6635.60	6905.83	278.542

1 psi = 0.006894757 MPa

Table A-3. Ternary blended concrete hardened properties.

Measure	Day	PC77.5FAF12.5GGBFS10	PC72.5FAC25SF2.5	PC77.5FAC12.5GGBFS10
Compressive Strength (psi)	3	4189	3493	3231
	7	4309	4396	3892
	14	4953	4535	4438
	28	5037	5061	5426
	56	5528	5659	5686
Electrical Resistivity (kΩ/cm)	3	9.5	6.6	7.6
	7	14.1	11.4	10.8
	14	17.0	11.8	16.5
	28	23.2	17.8	21.9
	56	25.6	25.8	25.1

1 psi = 0.006894757 MPa

Table A-4. PC77.5FAC12.5GGBFS10 ternary blended alkali-silica reaction.

Time (days)	Std Bar RDG (cm)	Specimen RDG (cm)	CRD	ΔL_x (%)	Mass (g)	Specimen RDG (cm)	CRD	ΔL_x (%)	Mass (g)	Specimen RDG (cm)	CRD	ΔL_x (%)	Mass (g)
		1				2				3			
−1	0.6734	0.7473	0.0291	0	0	0.7414	0.0268	0	0	0.74625	0.0287	0	0
0	0.6736	0.7554	0.0322	0	440.5	0.7516	0.0307	0	438.6	0.76530	0.0361	0	441.8
1	0.6734	0.7605	0.0343	0.021	441.1	0.7539	0.0317	0.01	440.1	0.76683	0.0368	0.007	442
3	0.6736	0.7633	0.0353	0.031	441.9	0.7559	0.0324	0.017	440.6	0.76937	0.0377	0.016	442.8
5	0.6736	0.7656	0.0362	0.04	442.3	0.7584	0.0334	0.027	440.9	0.77114	0.0384	0.023	443.1
7	0.6731	0.7661	0.0366	0.044	442.4	0.7582	0.0335	0.028	441	0.77114	0.0386	0.025	443.2
10	0.6731	0.7666	0.0368	0.046	443.1	0.7592	0.0339	0.032	441.9	0.77191	0.0389	0.028	444.3
14	0.672592	0.769112	0.038	0.058	443.4	0.761238	0.0349	0.042	442.1	0.7747	0.0402	0.034	444.2

ΔL_x = length change of specimen at any age, %.

CRD = difference between the comparator reading of the specimen and the reference bar at any age.

Std Bar RDG = reference bar reading.

Specimen RDG = specimen reading.

Table A-5. PC77.5FAF12.5GGBFS10 ternary blended alkali-silica reaction.

Time (days)	Std Bar RDG (cm)	Specimen RDG (cm)	CRD	ΔL_x (%)	Mass (g)	Specimen RDG (cm)	CRD	ΔL_x (%)	Mass (g)	Specimen RDG (cm)	CRD	ΔL_x (%)	Mass (g)
		1				2				3			
−1	0.6734	0.7513	0.0307	0	0	0.7584	0.0335	0	0	0.7513	0.0307	0	0
0	0.6736	0.7506	0.0303	0	433.2	0.7445	0.0279	0	440.6	0.7529	0.0312	0	437.2
1	0.6734	0.7521	0.031	0.007	433.9	0.7463	0.0287	0.008	441	0.7544	0.0319	0.007	437.8
3	0.6736	0.7534	0.0314	0.011	434.7	0.7478	0.0292	0.013	442	0.7559	0.0324	0.012	438.5
5	0.6736	0.7549	0.032	0.017	435.1	0.7493	0.0298	0.019	442.2	0.7577	0.0331	0.019	438.9
7	0.6731	0.7546	0.0321	0.018	435.3	0.7493	0.03	0.021	442.6	0.7571	0.0331	0.019	439.2
10	0.6731	0.7551	0.0323	0.02	436.1	0.7498	0.0302	0.023	443	0.7574	0.0332	0.02	439.9
14	0.6726	0.7574	0.0334	0.031	436.5	0.7523	0.0314	0.035	443.7	0.7597	0.0343	0.031	440

ΔL_x = length change of specimen at any age, %.

CRD = difference between the comparator reading of the specimen and the reference bar at any age.

Std Bar RDG = reference bar reading.

Specimen RDG = specimen reading.

Table A-6. PC72.5FAC25SF2.5 ternary blended alkali-silica reaction.

Time (days)	Std Bar RDG (cm)	Specimen RDG (cm)	CRD	ΔL_x (%)	Mass (g)	Specimen RDG (cm)	CRD	ΔL_x (%)	Mass (g)	Specimen RDG (cm)	CRD	ΔL_x (%)	Mass (g)
		1				2				3			
−1	0.6736	0.7488	0.0296	0	438.9	0.7386	0.0256	0	428.2	0.7303	0.0223	0	435.9
0	0.6734	0.7447	0.0281	0	438.6	0.7513	0.0307	0	430.4	0.7633	0.0354	0	441.4
1	0.6739	0.7483	0.0293	0.012	439.2	0.7557	0.0322	0.015	431.1	0.7668	0.0366	0.012	442
3	0.6736	0.7511	0.0305	0.024	439.8	0.7579	0.0332	0.025	431.5	0.7691	0.0376	0.022	442.5
5	0.6734	0.7523	0.0311	0.03	440	0.7592	0.0338	0.031	431.8	0.7704	0.0382	0.028	442.6
7	0.6734	0.7523	0.0311	0.03	440	0.7592	0.0338	0.031	432	0.7704	0.0382	0.028	443.3
10	0.6726	0.7534	0.0318	0.037	440.9	0.7602	0.0345	0.038	432.7	0.7714	0.0389	0.035	443.9
14	0.6728	0.7539	0.0319	0.038	441.3	0.7610	0.0347	0.04	433	0.7724	0.0392	0.038	444

ΔL_x = length change of specimen at any age, %.

CRD = difference between the comparator reading of the specimen and the reference bar at any age.

Std Bar RDG = reference bar reading.

Specimen RDG = specimen reading.

Table A-7. Blended NC hardened properties.

Measure	Day	NC	NC30	NC30T	NC50T
Compressive Strength (psi)	3	3894	4984	4152	4714
	7	4700	5351	5069	5662
	14	5030	5942	5435	6238
	28	5291	6186	5768	6571
	56	5943	6740	6125	7316
	90	6246		6894	7671
Elastic Modulus (ksi)	3	7217	7416	7916	8415
	7	7910	7798	8828	8983
	14	7837	7929	8502	8779
	28	8896	8728	8589	8145
	56	9854	9361	9455	8515
	90	9483		9433	9087
Electrical Resistivity (kΩ/cm)	3	7.9	8.4	6.8	6.2
	7	9.9	9.9	9.6	7.9
	14	11.3	12.7	12.1	10.8
	28	13.7	13.5	17.1	14.5
	56	18.0	16.7	22.0	20.2
	90	19.7		27.4	23.7
Modulus of Rupture (psi)	28	990	1034	1111	1013
	90	1045	1089	1108	1107

1 psi = 0.006894757 MPa; 1 ksi = 6.894757 MPa

Table A-8. RCA1 hardened properties.

Measure	Day	RCA1-50	RCA1-50T	RCA1-100T
Compressive Strength (kΩ/cm)	3	4342	4074	3721
	7	4839	4944	4222
	14	5342	5228	4437
	28	6025	5990	4979
	56	6258	6549	5303
	90	6521	6638	5579
Elastic Modulus (kΩ/cm)	3	6958	6050	3817
	7	6813	5347	3438
	14	7906	4037	4556
	28	9239	5107	4979
	56	6110	5880	4931
	90	6162	5432	4363
Electrical Resistivity (kΩ/cm)	3	7.3	5.4	4.4
	7	8.6	7.4	5.4
	14	9.7	9.8	8.8
	28	12.3	12.7	9.0
	56	12.1	16.3	10.4
	90	15.2	20.0	16.8
Modulus of Rupture (psi)	28	1049	968	746
	90	1044	1050	849

1 psi = 0.006894757 MPa

Table A-9. RCA2 hardened properties.

Measure	Day	RCA2-50	RCA2-50T	RCA2-100T
Compressive Strength (kΩ/cm)	3	3262	3181	2824
	7	4057	3514	2832
	14	4099	4048	3304
	28	4359	4539	3251
	56	4863	4535	3615
	90	4970	4857	3482
Elastic Modulus (kΩ/cm)	3	4026	4563	3264
	7	3797	4998	3281
	14	4121	4630	3642
	28	4143	4620	3902
	56	4900	4831	5853
	90	4504	5267	4458
Electrical Resistivity (kΩ/cm)	3	7.7	6.8	5.2
	7	10.8	9.6	6.3
	14	11.1	12.7	8.7
	28	12.2	15.7	11.8
	56	15.5	20.1	13.3
	90	16.3	26.4	16.1
Modulus of Rupture (psi)	28	904	969	848
	90	977	1033	732

1 psi = 0.006894757 MPa

Table A-10. RCA3 hardened properties.

Measure	Day	RCA3-50	RCA3-50T	RCA3-100T
Compressive Strength (kΩ/cm)	3	4098	4068	3504
	7	4337	4267	4183
	14	5133	5282	4554
	28	5178	5536	4779
	56	5891	6007	5419
	90	5858	6009	5454
Elastic Modulus (kΩ/cm)	3	3939	3893	3796
	7	5128	4944	4722
	14	5111	5697	4463
	28	5237	5743	5182
	56	5378	5197	4535
	90	5843	5715	4566
Electrical Resistivity (kΩ/cm)	3	6.0	5.8	3.7
	7	8.3	7.3	5.4
	14	8.5	10.4	6.9
	28	9.8	12.0	8.0
	56	11.3	16.4	11.5
	90	17.1	25.1	14.5
Modulus of Rupture (psi)	28	991	1001	830
	90	905	873	854

1 psi = 0.006894757 MPa

Table A-11. NC alkali-silica reaction.

Time (days)	Std Bar RDG (cm)	Specimen RDG (cm)	CRD	ΔL_x (%)	Mass (g)	Specimen RDG (cm)	CRD	ΔL_x (%)	Mass (g)	Specimen RDG (cm)	CRD	ΔL_x (%)	Mass (g)
		1				2				3			
−1	0.5964	0.6525	0.0221	0	444.88	0.6510	0.0215	0	440.14	0.6548	0.023	0	443.68
0	0.5969	0.6701	0.0288	0	444.6	0.6690	0.0284	0	440.64	0.6729	0.0299	0	444.09
1	0.5961	0.6711	0.0295	0.007	445.29	0.6690	0.0287	0.003	440.63	0.6741	0.0307	0.008	444.3
3	0.5964	0.6718	0.0297	0.009	445.51	0.6698	0.0289	0.005	441.41	0.6749	0.0309	0.01	444.86
5	0.5951	0.6728	0.0306	0.018	445.8	0.6701	0.0295	0.011	441.7	0.6749	0.0314	0.015	444.98
7	0.5966	0.6746	0.0307	0.019	445.5	0.6739	0.0304	0.02	441.28	0.6777	0.0319	0.02	444.84
10	0.5961	0.6769	0.0318	0.03	445.7	0.6754	0.0312	0.028	441.61	0.6784	0.0324	0.025	444.91
14	0.5972	0.6789	0.0322	0.034	445.48	0.6767	0.0313	0.029	441.2	0.6807	0.0329	0.03	444.75

Table A-12. NC30 alkali-silica reaction.

Time (days)	Std Bar RDG (cm)	Specimen RDG (cm)	CRD	ΔL_x (%)	Mass (g)	Specimen RDG (cm)	CRD	ΔL_x (%)	Mass (g)	Specimen RDG (cm)	CRD	ΔL_x (%)	Mass (g)
		1				2				3			
−1	0.5964	0.6507	0.0214	0	442.63	0.6584	0.0244	0	440.05	0.6527	0.0222	0	437.03
0	0.5969	0.6680	0.028	0	442.64	0.6759	0.0311	0	440.77	0.6690	0.0284	0	437.8
1	0.5961	0.6693	0.0288	0.008	442.75	0.6769	0.0318	0.007	440.7	0.6708	0.0294	0.01	437.86
3	0.5964	0.6701	0.029	0.01	443.42	0.6789	0.0325	0.014	441.28	0.6731	0.0302	0.018	438.5
5	0.5951	0.6711	0.0299	0.019	443.55	0.6802	0.0335	0.024	441.38	0.6749	0.0314	0.03	438.52
7	0.5966	0.6759	0.0312	0.032	443.57	0.6835	0.0342	0.031	441.35	0.6779	0.032	0.036	438.65
10	0.5961	0.6800	0.033	0.05	444.3	0.6883	0.0363	0.052	442.13	0.6787	0.0325	0.041	439.17
14	0.5972	0.6894	0.0363	0.083	444.27	0.6965	0.0391	0.08	442.37	0.6911	0.037	0.086	439.5

Table A-13. NC30T alkali-silica reaction.

Time (days)	Std Bar RDG (cm)	Specimen RDG (cm)	CRD	ΔL_x (%)	Mass (g)	Specimen RDG (cm)	CRD	ΔL_x (%)	Mass (g)	Specimen RDG (cm)	CRD	ΔL_x (%)	Mass (g)
		1				2				3			
−1	0.5979	0.6622	0.0253	0	439.2	0.6599	0.0244	0	432.1	0.6637	0.0259	0	438
0	0.5982	0.6797	0.0321	0	440.92	0.6759	0.0306	0	433.5	0.6799	0.0322	0	439.79
1	0.5964	0.6838	0.0344	0.023	441.26	0.6802	0.033	0.024	434.26	0.6842	0.0346	0.024	440.46
3	0.5964	0.6848	0.0348	0.027	441.22	0.6828	0.034	0.034	434.63	0.6870	0.0357	0.035	440.71
5	0.5964	0.6858	0.0352	0.031	441.94	0.6830	0.0341	0.035	435.02	0.6865	0.0355	0.033	441.07
7	0.5964	0.6883	0.0362	0.041	442.25	0.6871	0.0357	0.051	435.46	0.6898	0.0368	0.046	441.64
10	0.5974	0.6929	0.0376	0.055	442.53	0.6914	0.037	0.064	435.61	0.6941	0.0381	0.059	441.87
14	0.5969	0.7021	0.0414	0.093	443.71	0.7026	0.0416	0.11	442.7	0.6990	0.0402	0.08	436.63

Table A-14. NC50T alkali-silica reaction.

Time (days)	Std Bar RDG (cm)	Specimen RDG (cm)	CRD	ΔL_x (%)	Mass (g)	Specimen RDG (cm)	CRD	ΔL_x (%)	Mass (g)
		1				2			
−1	0.5979	0.6576	0.0235	0	431.7	0.6525	0.0215	0	438.6
0	0.5982	0.6728	0.0294	0	433.6	0.6698	0.0282	0	440.5
1	0.5964	0.6761	0.0314	0.02	434.13	0.6734	0.0303	0.021	440.35
3	0.5964	0.6767	0.0316	0.022	434.22	0.6772	0.0318	0.036	440.9
5	0.5964	0.6774	0.0319	0.025	435.9	0.6774	0.0319	0.037	441.55
7	0.5964	0.6830	0.0341	0.047	435.43	0.6817	0.0336	0.054	442.03
10	0.5974	0.6896	0.0363	0.069	435.96	0.6906	0.0367	0.085	442.35
14	0.5969	0.7041	0.0422	0.128	436.94	0.7036	0.042	0.138	443.19

Table A-15. NC50Tb alkali-silica reaction.

Time (days)	Std Bar RDG (cm)	Specimen RDG (cm)	CRD	ΔL_x (%)	Mass (g)	Specimen RDG (cm)	CRD	ΔL_x (%)	Mass (g)	Specimen RDG (cm)	CRD	ΔL_x (%)	Mass (g)
		1				2				3			
−1	0.5949	0.6599	0.0256	0	446.21	0.6523	0.0226	0	438.14	0.65151	0.0223	0	439.47
0	0.5949	0.6764	0.0321	0	445.3	0.6706	0.0298	0	440	0.67031	0.0297	0	442
1	0.5949	0.6789	0.0331	0.01		0.6718	0.0303	0.005		0.00000	−0.2342	0	
3	0.5949	0.6797	0.0334	0.013		0.6713	0.0301	0.003		0.67183	0.0303	0.006	
5	0.5949	0.6802	0.0336	0.015		0.6734	0.0309	0.011		0.67208	0.0304	0.007	
7	0.5949	0.6830	0.0347	0.026	449.4	0.6751	0.0316	0.018	441.9	0.67412	0.0312	0.015	443.7
10	0.5949	0.6838	0.035	0.029	449.8	0.6764	0.0321	0.023	442.5	0.67462	0.0314	0.017	444.1
14	0.5964	0.6901	0.0369	0.048	451	0.6822	0.0338	0.04	443	0.68148	0.0335	0.038	444

Table A-16. RCA1-50 alkali-silica reaction.

Time (days)	Date	Std Bar RDG (cm)	Specimen RDG (cm)	CRD	ΔL_x (%)	Mass (g)	Specimen RDG (cm)	CRD	ΔL_x (%)	Mass (g)	Specimen RDG (cm)	CRD	ΔL_x (%)	Mass (g)
			1				2				3			
−1	16-Feb	0.5964	0.6581	0.0243	0	435.2	0.6515	0.0217	0	431.3	0.6546	0.0229	0	441.05
0	17-Feb	0.5964	0.6746	0.0308	0	436.5	0.6701	0.029	0	433	0.6746	0.0308	0	443.4
1	18-Feb	0.5969	0.6767	0.0314	0.006	436.7	0.6721	0.0296	0.006	432.8	0.6759	0.0311	0.003	443
3	20-Feb	0.5964	0.6777	0.032	0.012	438.4	0.6728	0.0301	0.011	434.5	0.6764	0.0315	0.007	445.3
5	22-Feb	0.5964	0.6782	0.0322	0.014	437.2	0.6746	0.0308	0.018	433.2	0.6774	0.0319	0.011	443.3
7	24-Feb	0.5964	0.6820	0.0337	0.029	437.4	0.6779	0.0321	0.031	433.8	0.6789	0.0325	0.017	443.5
10	27-Feb	0.5964	0.6840	0.0345	0.037	437.5	0.6789	0.0325	0.035	434.1	0.6815	0.0335	0.027	443.8
14	3-Mar	0.5969	0.6970	0.0394	0.086	439.7	0.6922	0.0375	0.085	436.1	0.6977	0.0397	0.089	445.1

Table A-17. RCA1-50T alkali-silica reaction.

Time (days)	Date	Std Bar RDG (cm)	Specimen RDG (cm)	CRD	ΔL_x (%)	Mass (g)	Specimen RDG (cm)	CRD	ΔL_x (%)	Mass (g)	Specimen RDG (cm)	CRD	ΔL_x (%)	Mass (g)
			1				2				3			
−1	16-Feb	0.5964	0.6378	0.0163	0	443.8	0.6627	0.0261	0	433.16	0.6675	0.028	0	443.98
0	17-Feb	0.5964	0.6541	0.0227	0	448.1	0.6787	0.0324	0	437.2	0.6822	0.0338	0	445.2
1	18-Feb	0.5969	0.6574	0.0238	0.011	447.9	0.6820	0.0335	0.011	437	0.6861	0.0351	0.013	445.6
3	20-Feb	0.5964	0.6596	0.0249	0.022	448.7	0.6850	0.0349	0.025	437.9	0.6886	0.0363	0.025	450
5	22-Feb	0.5964	0.6627	0.0261	0.034	448.9	0.6855	0.0351	0.027	437.6	0.6904	0.037	0.032	446.7
7	24-Feb	0.5964	0.6622	0.0259	0.032	449.6	0.6868	0.0356	0.032	438.3	0.6909	0.0372	0.034	447.6
10	27-Feb	0.5964	0.6650	0.027	0.043	449.8	0.6896	0.0367	0.043	438.7	0.6934	0.0382	0.044	447.4
14	3-Mar	0.5964	0.6784	0.0323	0.096	451.5	0.7033	0.0421	0.097	440.5	0.7013	0.0413	0.075	449.4

Table A-18. RCA1-100T alkali-silica reaction.

Time (days)	Date	Std Bar RDG (cm)	Specimen RDG (cm)	CRD	ΔL_x (%)	Mass (g)	Specimen RDG (cm)	CRD	ΔL_x (%)	Mass (g)	Specimen RDG (cm)	CRD	ΔL_x (%)	Mass (g)
			1				2				3			
−1	20-Mar	0.5949	0.5192	−0.0298	0	417.19	0.4986	−0.0379	0	425.32	0.4468	−0.0583	0	428.92
0	21-Mar	0.5949	0.5385	−0.0222	0	420.7	0.5174	−0.0305	0	428.4	0.4669	−0.0504	0	433
1	22-Mar	0.5949	0.5464	−0.0191	0.031	-	0.5260	−0.0271	0.034	-	0.4740	−0.0476	0.028	-
3	24-Mar	0.5949	0.5484	−0.0183	0.039	-	0.5283	−0.0262	0.043	-	0.4770	−0.0464	0.04	-
5	26-Mar	0.5949	0.5512	−0.0172	0.05	-	0.5304	−0.0254	0.051	-	0.4790	−0.0456	0.048	-
7	28-Mar	0.5949	0.5573	−0.0148	0.074	422.5	0.5370	−0.0228	0.077	430.7	0.4862	−0.0428	0.076	434.6
10	31-Mar	0.5949	0.5631	−0.0125	0.097	422.8	0.5423	−0.0207	0.098	431.2	0.4912	−0.0408	0.096	435.4
14	4-Apr	0.5969	0.5771	−0.0078	0.144	425	0.5560	−0.0161	0.144	433	0.5070	−0.0354	0.15	436

Table A-19. RCA1-100Tb alkali-silica reaction.

Time (days)	Date	Std Bar RDG (cm)	Specimen RDG (cm)	CRD	ΔL_x (%)	Mass (g)	Specimen RDG (cm)	CRD	ΔL_x (%)	Mass (g)	Specimen RDG (cm)	CRD	ΔL_x (%)	Mass (g)
			1				2				3			
−1	4-May	0.5939	0.7247	0.0515	0	414.4	0.7155	0.0479	0	416.3	0.6071	0.0052	0	415.9
0	5-May	0.5939	0.7389	0.0571	0	423.1	0.7330	0.0548	0	425	0.6253	0.0124	0	426.3
1	6-May	0.5939	0.7430	0.0587	0.016	423.2	0.7341	0.0552	0.004	425	0.6259	0.0126	0.002	426.3
3	8-May	0.5939	0.7447	0.0594	0.023	423.9	0.7361	0.056	0.012	425.8	0.6271	0.0131	0.007	426.8
5	10-May	0.5941	0.7455	0.0596	0.025	424.2	0.7371	0.0563	0.015	426.3	0.6281	0.0134	0.01	427.3
7	12-May	0.5944	0.7470	0.0601	0.03	425	0.7389	0.0569	0.021	427	0.6294	0.0138	0.014	427.9
10	15-May	0.5931	0.7483	0.0611	0.04	424.8	0.7389	0.0574	0.026	426.7	0.6297	0.0144	0.02	427.8
14	19-May	0.5931	0.7529	0.0629	0.058	425.5	0.7432	0.0591	0.043	427.3	0.6340	0.0161	0.037	428.4

Table A-20. RCA2-50 alkali-silica reaction.

Time (days)	Date	Std Bar RDG (cm)	Specimen RDG (cm)	CRD	ΔL_x (%)	Mass (g)	Specimen RDG (cm)	CRD	ΔL_x (%)	Mass (g)	Specimen RDG (cm)	CRD	ΔL_x (%)	Mass (g)
			1				2				3			
−1	19-Apr	0.5951	0.6690	0.0291	0	444.6	0.5331	−0.0244	0	446.5	0.6213	0.0103	0	448.6
0	20-Apr	0.5951	0.6850	0.0354	0		0.0000	−0.2343	0		0.6264	0.0123	0	
1	21-Apr	0.5949	0.6888	0.037	0.016	444.6	0.5522	−0.0168	0	447.6	0.6406	0.018	0	450.1
3	23-Apr	0.5949	0.6901	0.0375	0.021		0.5525	−0.0167	0.001		0.6414	0.0183	0.003	
5	25-Apr	0.5949	0.6929	0.0386	0.032	445.4	0.5547	−0.0158	0.01	448.7	0.6436	0.0192	0.069	450.9
7	27-Apr	0.5949	0.6949	0.0394	0.04	445.7	0.5570	−0.0149	0.019	449.9	0.6459	0.0201	0.078	451.2
10	30-Apr	0.5954	0.6988	0.0407	0.053	447.6	0.5606	−0.0137	0.031	451.5	0.6492	0.0212	0.089	452.5
14	4-May	0.5954	0.7054	0.0433	0.079	448.3	0.5669	−0.0112	0.056	452.9	0.6561	0.0239	0.116	452.9

Table A-21. RCA2-50T alkali-silica reaction.

Time (days)	Date	Std Bar RDG (cm)	Specimen RDG (cm)	CRD	ΔL_x (%)	Mass (g)	Specimen RDG (cm)	CRD	ΔL_x (%)	Mass (g)	Specimen RDG (cm)	CRD	ΔL_x (%)	Mass (g)
			1				2				3			
−1	19-Apr	0.5951	0.6690	0.0291	0	432.7	0.6655	0.0277	0	426.9	0.6820	0.0342	0	435.4
0	20-Apr	0.5951	0.7000	0.0413	0		0.6830	0.0346	0		0.6944	0.0391	0	
1	21-Apr	0.5949	0.7021	0.0422	0.009	438.2	0.6848	0.0354	0.008	429.6	0.6906	0.0377	-0.014	
3	23-Apr	0.5949	0.6909	0.0378	−0.035	437.1	0.6909	0.0378	0.032	431.1	0.7038	0.0429	0.038	439.4
5	25-Apr	0.5949	0.6929	0.0386	−0.027	437.3	0.6922	0.0383	0.037	431.3	0.7064	0.0439	0.048	439.8
7	27-Apr	0.5949	0.6952	0.0395	−0.018	437	0.6934	0.0388	0.042	431.5	0.7089	0.0449	0.058	440
10	30-Apr	0.5954	0.6982	0.0405	−0.008	437.6	0.6955	0.0394	0.048	431.7	0.7122	0.046	0.069	440.5
14	4-May	0.5954	0.7010	0.0416	0.003	438.3	0.6982	0.0405	0.059	432.4	0.7163	0.0476	0.085	441.1

Table A-22. RCA2-100T alkali-silica reaction.

Time (days)	Date	Std Bar RDG (cm)	Specimen RDG (cm)	CRD	ΔL_x (%)	Mass (g)	Specimen RDG (cm)	CRD	ΔL_x (%)	Mass (g)	Specimen RDG (cm)	CRD	ΔL_x (%)	Mass (g)
			1				2				3			
−1	4-May	0.5939	0.6071	0.0052	0	409.4	0.5243	−0.0274	0	408	0.6502	0.0222	0	412.4
0	5-May	0.5939	0.6243	0.012	0	417.1	0.5420	−0.0204	0	415.5	0.6685	0.0294	0	420.6
1	6-May	0.5939	0.6266	0.0129	0.009	417.3	0.5443	−0.0195	0.009	415.6	0.6708	0.0303	0.009	420.9
3	8-May	0.5939	0.6284	0.0136	0.016	418.4	0.5466	−0.0186	0.018	416.9	0.6728	0.0311	0.017	421.8
5	10-May	0.5941	0.6314	0.0147	0.027	418	0.5499	−0.0174	0.03	417.3	0.6759	0.0322	0.028	422.3
7	12-May	0.5944	0.6340	0.0156	0.036	419.5	0.5519	−0.0167	0.037	417.9	0.6779	0.0329	0.035	422.9
10	15-May	0.5931	0.6368	0.0172	0.052	419.2	0.5547	−0.0151	0.053	417.9	0.6810	0.0346	0.052	422.8
14	19-May	0.5931	0.6426	0.0195	0.075	420	0.5606	−0.0128	0.076	418.5	0.6861	0.0366	0.072	423.6

Table A-23. RCA3-50 alkali-silica reaction.

Time (days)	Date	Std Bar RDG (cm)	Specimen RDG (cm)	CRD	ΔL_x (%)	Mass (g)	Specimen RDG (cm)	CRD	ΔL_x (%)	Mass (g)	Specimen RDG (cm)	CRD	ΔL_x (%)	Mass (g)
			1				2				3			
−1	24-May	0.5954	0.6322	0.0145	0	443.67	0.4948	−0.0396	0	444.89	0.5166	−0.031	0	444.93
0	25-May	0.5949	0.6482	0.021	0	445.3	0.5105	−0.0332	0	446.3	0.5331	−0.0243	0	454.72
1	26-May	0.5944	0.6485	0.0213	0.003	445.5	0.5113	−0.0327	0.005	447.1	0.5331	−0.0241	0.002	447.1
3	28-May	0.5939	0.6480	0.0213	0.003	444.5	0.5110	−0.0326	0.006	446.2	0.5331	−0.0239	0.004	446.4
5	30-May	0.5951	0.6502	0.0217	0.007	445.7	0.5131	−0.0323	0.009	447.1	0.5352	−0.0236	0.007	448.9
7	1-Jun	0.5944	0.6520	0.0227	0.017	445.7	0.5136	−0.0318	0.014	446.7	0.5364	−0.0228	0.015	447.1
10	4-Jun	0.5939	0.6533	0.0234	0.024	445.9	0.5164	−0.0305	0.027	447.2	0.5385	−0.0218	0.025	447.7
14	8-Jun	0.5936	0.6566	0.0248	0.038	445.9	0.5199	−0.029	0.042	447.4	0.5420	−0.0203	0.04	448

Table A-24. RCA3-50T alkali-silica reaction.

Time (days)	Date	Std Bar RDG (cm)	Specimen RDG (cm)	CRD	ΔL_x (%)	Mass (g)	Specimen RDG (cm)	CRD	ΔL_x (%)	Mass (g)	Specimen RDG (cm)	CRD	ΔL_x (%)	Mass (g)
			1				2				3			
−1	24-May	0.5954	0.6640	0.027	0	443.08	0.5933	−0.0008	0	443.88	0.6510	0.0219	0	454.72
0	25-May	0.5949	0.6802	0.0336	0	446.2	0.6096	0.0058	0	446.8	0.6675	0.0286	0	457.3
1	26-May	0.5944	0.6805	0.0339	0.003	447	0.6099	0.0061	0.003	447.6	0.6675	0.0288	0.002	458
3	28-May	0.5939	0.6807	0.0342	0.006	447.2	0.6104	0.0065	0.007	447.7	0.6673	0.0289	0.003	458.1
5	30-May	0.5951	0.6838	0.0349	0.013	447.6	0.6137	0.0073	0.015	448.6	0.6703	0.0296	0.01	458.5
7	1-Jun	0.5944	0.6843	0.0354	0.018	447.4	0.6142	0.0078	0.02	448.3	0.6721	0.0306	0.02	458.8
10	4-Jun	0.5939	0.6873	0.0368	0.032	447.9	0.6175	0.0093	0.035	448.7	0.6744	0.0317	0.031	459.1
14	8-Jun	0.5936	0.6906	0.0382	0.046	448.8	0.6200	0.0104	0.046	449.3	0.6772	0.0329	0.043	459.3

Table A-25. RCA3-100T alkali-silica reaction.

Time (days)	Date	Std Bar RDG (cm)	Specimen RDG (cm)	CRD	ΔL_x (%)	Mass (g)	Specimen RDG (cm)	CRD	ΔL_x (%)	Mass (g)	Specimen RDG (cm)	CRD	ΔL_x (%)	Mass (g)
			1				2				3			
−1	20-Jun	0.5966	0.6736	0.0303	0	438.3	0.6713	0.0294	0	436.4	0.6693	0.0286	0	439.8
0	21-Jun	0.5969	0.6937	0.0381	0	440.3	0.6919	0.0374	0	438.4	0.6899	0.0366	0	442
1	22-Jun	0.5966	0.6947	0.0386	0.005	441.1	0.6922	0.0376	0.002	439.2	0.6906	0.037	0.004	442.9
3	24-Jun	0.5964	0.6957	0.0391	0.01	441.6	0.6939	0.0384	0.01	439.5	0.6916	0.0375	0.009	443
5	26-Jun	0.5972	0.6990	0.0401	0.02	441.9	0.6970	0.0393	0.019	440	0.6955	0.0387	0.021	443.7
7	28-Jun			0	0.02			0	0.019			0.0000	0.021	
10	1-Jul			0	0.02			0	0.019			0.0000	0.021	
14	5-Jul			0	0.02			0	0.019			0.0000	0.021	

1 in. = 0.0254 m

A.1 JMP statistical analysis of Class F fly ash—silica fume combination

Response fc (MPa)
Whole Model
Actual by Predicted Plot

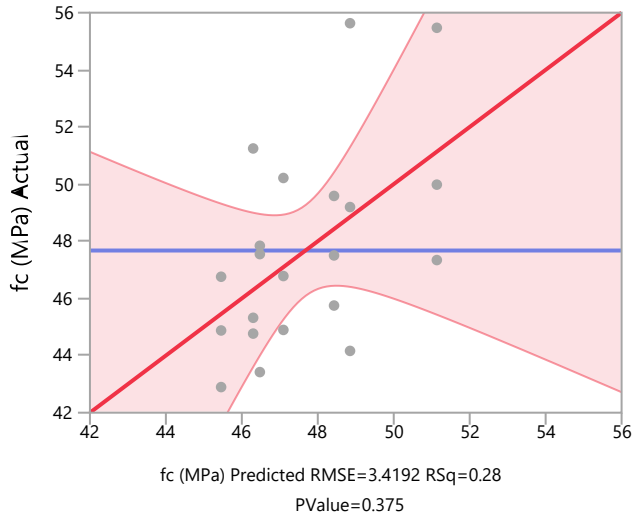

Effect Summary

Source	LogWorth	PValue
FAF (%)	1.131	0.07392
FAF (%)*SF (%)	0.659	0.21939
SF (%)	0.195	0.63755 ^
FAF (%)*FAF (%)	0.113	0.77124
SF (%)*SF (%)	0.065	0.86096

Lack of Fit

Source	DF	Sum of Squares	Mean Square	F Ratio
Lack Of Fit	1	7.45893	7.4589	0.6219
Pure Error	14	167.90040	11.9929	**Prob > F**
Total Error	15	175.35934		0.4435
				Max RSq
				0.3088

Residual by Predicted Plot

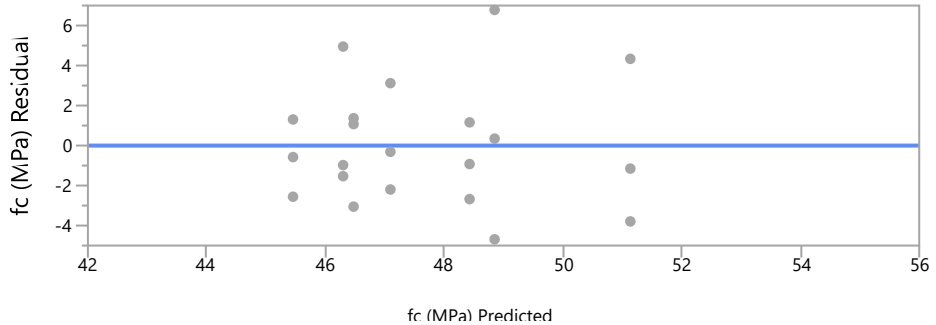

Summary of Fit

RSquare	0.278127
RSquare Adj	0.037503
Root Mean Square Error	3.419155
Mean of Response	47.67604
Observations (or Sum Wgts)	21

Analysis of Variance

Source	DF	Sum of Squares	Mean Square	F Ratio
Model	5	67.56344	13.5127	1.1559
Error	15	175.35934	11.6906	**Prob > F**
C. Total	20	242.92278		0.3750

Parameter Estimates

Term	Estimate	Std Error	t Ratio	Prob>|t|	Lower 95%	Upper 95%
Intercept	49.906609	2.86806	17.40	<.0001*	43.793483	56.019735
FAF (%)	-0.153138	0.07971	-1.92	0.0739	-0.323037	0.0167608
SF (%)	0.1916483	0.398552	0.48	0.6376	-0.657846	1.0411426
(FAF (%)-14.2857)*(FAF (%)-14.2857)	-0.003548	0.011986	-0.30	0.7712	-0.029095	0.0219982
(SF (%)-2.85714)*(SF (%)-2.85714)	-0.053392	0.29964	-0.18	0.8610	-0.692059	0.5852748
(FAF (%)-14.2857)*(SF (%)-2.85714)	-0.040484	0.031585	-1.28	0.2194	-0.107805	0.0268379

Prediction Expression

49.906609155

+ -0.153138051 • FAF (%)

+ 0.1916482809 • SF (%)

+ (FAF (%) − 14.285714286) • ((FAF (%) − 14.285714286) • -0.003548446)

+ (SF (%) − 2.8571428571) • ((SF (%) − 2.8571428571) • -0.053392168)

+ (FAF (%) − 14.285714286) • ((SF (%) − 2.8571428571) • -0.040483545)

A.2 JMP statistical analysis of Class F fly ash—ground granulated blast furnace slag combination

Response fc (MPa)
Whole Model
Actual by Predicted Plot

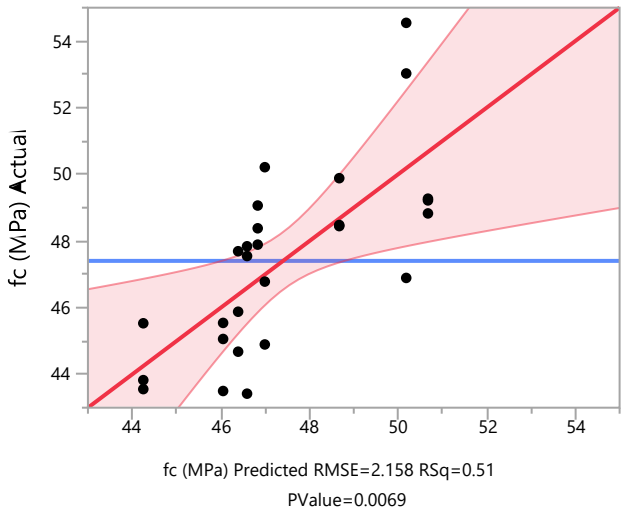

Effect Summary

Source	LogWorth	PValue
FAF (%)	2.711	0.00195
FAF (%)*FAF (%)	2.438	0.00365
GGBFS (%)	1.142	0.07204
GGBFS (%)*GGBFS (%)	0.502	0.31481
FAF (%)*GGBFS (%)	0.317	0.48158

Lack of Fit

Source	DF	Sum of Squares	Mean Square	F Ratio
Lack Of Fit	3	26.857396	8.95247	2.2717
Pure Error	18	70.935392	3.94086	**Prob > F**
Total Error	21	97.792789		0.1150
				Max RSq
				0.6450

Residual by Predicted Plot

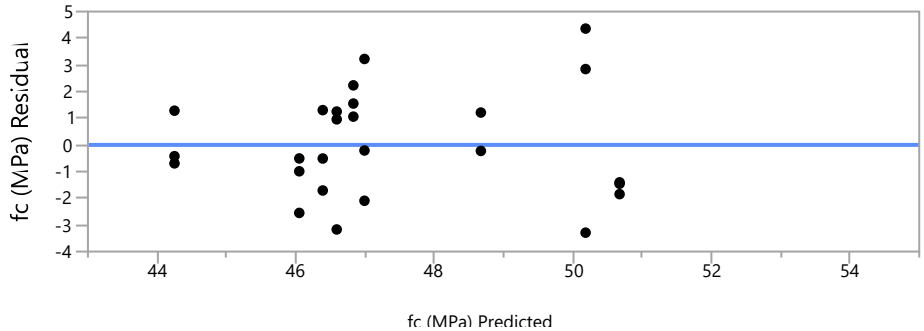

Summary of Fit

RSquare	0.510538
RSquare Adj	0.394
Root Mean Square Error	2.157962
Mean of Response	47.40406
Observations (or Sum Wgts)	27

Analysis of Variance

Source	DF	Sum of Squares	Mean Square	F Ratio
Model	5	102.00388	20.4008	4.3809
Error	21	97.79279	4.6568	**Prob > F**
C. Total	26	199.79667		0.0069*

Parameter Estimates

Term	Estimate	Std Error	t Ratio	Prob>|t|	Lower 95%	Upper 95%
Intercept	54.008973	1.567383	34.46	<.0001*	50.749422	57.268524
FAF (%)	-0.173895	0.049141	-3.54	0.0019*	-0.276089	-0.071702
GGBFS (%)	-0.072527	0.038286	-1.89	0.0720	-0.152148	0.0070942
(FAF (%)-15.2778)*(FAF (%)-15.2778)	-0.021457	0.00656	-3.27	0.0036*	-0.035098	-0.007816
(GGBFS (%)-16.6667)*(GGBFS (%)-16.6667)	-0.005105	0.004957	-1.03	0.3148	-0.015413	0.0052035
(FAF (%)-15.2778)*(GGBFS (%)-16.6667)	-0.00232	0.003238	-0.72	0.4816	-0.009053	0.0044134

A.3 JMP statistical analysis of Class C fly ash—silica fume combination

Response fc (MPa)
Whole Model
Actual by Predicted Plot

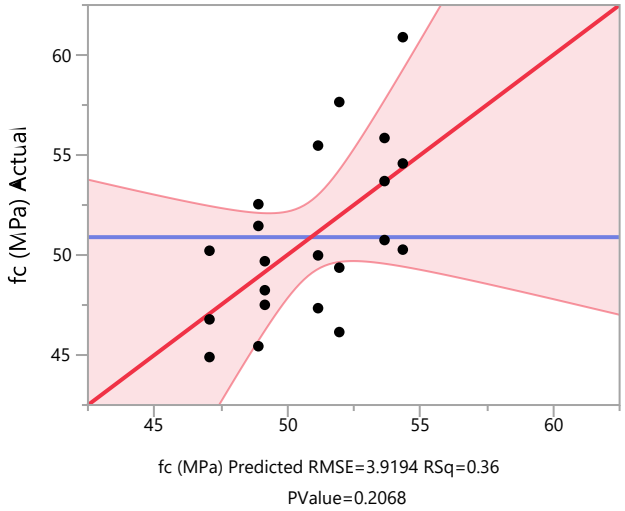

Effect Summary

Source	LogWorth	PValue
FAC (%)*SF (%)	1.112	0.07723
SF (%)*SF (%)	0.719	0.19106
SF (%)	0.537	0.29060 ^
FAC (%)	0.506	0.31221 ^
FAC (%)*FAC (%)	0.244	0.57074

Lack of Fit

Source	DF	Sum of Squares	Mean Square	F Ratio
Lack Of Fit	1	9.11864	9.1186	0.5769
Pure Error	14	221.30236	15.8073	**Prob > F**
Total Error	15	230.42100		0.4601
				Max RSq
				0.3807

Residual by Predicted Plot

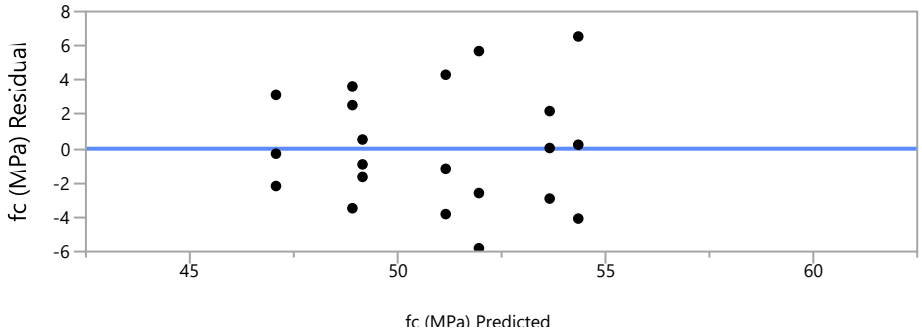

Summary of Fit

RSquare	0.355136
RSquare Adj	0.140182
Root Mean Square Error	3.919362
Mean of Response	50.89309
Observations (or Sum Wgts)	21

Analysis of Variance

Source	DF	Sum of Squares	Mean Square	F Ratio
Model	5	126.89647	25.3793	1.6521
Error	15	230.42100	15.3614	**Prob > F**
C. Total	20	357.31747		0.2068

Parameter Estimates

Term	Estimate	Std Error	t Ratio	Prob>|t|	Lower 95%	Upper 95%
Intercept	52.090275	3.287644	15.84	<.0001*	45.082827	59.097723
FAC (%)	0.0955576	0.091372	1.05	0.3122	-0.099197	0.2903119
SF (%)	-0.500464	0.456859	-1.10	0.2906	-1.474236	0.4733073
(FAC (%)-14.2857)*(FAC (%)-14.2857)	0.0079641	0.013739	0.58	0.5707	-0.02132	0.0372482
(SF (%)-2.85714)*(SF (%)-2.85714)	-0.470322	0.343476	-1.37	0.1911	-1.202423	0.2617794
(FAC (%)-14.2857)*(SF (%)-2.85714)	-0.068687	0.036206	-1.90	0.0772	-0.145857	0.008483

A.4 JMP statistical analysis of Class C fly ash—ground granulated blast furnace slag combination

Response fc (MPa)
Whole Model
Actual by Predicted Plot

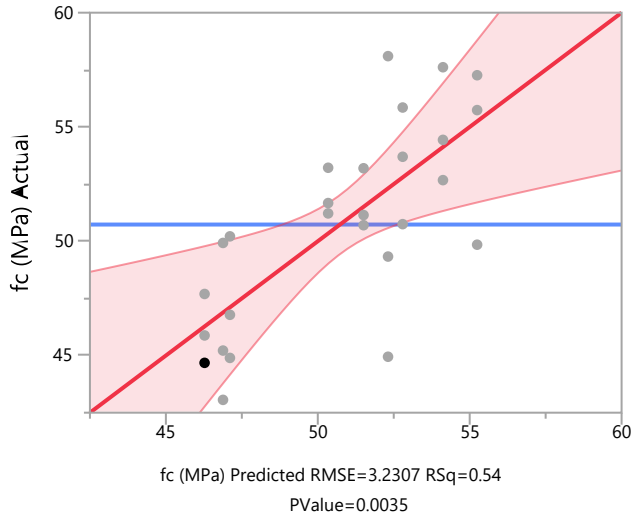

Effect Summary

Source	LogWorth	PValue
FAC (%)*FAC (%)	2.379	0.00418
GGBFS (%)	1.895	0.01273
FAC (%)*GGBFS (%)	0.752	0.17700
GGBFS (%)*GGBFS (%)	0.485	0.32703
FAC (%)	0.378	0.41859 ^

Lack of Fit

Source	DF	Sum of Squares	Mean Square	F Ratio
Lack Of Fit	3	23.67601	7.8920	0.7266
Pure Error	18	195.50357	10.8613	**Prob > F**
Total Error	21	219.17958		0.5493
				Max RSq
				0.5933

Residual by Predicted Plot

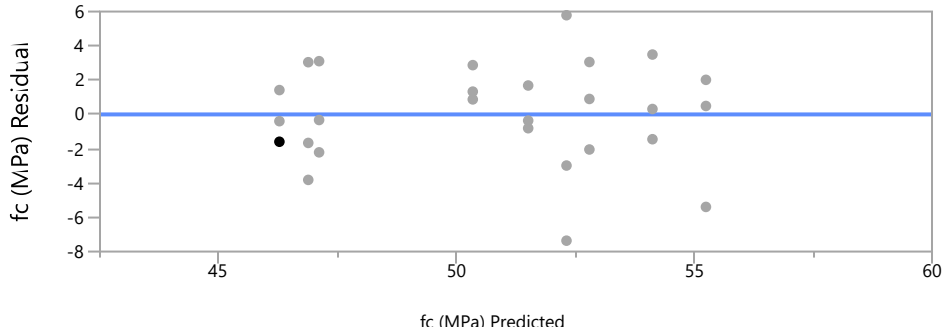

Summary of Fit

RSquare	0.544084
RSquare Adj	0.435533
Root Mean Square Error	3.230654
Mean of Response	50.73116
Observations (or Sum Wgts)	27

Analysis of Variance

Source	DF	Sum of Squares	Mean Square	F Ratio
Model	5	261.56620	52.3132	5.0122
Error	21	219.17958	10.4371	**Prob > F**
C. Total	26	480.74578		0.0035*

Parameter Estimates

Term	Estimate	Std Error	t Ratio	Prob>|t|
Intercept	58.264507	2.346506	24.83	<.0001*
FAC (%)	-0.0607	0.073568	-0.83	0.4186
GGBFS (%)	-0.156105	0.057318	-2.72	0.0127*
(FAC (%)-15.2778)*(FAC (%)-15.2778)	-0.031547	0.00982	-3.21	0.0042*
(GGBFS (%)-16.6667)*(GGBFS (%)-16.6667)	-0.007447	0.007421	-1.00	0.3270
(FAC (%)-15.2778)*(GGBFS (%)-16.6667)	-0.006771	0.004847	-1.40	0.1770

REPORT DOCUMENTATION PAGE

Form Approved
OMB No. 0704-0188

1. REPORT DATE (DD-MM-YYYY)	2. REPORT TYPE	3. DATES COVERED (From - To)
May 2021	Technical Report / Final	FY18–FY19

4. TITLE AND SUBTITLE

Long-Term Performance of Sustainable Pavements Using Ternary Blended Concrete with Recycled Aggregates

5a. CONTRACT NUMBER

5b. GRANT NUMBER

5c. PROGRAM ELEMENT
0602784A

6. AUTHOR(S)
Gilson R. Lomboy, Douglas B. Cleary, Seth M. Wagner, Yusuf Mehta, Danielle E. Kennedy, Benjamin E. Watts, Peter G. Bly, and Jared I. Oren

5d. PROJECT NUMBER
T26

5e. TASK NUMBER

5f. WORK UNIT NUMBER

7. PERFORMING ORGANIZATION NAME(S) AND ADDRESS(ES)

Rowan University
CREATEs
107 Gilbreth Parkway
Mullica Hill, NJ 08062-4446

U.S. Army Engineer Research and Development Center
Cold Regions Research and Engineering Laboratory
72 Lyme Road
Hanover, NH 03755-1290

U.S. Army Engineer Research and Development Center
Geotechnical and Structures Laboratory
3909 Halls Ferry Road
Vicksburg, MS 39180-6199

8. PERFORMING ORGANIZATION REPORT NUMBER

ERDC TR-21-8

9. SPONSORING / MONITORING AGENCY NAME(S) AND ADDRESS(ES)

Headquarters, U.S. Army Corps of Engineers
Washington, DC 20314-1000

10. SPONSOR/MONITOR'S ACRONYM(S)
USACE

11. SPONSOR/MONITOR'S REPORT NUMBER(S)

12. DISTRIBUTION / AVAILABILITY STATEMENT

Approved for public release; distribution is unlimited.

13. SUPPLEMENTARY NOTES

14. ABSTRACT

Dwindling supplies of natural concrete aggregates, the cost of landfilling construction waste, and interest in sustainable design have increased the demand for recycled concrete aggregates (RCA) in new portland cement concrete mixtures. RCA repurposes waste material to provide useful ingredients for new construction applications. However, RCA can reduce the performance of the concrete.

This study investigated the effectiveness of ternary blended binders, mixtures containing portland cement and two different supplementary cementitious materials, at mitigating performance losses of concrete mixtures with RCA materials. Concrete mixtures with different ternary binder combinations were batched with four recycled concrete aggregate materials. For the materials used, the study found that a blend of portland cement, Class C fly ash, and blast furnace slag produced the highest strength of ternary binder. At 50% replacement of virgin aggregates and ternary blended binder, some specimens showed comparable mechanical performance to a control mix of only portland cement as a binder and no RCA substitution. This study demonstrates that even at 50% RCA replacement, using the appropriate ternary binder can create a concrete mixture that performs similarly to a plain portland cement concrete without RCA, with the added benefit of being environmentally beneficial.

15. SUBJECT TERMS

Aggregates (Building materials), Binders (Materials), Concrete--Mixing, Waste products as building materials

16. SECURITY CLASSIFICATION OF:			17. LIMITATION OF ABSTRACT	18. NUMBER OF PAGES	19a. NAME OF RESPONSIBLE PERSON
a. REPORT	b. ABSTRACT	c. THIS PAGE			19b. TELEPHONE NUMBER (include area code)
Unclassified	Unclassified	Unclassified	SAR	117	